

NASA Contractor Report 3287

NASA
CR
3287
c.1

LOAN COPY
AFWL TECHNICAL
KIRILAND AFB

0062051

TECH LIBRARY KAFB, NM

Nonlinear Transient Analysis by Energy Minimization - A Theoretical Basis for the "ACTION" Computer Code

Manohar P. Kamat

CONTRACT NAS1-15080
JULY 1980

NASA



NASA Contractor Report 3287

Nonlinear Transient Analysis by Energy Minimization - A Theoretical Basis for the "ACTION" Computer Code

Manohar P. Kamat

*Virginia Polytechnic Institute and State University
Blacksburg, Virginia*

Prepared for
Langley Research Center
under Contract NAS1-15080



National Aeronautics
and Space Administration

**Scientific and Technical
Information Office**

1980

FOREWORD

The computer program ACTION was developed to support NASA Langley Research Center's program to improve crashworthiness of general aviation aircraft. The development of the ACTION program was supported by NASA Langley under grants NGR 47-004-114, NSG-1546 and other task orders.

This project, during its first phase, was under the cognizance of Dr. Edwin Kruszewski, then Branch Chief, Dynamics Branch. For the follow-on phases the development work was under the cognizance of Dr. Robert Thomson, Head, Loads Control Section, Dynamics Branch. The technical monitor, Dr. Robert Hayduk, of this branch was the responsible government officer and assisted in some of the work. For the first two phases the co-principal investigators at VPI & SU were Dr. Robert Melosh and Dr. George Swift. Dr. Manohar Kamat, Mr. Ben Brennenman, and the late Mr. Jon Dana provided technical support. For the third phase the co-principal investigators were Dr. Manohar Kamat and Dr. George Swift. Mr. Douglas Killian provided technical support on the second and third phases of the project. Dr. Manohar Kamat was the principal investigator for the final phases. Mr. Norman Knight, Jr., and Mr. Linh T. Duong provided technical support.

The computer code CRASH previously developed by the Department of Transportation was the basis of the ACTION computer code which finally came to fruition only as a result of the efforts and dedication of several people, especially those of the graduate students. The author of this document is indebted to all of them for their contributions. The directions

and the continued encouragement of grant monitors Robert Thomson and Robert Hayduk of NASA Langley during the development of this program were as always invaluable. The hitherto taken-for-granted assistance of Ms. Barbara Durling of NASA Langley on several occasions during the development of the ACTION program certainly merits a great deal of appreciation. Finally, a word of gratitude is in order to Marlene Taylor, Fran Carter, B. J. Vickers, and Jane Harrison for typing many versions of this document.

TABLE OF CONTENTS

<u>Section</u>	<u>Page</u>
1. INTRODUCTION	1
2. FORMULATION OF ACTION	4
3. DEFORMATION MODEL	8
3.1 Truss Element	8
3.1.1 Deformation	9
3.2 Frame Element	11
3.2.1 Geometry of Deformation of a Frame Element	12
3.2.2 Strain-Displacement Relations	23
3.2.3 Deformation Modeshapes: Linear- Elastic Material	23
3.2.4 Deformation Modeshapes: Inelastic Material	29
3.2.5 Shear Flow Theory	32
3.3 Membrane Element	35
3.3.1 Geometry of Deformation of a Membrane Element	35
3.3.2 Deformation Mode Shapes, Stresses and Strains	38
4. MATERIAL MODEL	41
4.1 Basic Assumptions	41
4.2 Modeling of Stress-Strain Curve and the Treatment of Stress-Strain History	43
4.3 Evaluation of Dissipative Strain Energy Density	47
5. KINEMATIC CONSTRAINTS	51
5.1 Rigid link Element	51
5.2 Impenetrable Contact Plane (Terrain Model)	52
5.2.1 Node Capture and Release	52
6. ANALYSIS BY ENERGY MINIMIZATION	55
6.1 Background Information	55
6.2 Solution Basis	56
6.3 Minimization Algorithms	57
6.3.1 BFGS Variable Metric Algorithm	58

<u>Section</u>	<u>Page</u>
6.3.2 Powell's Conjugate Gradient Algorithm	60
6.4 Evaluation of the Function and its Gradient	61
6.4.1 Function Evaluation	61
6.4.2 Gradient Evaluation	66
7. SOLUTION ERROR CONTROL	75
8. APPENDIX A - FRAME ELEMENT CROSS-SECTION DETAILS	78
A.1 The Box Cross-Section	78
A.2 The IE Cross-Section	82
A.3 The Circular Tube Cross-Section	91
A.4 The Elliptical Tube Cross-Section	94
A.5 The Solid Rectangular Cross-Section	96
9. BIBLIOGRAPHY	99

LIST OF FIGURES

<u>Figure</u>		<u>Page</u>
3-1	Geometry and Deformation of the Truss Element	10
3-2	Initial Orientation of the Frame Element	13
3-3	Finite Motion of the Frame Element	16
3-4	Generalized Displacements of the Frame Element	21
3-5	Generalized Forces of the Frame Element	25
3-6	Free Body Diagram of a Thin-walled Section	33
3-7	Deformation of the Membrane Element	36
4-1	Representation of the Stress-Strain Curve	44
4-2	Typical Stress-Strain Curve	46
4-3	Loading and Unloading Paths	48
4-4	Evaluation of Strain Energy Densities	49
6-1	A Model for Strain Energy Integration	65
A-1	Box Cross-Section Definition	79
A-2	Quadrature Points for the Box Cross-section	81
A-3	IE Cross-section Definition	83
A-4	Method for Determining Shear Stresses τ_y	85
A-5	Quadrature Points for IE Cross-Section	87
A-6	Circular Tube Cross-Section Details	90
A-7	Elliptical Tube Cross-Section Details	93
A-8	Solid Rectangular Cross-Section Details	97

Section 1

INTRODUCTION

A structural engineer is often faced with the need to predict the response of structures under failure conditions in attempting to make them fail-safe or crashworthy. Under failure conditions the load magnitudes may be large and the structural response may involve large permanent deformations, rupture and tearing.

With finite deformations the equations of motion of the structure are coupled in products of the derivatives of displacements and stresses: the unknowns of the problem. Material yielding may introduce non-linear stress-strain relations. Thus, nonlinear transient response prediction requires the evaluation of deflections, velocities, accelerations, stresses and strains in a structure of complex geometry and ductile material under time-varying loads that may cause the members of the structure to undergo large motions and deformations and/or respond plastically.

A number of well-known computer codes which can be used for post-impact studies of aircraft may be identified [1,2]. They can be classified as general or special purpose programs. General purpose programs such as MARC and NASTRAN¹ include some of the capabilities necessary for crash simulations. Special purpose programs such as the present computer program ACTION, provide in addition special modeling and evaluation processes which are particularly useful for crash. Because special purpose programs focus on a particular problem class, they are potentially more efficient for that class, and presumably require less computer resources, and are more manageable.

In the partitioned spectrum of crash simulators defined by McIvor,

¹NASTRAN: Registered trademark of the National Aeronautics and Space Administration.

[1], ACTION qualifies as a level four code: providing the capability to represent the material and geometric nonlinear transient behavior of a structure composed of truss, frame and membrane elements. In comparison with other level four simulators, ACTION offers the following unique features:

1. The ability to automatically control time discretization error.
2. Representation of impact with a rigid barrier including treatment of gapping and friction effects.
3. Logic specifically designed to minimize data transfers by keeping all working data in core and providing an analysis mode which avoids generation of large stiffness matrices in explicit form.
4. Response data defining the allocation of stored and dissipated energies.

The ACTION code, although quite suitable for nonlinear static analysis is primarily designed for analyzing response of vehicles crashing into a rigid or a deformable barrier. The objective is to predict analytically the response of a lightweight aircraft during a crash. The simulation is based on a discretized model of the structure using finite elements which may undergo finite motions and deformations and may respond plastically. A transient analysis of such a model then yields the displacements, velocities, accelerations, internal loads and stresses, at points of interest, under time varying loads that may cause complete failure of the structure.

The objective of such a nonlinear transient analysis is to develop an understanding of the multi-faceted relationship between the complex structural configuration of an aircraft and its response during crash. Such an understanding can provide the basis for crashworthy design of

lightweight aircraft, better restraint systems and efficient energy absorption devices which will reduce passenger trauma.

This report outlines the theoretical basis for the ACTION computer code. Instructions for the preparation of input and the interpretation of results can be found in reference [3].

Section 2

FORMULATION OF ACTION

This section describes the basis and highlights the intricacies of nonlinear transient analysis of a structure. Because of the complexity of structural geometry and response it is necessary to construct an approximate mathematical model. The objective is to predict the displacements, velocities, accelerations, internal loads and stresses at points of interest under time-varying loads that may cause complete failure of the structural model.

The mathematical model is a finite element displacement model. Simulation consists of discretizing the actual structure by finite elements, approximating the response of each element by a finite number of deformation states expressed as linear functions of generalized joint displacements and analyzing the mathematical model numerically.

Most researchers prefer to use a step-by-step incrementally linear approach for the solution of the nonlinear equations of the finite element model. In this process, sometimes referred to as the vector approach, the load is applied in increments which are sufficiently small so that a linear analysis will approximately represent the structural response for in increment. An iterative technique at constant load is used to satisfy equilibrium exactly for the partial load. The deformed geometry and stress state for a partial load is used as the initial state for the next load increment. Turner et al. [4], in their pioneering paper, provide a description of the process for finite deflection analysis by the step-by-step technique. Martin [5] provides some illustrations. Oden [6] and Hibbitt et al. [7] show applications to problems involving large strains and finite displacements. A comprehensive re-

view of the many aberrations of the incremental method for geometrically nonlinear problems is provided by Haisler et al [8]. Armen et al. [9], [10] Belytschko [11], [12] generalize the step-by-step process to problems involving both geometric and material nonlinearities. The work of these authors represents the many applications of the step-by-step approach that may be found in the literature.

ACTION represents the structural characteristics by a scalar function. The equilibrium configuration is established based on derivatives of the function. This approach, sometimes referred to as the scalar approach, has been successfully used in nonlinear structural analysis by Bogner et al. [13]. Mallet and Berke [14] show results of applying the process to truss structures. For transient analysis the formulation couples a step-by-step numerical integration in time with the function minimization procedure. Discrete steps are taken in the time co-ordinate and function minimization is used at each discrete time point to find the solution. Young [15] was probably the first to illustrate the use of this approach for nonlinear transient response simulation.

The approach consists briefly of the following steps:

1. Assume suitable element displacement field as a function of the local spatial co-ordinates with generalized joint displacements as unknown coefficients.
2. Relate the element generalized displacements to global generalized displacements of the system accounting for prescribed boundary conditions.
3. Develop expressions for strains in each element as functions of the global generalized displacements. (These expressions will account for nonlinearities in the derivatives of the displacement field.)

4. Determine the corresponding stresses and strain energy densities in each of the elements of the assemblage using respective material models.
5. Integrate the strain energy density over the volume of each element to yield element strain energy as a function of the global generalized displacements.
6. For transient analysis, knowing the values of the generalized displacements, velocities, accelerations, etc., at time t extrapolate assuming displacements vary as prescribed functions of time.
7. Determine by energy minimization, the configuration which implies satisfaction of equilibrium at the end of the next (load) time increment.

The simulation provides accurate results for static analysis with linear material behavior. For transient analysis with inelastic material behavior several factors limit the accuracy:

1. Because of the assumed displacement-time relations for the response the approximation does not accurately describe the response for large time steps. Depending upon the type of the temporal integration scheme used, there is a possibility of divergence of the solution from the true solution as time steps accumulate.
2. For inelastic stresses, the evaluation of the strain energy may be in error for certain deformation states due to approximations in integration. This error may be reduced by modeling the affected element with a number of smaller elements.
3. Because of discretization of the actual structure by an assemb-

lage of kinematically admissible finite elements, in general, the calculated solution can be expected to be in error from the true solution for the actual structure due to large geometry changes of particular elements. This error can also be reduced by modeling the given structure with more elements.

4. The inelastic material representation may be inadequate in some cases because the constitutive equations of ACTION are rather simple idealizations of true behavior.

Section 3

DEFORMATION MODEL

The deformation model is a mathematical model which characterizes the deformation of the structure in terms of unknown variables. The model is synthesized from deformation states of each element of the structure. These deformations are expressed in terms of displacements of "joints" of the system, points at which the elements interface.

The displacement field within each element is chosen as a continuously differentiable function of the local spatial co-ordinates and the joint displacements. The field maintains interelement continuity of the essential derivatives and includes constant strain states so that the representation provides a Galerkin model of the system. The generalized joint displacements of each element are related to the global displacements of the assemblage of the elements. These relations, which can be interpreted as transformations of the local generalized displacements, may be linear or nonlinear depending upon whether the motions and deformations of the elements are infinitesimally small or finite. For large angular changes, these transformations are accomplished using Euler angles which are linearly independent by virtue of the fact that the rotations are performed in a prescribed order.

The remainder of this section formulates the deformation characteristics of each type of element used in the ACTION simulator and the transformations to relate element behavior to the common rectangular cartesian coordinate system.

3.1 TRUSS ELEMENT [15]

A truss or a rod element is a structural component of uniform cross-

section which is initially straight. It is assumed that the element is capable of resisting only axial deformation imposed by joint displacements through momentless connections. Using a linear interpolation function for the axial displacement, closed form expressions for stresses and strain energy for the linear elastic range are developed. For the inelastic range development of the expression for the strain energy involves the use of the material model of the element.

3.1.1 Deformation

Figure 3-1 shows the initial and deformed positions of a typical truss element specified by the co-ordinates of the two joints, p and q, which it connects. These co-ordinates are defined with respect to a fixed global system of reference axes X, Y and Z. x and y denote the local co-ordinates axes corresponding to the deformed nodal configuration. Motion of the element is defined by finite displacement vectors \underline{U}_p and \underline{U}_q of the two joints. The components of the displacement vector \underline{U} in the X, Y, Z co-ordinate directions are denoted by U, V and W respectively. Element deformations are denoted by an axial displacement function $u(x)$. It is convenient to express the element strains with reference to the deformed nodal configuration, finite nodal displacements being accounted for in the transformation from global to the local displacements.

From Fig. 3-1 the initial length, L, of the element is given by

$$L = [(X_q - X_p)^2 + (Y_q - Y_p)^2 + (Z_q - Z_p)^2]^{1/2} \quad (3-1)$$

The deformed length, \tilde{L} , is given by

$$\tilde{L} = [(X_q + U_q - X_p - U_p)^2 + (Y_q + V_q - Y_p - V_p)^2 + (Z_q + W_q - Z_p - W_p)^2]^{1/2} \quad (3-2)$$

Hence, the change in length, DL, is given by

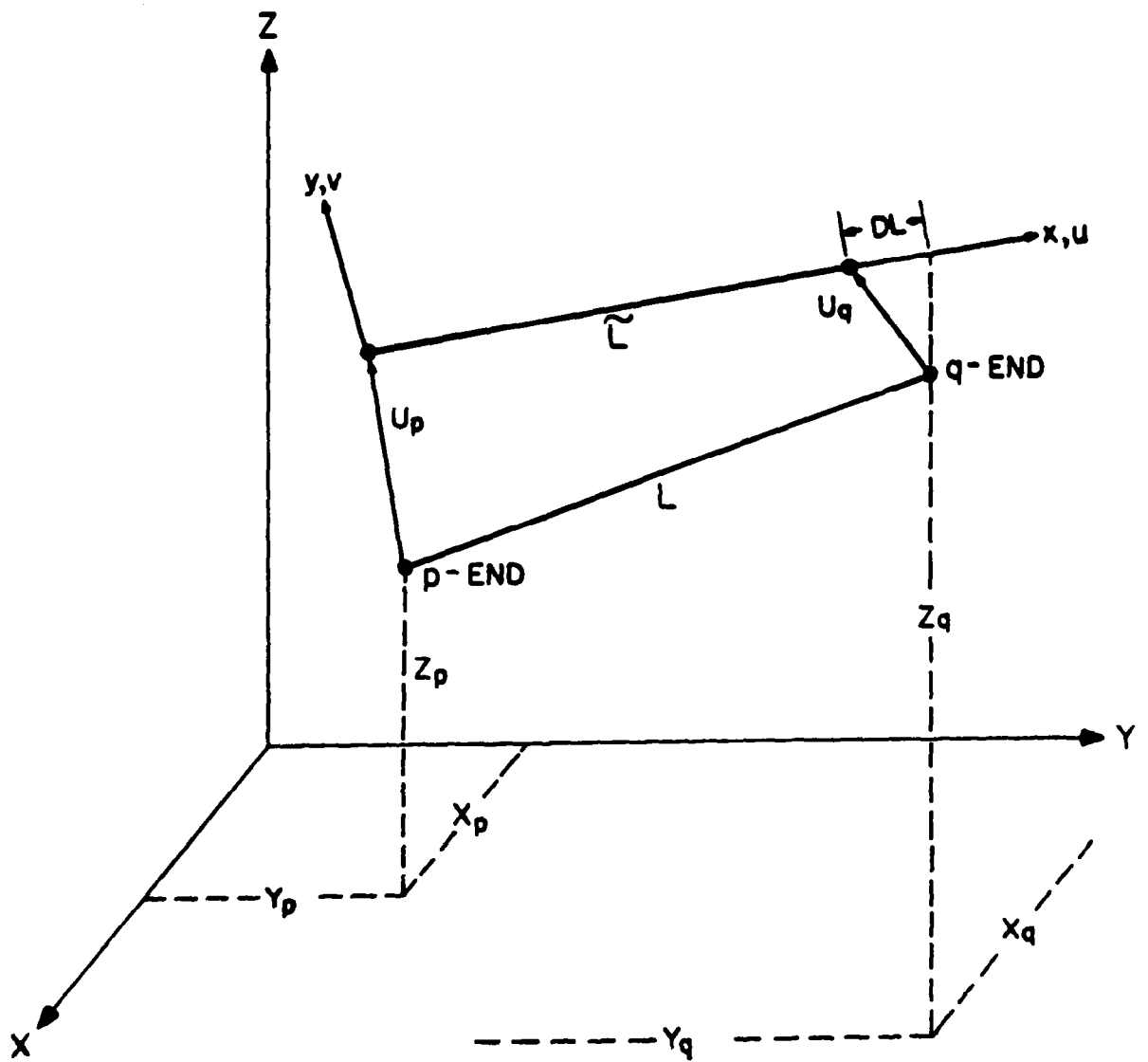


Fig. 3-1 Geometry and Deformation of the Truss Element.

$$DL = L[1 + \frac{2(\Delta X \Delta U + \Delta Y \Delta V + \Delta Z \Delta W)}{L^2} + \frac{\Delta U^2 + \Delta V^2 + \Delta W^2}{L^2}]^{1/2} - L \quad (3-3)$$

where Δ is the difference operator for q and p end values.

Equation (3-3) gives the change in length for joint displacements of any magnitude. The quantity inside the brackets in Eq. (3-3) should be positive but due to manipulation errors, values less than zero may be realized. Then DL is assumed to be -L: the maximum value physically possible. For values of the quantity inside the brackets close to one, DL is evaluated by using a binomial expansion.

Next, the assumption of the usual linear interpolation function in the corotational co-ordinate system yields

$$\delta u = x \left(\frac{DL}{L} \right) \quad (3-4)$$

whence

$$\epsilon = \left(\frac{DL}{L} \right) \quad (3-5)$$

δu being the relative displacement of the end q relative to the end p in the corotational system and ϵ being the strain.

3.2 FRAME ELEMENT [15]

A frame element is a structural component which is initially straight and which undergoes axial, bending and torsional deformations resulting from finite displacements and rotations of its ends. A frame element of general cross-section resists loads mainly by three types of stresses namely σ_x , τ_{xy} and τ_{xz} . For such a frame element, a general treatment of shear deformations is quite complex hence only thin-walled cross-section frame elements, wherein the plastic strain energy due to shear deformations can be ignored, are implemented in ACTION.

For the linear elastic case a closed form expression for the elastic strain energy density is developed.

For the inelastic case, however, the calculation of the elastic portion of the total strain energy density is based on the shear flow theory for beams with thin-walled cross-section and the incremental dissipative strain energy density U_D^* is assumed to be that due to the effects of normal stress and strain alone.

3.2.1 Geometry of Deformation of a Frame Element

Figure 3-2 shows the initial position, of a typical frame element, specified by the co-ordinates of its end points (the p and q joints it connects) with respect to a fixed system of global axes X, Y and Z. Roll orientation is specified by the angle between a reference axis of the cross-section and the plane formed by the member and its projection in the XY plane. This angle is denoted by γ . (If the member is parallel to the Z axis, γ is measured from the X axis.)

The longitudinal axis of the element and two reference axes of the cross-section form member axes x_1 , y_1 and z_1 . A vector, $\{V\}$, known in the global co-ordinate system can be described with respect to the member co-ordinate system as vector $\{V_1\}$ given by

$$\{V_1\} = [T_1]\{V\} \quad (3-6)$$

where $[T_1]$ is an orthogonal transformation matrix with the property

$$[T_1]^T [T_1] = [I] \quad (3-7)$$

where $[I]$ is the identity matrix. Premultiplication of both sides of Eq. (3-6) thus yields

$$\{V\} = [T_1]^T \{V_1\} \quad (3-8)$$

The transformation matrix, $[T_1]$, which describes large angular rotations from global axes X, Y, Z to axes x_1 , y_1 , z_1 are given by [16] as

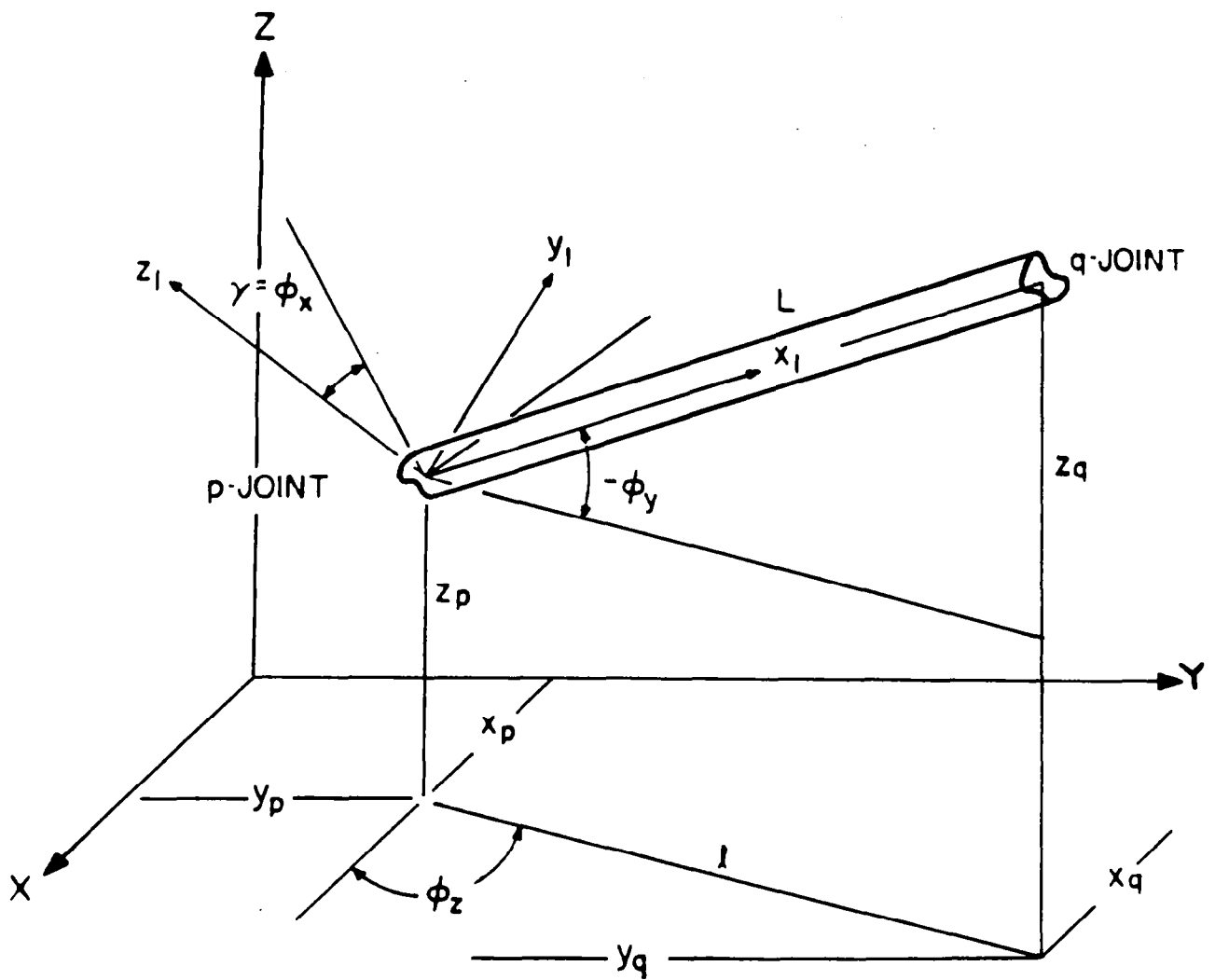


Fig. 3-2 Initial Orientation of the Frame Element.

$$[T_1] = \begin{bmatrix} c_y c_z & c_y s_z & -s_y \\ -c_x s_z + s_x s_y c_z & c_x c_z + s_x s_y s_z & s_x c_y \\ s_x s_z + c_x s_y c_z & -s_x c_z + c_x s_y s_z & c_x c_y \end{bmatrix} \quad (3-9)$$

where $c_i = \cos\phi_i$ and $s_i = \sin\phi_i$ for $i = x, y, z$. Angles ϕ_x, ϕ_y, ϕ_z are defined in Fig. 3-2 and the rotations have been performed in the order ϕ_z, ϕ_y and ϕ_x . From this figure it can be deduced that

$$\begin{aligned} \cos\phi_x &= \cos\gamma & \sin\phi_x &= \sin\gamma \\ \cos\phi_y &= \frac{\ell}{L} & \sin\phi_y &= -\frac{z_q - z_p}{L} \\ \cos\phi_z &= \frac{x_q - x_p}{\ell} & \sin\phi_z &= \frac{y_q - y_p}{\ell} \end{aligned}$$

where

$$\ell = \sqrt{(x_q - x_p)^2 + (y_q - y_p)^2} \quad \text{and} \quad L = \sqrt{\ell^2 + (z_q - z_p)^2}$$

Motion of the frame element is characterized as the superposition of a rigid body motion and deformations. There is no limit on the size of the rigid-body motion; however, the deformations are assumed to be small. Motion of the frame element is a function of the three translational displacements and the three rotational displacements of the two joints which the member connects.

To define joint displacements and rotations a set of joint axes, at the joint p which are initially parallel to the global axes X, Y, Z, are introduced. The joint displacements are denoted by the vector \underline{U} which has components U, V and W in the X, Y and Z directions respectively. The rotations of the joint p, $\theta_x, \theta_y, \theta_z$, are about the joint axes which are initially parallel to the global axes. Motion of the element is, thus, separated into two parts: a rigid-body motion which is described by the displacements and rotations of joint p, and a deformation which is

described by the motion of joint q relative to joint p.

Initially the joint axes are situated parallel to the global axes with the origin at joint p. The rigid body motion translates and rotates the joint axes to the position x' , y' , z' as shown in Fig. (3-3). The translation is given by the vector \underline{U}_p and the rotation is described by the transformation $[T_2]_p$ which relates vectors in global system to vectors in the displaced x' , y' , z' position of the joint axes,

$$\{V'\} = [T_2]_p \{V_1\} \quad (3-10)$$

The transformation $[T_2]_p$ is identical in form to $[T_1]$ of Eq. (3-6) except that the angles θ_{xp} , θ_{yp} , θ_{zp} are used in place of ϕ_x , ϕ_y , ϕ_z . The rotations must be specified in the order θ_{zp} , θ_{yp} , θ_{xp} to be able to use a form for $[T_2]$ similar to $[T_1]$. The member axes remain fixed with respect to the joint axes. Rigid-body motion carries the joint axes from their initial position parallel to the global axes) to the position x' , y' , z' . Likewise, the member axes x_1 , y_1 , z_1 become axes x_2 , y_2 , z_2 after the rigid-body motion. However, the new member axes x_2 , y_2 , z_2 are oriented exactly in the same manner with respect to the joint axes x' , y' , z' as were the member axes x_1 , y_1 , z_1 with respect to the global axes. Hence, any vector $\{V_2\}$ described with respect to the new member axes x_2 , y_2 , z_2 is related to the vector $\{V'\}$ described with respect to the x' , y' , z' axes by the relation

$$\{V_2\} = [T_1]\{V'\} \quad (3-11)$$

Accordingly, use of Eq. (3-9) yields

$$\{V_2\} = [T_1][T_2]_p \{V_1\}$$

or

$$\{V_2\} = [T_3]_p \{V_1\} \quad (3-12)$$

where

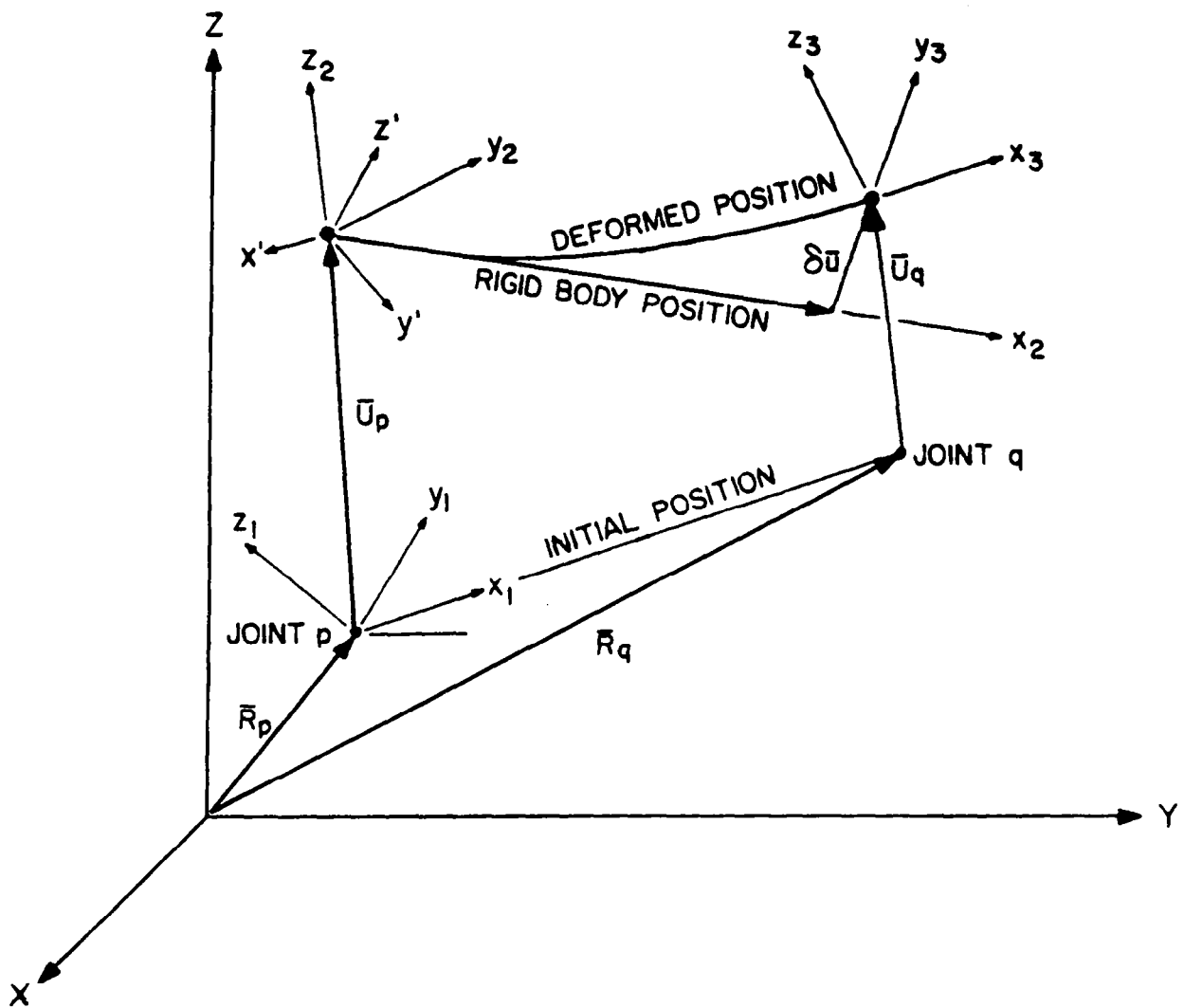


Fig. 3-3 Finite Motion of the Frame Element.

$$[T_3]_p = [T_1][T_2]_p \quad (3-13)$$

Since, both $[T_1]$ and $[T_2]_p$ are orthogonal transformations, their product is also an orthogonal transformation i.e.

$$[T_3]_p^T [T_3]_p = [I]$$

Thus, vectors specified in the global axes can be expressed in the deformation axes (member axes after rigid body motion) x_2, y_2, z_2 by the relation

$$\{V_1\} = [T_3]_p^T \{V_2\} \quad (3-14)$$

To describe the deformation of the element, the displacements of the joint q need be expressed with respect to the deformation axes.

From Fig. 3-3 it follows

$$\begin{aligned} \delta \underline{u} &= \underline{R}_q + \underline{U}_q - \underline{L} - \underline{U}_p - \underline{R}_p \\ &= (\underline{R}_q - \underline{R}_p) - \underline{L} + (\underline{U}_q - \underline{U}_p). \end{aligned}$$

where $\delta \underline{u}$ is a vector described with respect to the deformation axes.

Use of Eq. (3-12) then yields

$$\begin{Bmatrix} \delta u \\ \delta v \\ \delta w \end{Bmatrix} = [T_3]_p \begin{Bmatrix} X_q - X_p \\ Y_q - Y_p \\ Z_q - Z_p \end{Bmatrix} - \begin{Bmatrix} L \\ 0 \\ 0 \end{Bmatrix} + [T_3]_p \begin{Bmatrix} U_q - U_p \\ V_q - V_p \\ W_q - W_p \end{Bmatrix} \quad (3-15)$$

where $\delta u, \delta v, \delta w$ are the displacements of joint q relative to joint p along x_2, y_2, z_2 axes respectively; X, Y, Z are the co-ordinates and U, V, W the translational displacements of the joints measured with respect to the global axes.

For numerical calculations, the arrangement of terms in Eq. (3-15) is poor, requiring the differencing of nearly equal numbers. Since

$$\begin{Bmatrix} L \\ 0 \\ 0 \end{Bmatrix} = [T_1] \begin{Bmatrix} \Delta X \\ \Delta Y \\ \Delta Z \end{Bmatrix}$$

The terms are rearranged to:

$$\begin{Bmatrix} \delta u \\ \delta v \\ \delta w \end{Bmatrix} = [T_1] \left[[T_4]_p \begin{Bmatrix} \Delta X \\ \Delta Y \\ \Delta Z \end{Bmatrix} + [T_2]_p \begin{Bmatrix} \Delta U \\ \Delta V \\ \Delta W \end{Bmatrix} \right] \quad (3-16)$$

$$\text{where } [T_4]_p = [T_2]_p - [I] \quad (3-17)$$

and Δ is a difference operator for q and p end values in the global axes. After manipulation of the trigonometric terms in $[T_2]_p$, $[T_4]_p$ may be expressed as

$$[T_4]_p = \begin{bmatrix} -2(s_{y2}^2 c_{z2}^2 + c_{y2}^2 s_{z2}^2) & c_y s_z & -s_y \\ -c_x s_z + s_x s_y c_z & -2(s_{x2}^2 c_{z2}^2 + c_{x2}^2 s_{z2}^2) + s_x s_y s_z & s_x c_y \\ s_x s_z + c_x s_y c_z & -s_x c_z + c_x s_y s_z & -2(s_{x2}^2 c_{y2}^2 + c_{x2}^2 s_{y2}^2) \end{bmatrix}_p \quad (3-18)$$

where the subscript "2" denotes one-half of the indicated angle, the angles involved being θ_{xp} , θ_{yp} and θ_{zp} .

To complete the description of the deformation, expressions for rotation of joint q with respect to the deformation axes are required. In the development of these expressions, the rotations of each joint are permitted to be large but the differences between the rotations defined by

$$\Delta\theta_x = \theta_{xq} - \theta_{xp}, \quad \Delta\theta_y = \theta_{yq} - \theta_{yp}, \quad \Delta\theta_z = \theta_{zq} - \theta_{zp},$$

are assumed to be small, so that $\cos\Delta\theta \approx 1$ and $\sin\Delta\theta \approx \Delta\theta$. The intent is to permit large rigid body motion of the element but limit the deformation of the element to small rotations. With this restriction, the relative rotations ψ_x , ψ_y and ψ_z of the joint q with respect to the deformation axes are similarly given by

$$\begin{Bmatrix} \psi_x \\ \psi_y \\ \psi_z \end{Bmatrix} = [T_1][T_2]_p \begin{Bmatrix} \Delta\theta_x \\ \Delta\theta_y \\ \Delta\theta_z \end{Bmatrix} = [T_3]_p \begin{Bmatrix} \Delta\theta_x \\ \Delta\theta_y \\ \Delta\theta_z \end{Bmatrix} \quad (3-19)$$

Equations (3-19) have been obtained based on the fact that infinitesimal rotations can be treated as a vector.

Thus, deformation of the frame element is specified by the relative displacements and rotations of joint q with respect to joint p. The relative displacements δu , δv , δw are given by Eqs. (3-16) and the small rotations ψ_x , ψ_y , ψ_z are given by Eqs. (3-19). These equations contain large angle transformations which entail considerable calculation effort. For problems with small joint displacements and rotations, approximate transformations may be employed with considerable savings in calculations. This is achieved by replacing the trigonometric functions by their power series expansion and retaining only terms of the second-order. The resulting approximation is given by:

$$\begin{Bmatrix} \delta u \\ \delta v \\ \delta w \end{Bmatrix} = [T_1] \begin{bmatrix} -\frac{1}{2}(\theta_y^2 + \theta_z^2) & \theta_z & -\theta_y \\ -\theta_z + \theta_x \theta_y & -\frac{1}{2}(\theta_x^2 + \theta_z^2) & \theta_x \\ \theta_y + \theta_x \theta_z & -\theta_x + \theta_y \theta_z & -\frac{1}{2}(\theta_x^2 + \theta_y^2) \end{bmatrix} \begin{Bmatrix} \Delta X \\ \Delta Y \\ \Delta Z \end{Bmatrix} + \begin{bmatrix} 1 & \theta_z & -\theta_y \\ -\theta_z & 1 & \theta_x \\ \theta_y & -\theta_x & 1 \end{bmatrix} \begin{Bmatrix} \Delta U \\ \Delta V \\ \Delta W \end{Bmatrix} \quad (3-20a)$$

$$\begin{Bmatrix} \psi_x \\ \psi_y \\ \psi_z \end{Bmatrix} = [T_1] \begin{Bmatrix} \Delta\theta_x - \theta_{yp} \Delta\theta_z \\ \Delta\theta_y + \theta_{xp} \Delta\theta_z \\ -\theta_{xp} \Delta\theta_y + \Delta\theta_z \end{Bmatrix} \quad (3-20b)$$

If all second-order terms are neglected in the above expressions, the linear deformation equations are obtained

$$\begin{Bmatrix} \delta u \\ \delta v \\ \delta w \end{Bmatrix} = [T_1] \begin{bmatrix} 0 & \theta_z & -\theta_y \\ -\theta_z & 0 & \theta_x \\ \theta_y & -\theta_x & 0 \end{bmatrix}_p \begin{Bmatrix} \Delta X \\ \Delta Y \\ \Delta Z \end{Bmatrix} + \begin{Bmatrix} \Delta U \\ \Delta V \\ \Delta W \end{Bmatrix} \quad (3-21a)$$

$$\begin{Bmatrix} \psi \\ \psi_x \\ \psi_y \\ \psi_z \end{Bmatrix} = [T_1] \begin{Bmatrix} \Delta \theta \\ \Delta \theta_x \\ \Delta \theta_y \\ \Delta \theta_z \end{Bmatrix} \quad (3-21b)$$

These results may be used for problems where the displacements and rotations are small (i.e., (rotations)² << order (relative joint displacements)). If non-linear deformation effects are to be represented as in the case of buckling problems, the second-order approximation must be employed.

The parameters δu , δv , δw , ψ_x , ψ_y , ψ_z are the generalized displacements as seen at the end point q relative to the end point p of the element. Deformation along the length of the element is described by introducing displacement functions $u_o(x)$, $v_o(x)$, $w_o(x)$ of a longitudinal reference axis and the angle of twist $\beta_o(x)$ about the reference axis as shown in Fig. 3-4. The x , y , z axes of Fig. 3-4 are the x_2 , y_2 , z_2 axes of Fig. 3-3. The subscript is dropped to simplify the notation in the development to follow.

The displacement functions $u_o(x)$, $v_o(x)$, $w_o(x)$ and $\beta_o(x)$ define deformations of the reference axis. Displacements of points off the reference axis are obtained by making the usual kinematic assumptions of the engineering theory of beams under bending and torsion. For the sake of simplicity, the equations of equilibrium with bending and torsional deformations, lateral displacements and twists are referenced to a longitudinal axis through the shear center and are denoted by $v(x)$, $w(x)$ and $\beta(x)$ respectively as shown in Fig. 3-4. Based on the results

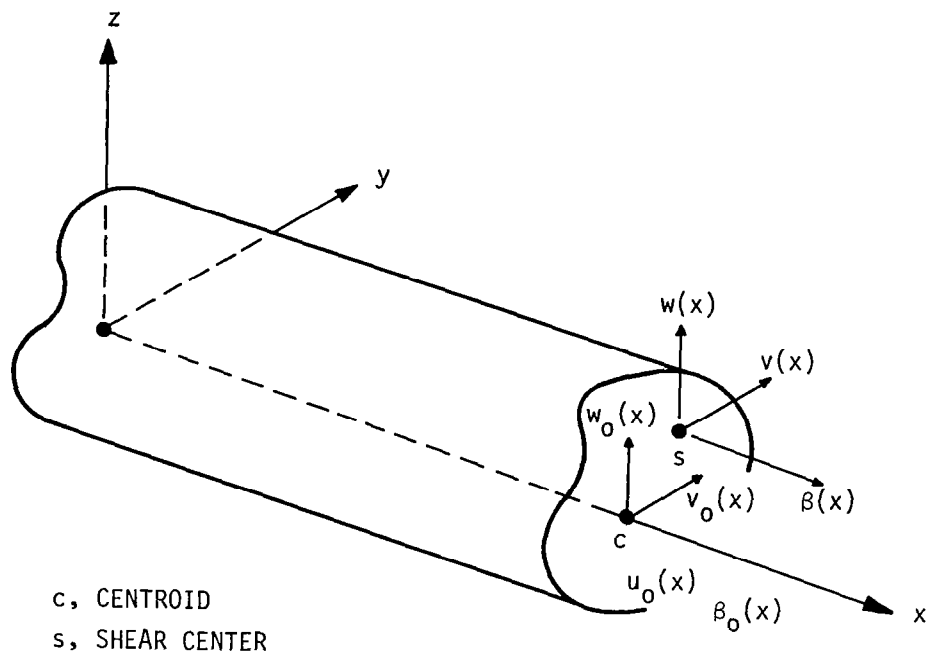


Fig. 3-4 Generalized Displacements of the Frame Element.

from strength of materials and elasticity [17] the following expressions are assumed for the displacements u^* , v^* , w^* of points off the centroidal reference axis:

$$\begin{aligned}
 u^*(x) &= u(x) - y \frac{dv_b(x)}{dx} - z \frac{dw_b(x)}{dx} + \phi_1(y,z) \frac{dv_s(x)}{dx} + \phi_2(y,z) \frac{dw_s(x)}{dx} \\
 &\quad + \phi_3(y,z) \frac{d\beta(x)}{dx} \\
 v^*(x) &= v_b(x) + v_s(x) - (z - z_s) \beta(x) \\
 w^*(x) &= w_b(x) + w_s(x) + (y - y_s) \beta(x)
 \end{aligned}
 \tag{3-22}$$

The subscripts "b" and "s" indicate lateral displacement due to bending and shear and the functions ϕ_1 , ϕ_2 , ϕ_3 describe cross-section warping. The total lateral displacement at the shear center is the sum of the bending and shear components

$$v = v_b + v_s, \quad w = w_b + w_s \tag{3-23}$$

The deformations of the reference axis can be obtained by setting $y = z = 0$ in Eqs. (3-22). It is implicitly assumed in Eqs. (3-22) that longitudinal warping is unrestrained and that plane sections remain plane during stretching and bending even though the total deformation produces nonplanar cross-sections.

For thin-walled closed cross-sections, the stresses produced by restrained warping are small. The same is not true of a thin-walled open section where a deformation model with restrained warping would be desirable. The assumptions of plane sections remaining plane during bending deformations and of plane rotations during torsional deformations are quite adequate for inelastic material behavior. However, warping

functions become complex functions of the distortion parameters and the material properties. The secondary, self-equilibrating stresses due to restrained warping, if any, are neglected for elastic and inelastic material behavior for sake of convenience.

3.2.2 Strain-Displacement Relations

With the assumption of unrestrained warping, the axial strain consistent with the deformations assumed in Eqs. (3-22) is given by

$$\epsilon_x = \frac{du}{dx} - y \frac{d^2 v_b}{dx^2} - z \frac{d^2 w_b}{dx^2} + \frac{1}{2} \left[\left(\frac{dv}{dx} \right)^2 + \left(\frac{dw}{dx} \right)^2 \right] \quad (3-24)$$

Implicit in the Eq. (3-24) is the assumption that squares of rotations are negligible in comparison to unity. Equation (3-24) is adequate for describing the initiation of buckling but not adequate for describing post buckling behavior. A rigorous treatment of shear distortion based on the theory of elasticity is quite involved even for the elastic case. Hence, to simplify the treatment of shear distortion, especially for the inelastic range, an approximate strength of materials approach is used.

3.2.3 Deformation Modeshapes: Linear-Elastic Material

Based on the results from engineering beam theory, deformation modeshapes are assumed and axial and shear strains are derived as functions of relative joint displacements. The deformation modeshapes describe deformation along the length of the member as caused by relative joint displacements δu , δv , δw , ψ_x , ψ_y , ψ_z defined in Section 3.2.1. Neglecting shear deformations and assuming unrestrained warping these results are

$$\frac{u}{L} = \eta \frac{\delta u}{L}$$

$$\frac{v_b}{L} = (3\eta^2 - 2\eta^3) \frac{\delta v_b}{L} + (\eta^3 - \eta^2)\psi_z$$

$$\frac{w_b}{L} = (3\eta^2 - 2\eta^3) \frac{\delta w_b}{L} - (\eta^3 - \eta^2)\psi_y$$

(3-25 a-d)

$$\beta = \eta\psi_x$$

where,

$$\delta v = \delta v_b + z_s \psi_x, \quad \delta w = \delta w_b - y_s \psi_x \quad (3-25 e, f)$$

$\eta = x/L$ and y_s, z_s are the co-ordinates of the shear center of the cross-section of the beam.

The stress resultants associated with the deformation shapes of Eqs. (3-25) are given by

$$N = EA \frac{du}{dx}$$

$$M_z = EI_z \frac{d^2 v_b}{dx^2} + EI_{yz} \frac{d^2 w_b}{dx^2}$$

$$-M_y = EI_{yz} \frac{d^2 v_b}{dx^2} + EI_y \frac{d^2 w_b}{dx^2}$$

(3-26 a-d)

$$T = GJ \frac{d\beta}{dx}$$

where,

$$A = \int_A dA, \quad I_y = \int_A z^2 dA, \quad I_z = \int_A y^2 dA, \quad I_{yz} = \int_A yz dA$$

the parameter J is the torsional constant for the cross-section and the parameters E and G are the material elastic moduli in tension and shear, respectively. Equilibrium of the frame element in Fig. (3-5), gives

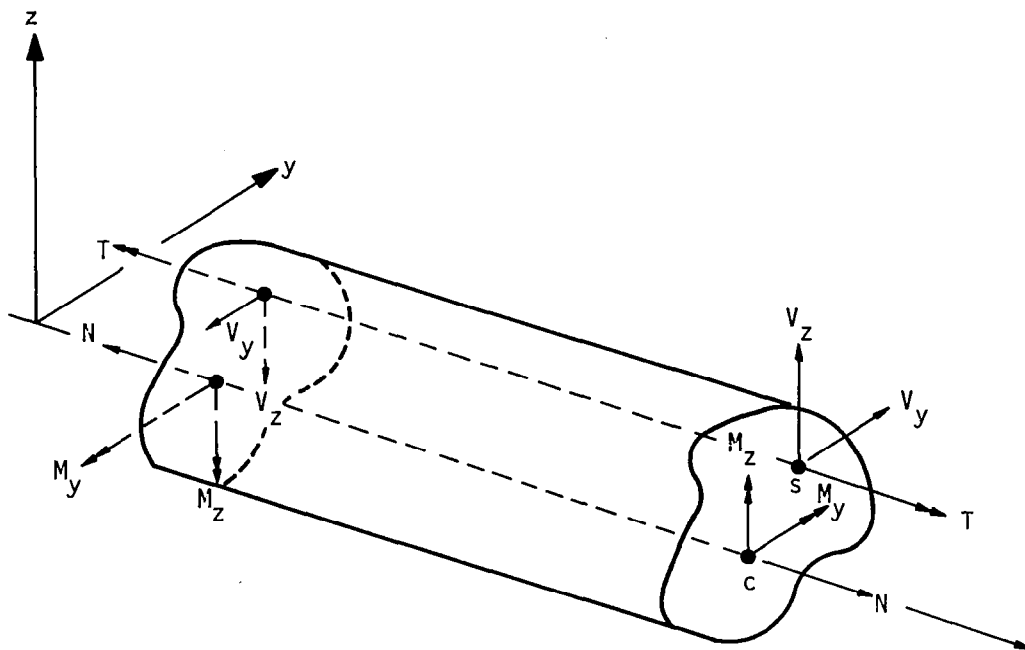


Fig. 3-5 Generalized Forces of the Frame Element.

$$\begin{aligned}
V_y &= -\frac{dM_z}{dx} = -EI_z \frac{d^3 v_b}{dx^3} - EI_{yz} \frac{d^3 w_b}{dx^3} \\
V_z &= -\frac{dM_y}{dx} = -EI_{yz} \frac{d^3 v_b}{dx^3} - EI_y \frac{d^3 w_b}{dx^3}
\end{aligned}
\tag{3-26e,f}$$

In the development of Eqs.(3-25), it is assumed that the x-axis or the straight line defined by the joints p and q, passes through the centroid of the cross-section. Thus, eccentricity between the structural joints and the centroidal axis of the element is not represented. Note that in Eqs. (3-26) torsion and bending are uncoupled, since twisting and lateral displacements are referenced to the shear center.

The effect of shear deformation due to bending is approximated. The gross shear distortion of the beam is described by an effective shear strain. From the geometry of shear deformation, the shear strain-displacement relations are given by

$$\gamma_{sxy} = \frac{dv_s}{dx}, \quad \gamma_{sxz} = \frac{dw_s}{dx} \tag{3-27a,b}$$

where the subscript "s" indicates the shear component of deflection.

The shear strains produce shear forces based on a gross response described by the expressions

$$V_y = \frac{AG}{k_y} \frac{dv_s}{dx} + \frac{AG}{k_{yz}} \frac{dw_s}{dx} \tag{3-28a}$$

$$V_z = \frac{AG}{k_{zy}} \frac{dv_s}{dx} + \frac{AG}{k_z} \frac{dw_s}{dx} \tag{3-28b}$$

The constants k_y , k_{yz} , k_{zy} , k_z are to be determined so that the gross shear model best represents the shear deformation in bending. From among the various methods available for the calculation of the shear constants the maximum-strain method is the one used in the ACTION simulator. In this method, the maximum strain at the centroidal plane is

assumed to be the effective strain and

$$k_y = \frac{(\gamma_{xy})_{\text{centroid}}}{(V_y/AG)} = \left[\frac{Q_z V_y}{b_z I_z G} \right]_{\text{centroid}} / (V_y/AG) = \left[\frac{AQ_z}{b_z I_z} \right]_{\text{centroid}} \quad (3-29 \text{ a,b})$$

$$k_z = \frac{(\gamma_{xz})_{\text{centroid}}}{(V_z/AG)} = \left[\frac{Q_y V_z}{b_y I_y G} \right]_{\text{centroid}} / (V_z/AG) = \left[\frac{AQ_y}{b_y I_y} \right]_{\text{centroid}}$$

where Q_z and Q_y are the first moments of area (on either side of the centroidal axis) about the centroidal axes z and y respectively. These constants are easily evaluated and results are found in strength of materials books [18] for a variety of common cross-sections.

The constants k_y , k_{yz} , k_{zy} , k_z must satisfy the reciprocity relations

$$k_{yz} = k_z \frac{I_y}{I_{yz}} = k_{zy} = k_y \frac{I_z}{I_{yz}} \quad (3-29 \text{ c,d})$$

However, if these constants are obtained by the maximum-strain method as outlined above, they may not satisfy the reciprocity relations for certain cross-sections.

Next, solving for v_s and w_s from Eqs. (3-28) with the help of Eqs. (3-26 e,f) and (3-29 c,d) gives

$$\frac{dv_s}{dx} = -k_y \frac{EI_z}{GA} \frac{d^3 v_b}{dx^3}, \quad \frac{dw_s}{dx} = -k_z \frac{EI_y}{GA} \frac{d^3 w_b}{dx^3}$$

which have the solutions

$$\frac{v_s}{L} = \eta \frac{\delta v_s}{L}, \quad \frac{w_s}{L} = \eta \frac{\delta w_s}{L} \quad (3-30 \text{ a,b})$$

where

$$\frac{\delta v_s}{L} = \frac{12k_y EI_z}{GAL^2} \left[\frac{\delta v_b}{L} - \frac{1}{2} \psi_z \right], \quad \frac{\delta w_s}{L} = \frac{12k_z EI_y}{GAL^2} \left[\frac{\delta w_b}{L} + \frac{1}{2} \psi_y \right] \quad (3-30 \text{ c,d})$$

Equations (3-30) are simple linear mode shapes that describe the deformation caused by bending shear. Adding these to the initial mode shapes

from Eqs. (3-25) gives

$$\frac{u}{L} = \eta \frac{\delta u}{L}$$

$$\frac{v}{L} = (3\eta^2 - 2\eta^3) \frac{\delta v_b}{L} + (\eta^3 - \eta^2)\psi_z + \eta \frac{\delta v_s}{L} + \eta \left(\frac{z_s}{L}\right) \psi_x \quad (3-31 \text{ a-d})$$

$$\frac{w}{L} = (3\eta^2 - 2\eta^3) \frac{\delta w_b}{L} - (\eta^3 - \eta^2)\psi_y + \eta \frac{\delta w_s}{L} - \eta \left(\frac{y_s}{L}\right) \psi_x$$

$$\beta = \eta\psi_x$$

where $\delta v = \delta v_b + \delta v_s + \left(\frac{z_s}{L}\right)\psi_x$, $\delta w = \delta w_b + \delta w_s - \left(\frac{y_s}{L}\right)\psi_x$

The deformation modeshapes of Eqs. (3-31) represent a linear deformation theory. These results may be extended to include the nonlinear coupling between axial and lateral deformations. An axial deformation of the following form is assumed

$$\frac{du}{dx} = K - \frac{1}{2} \left[\left[\frac{dv}{dx} \right]^2 + \left[\frac{dw}{dx} \right]^2 \right] \quad (3-32a)$$

where K is a constant given by the relation

$$K = \frac{\delta u}{L} + \frac{1}{2L^2} \int_0^1 \left[\left[\frac{dv}{d\eta} \right]^2 + \left[\frac{dw}{d\eta} \right]^2 \right] d\eta \quad (3-32b)$$

Equation (3-32) replaces the first of Eqs. (3-31).

Collecting results from Eqs. (3-31), (3-32) the deformation mode shapes for the linear elastic frame element are summarized as follows:

$$\begin{aligned} \frac{du}{d\eta} &= KL - \frac{1}{2L} \left[\left(\frac{dv}{d\eta} \right)^2 + \left(\frac{dw}{d\eta} \right)^2 \right] \\ \frac{v}{L} &= (3\eta^2 - 2\eta^3) \frac{\delta v_b}{L} + (\eta^3 - \eta^2)\psi_z + \eta \frac{\delta v_s}{L} \\ \frac{w}{L} &= (3\eta^2 - 2\eta^3) \frac{\delta w_b}{L} - (\eta^3 - \eta^2)\psi_y + \eta \frac{\delta w_s}{L} \\ \beta &= \eta\psi_x \end{aligned} \quad (3-33 \text{ a-d})$$

where

$$\delta_v = \delta v_b + \delta v_s + z_s \psi_x, \quad \delta_w = \delta w_b + \delta w_s - y_s \psi_x \quad (3-33 \text{ e,f})$$

and K is given by Eq. (3-32b).

Equations (3-30) and 3-33 e,f) can be solved simultaneously to obtain

$$\frac{\delta v_b}{L} = \frac{\frac{\delta v}{L} + \frac{\alpha_y}{2} \psi_z - \frac{z_s}{L} \psi_x}{1 + \alpha_y}, \quad \frac{\delta w_b}{L} = \frac{\frac{\delta w}{L} - \frac{\alpha_z}{2} \psi_y + \frac{y_s}{L} \psi_x}{1 + \alpha_z}$$

where,

$$\alpha_y = \frac{12k_y EI_z}{GAL^2}, \quad \alpha_z = \frac{12k_z EI_y}{GAL^2} \quad (3-34a,b)$$

The parameters α_y and α_z are a measure of the relative importance of shear deformation. For a lateral displacement imposed at the end of the element, α is the ratio of shear deformation to bending deformation.

With the deformation mode shapes defined the constant K of Eq.

(3-32b) can be evaluated. The expression for K is

$$\begin{aligned} K = & \frac{\delta u}{L} + \frac{3}{5} \left(\frac{\delta v_b}{L} \right)^2 - \frac{1}{10} \frac{\delta v_b}{L} \psi_z + \frac{1}{15} \psi_z^2 + \frac{\delta v_s}{L} \left(\frac{\delta v_b}{L} + \frac{1}{2} \frac{\delta v_s}{L} \right) \\ & + \frac{3}{5} \left(\frac{\delta w_b}{L} \right)^2 + \frac{1}{10} \frac{\delta w_b}{L} \psi_y + \frac{1}{15} \psi_y^2 + \frac{\delta w_s}{L} \left(\frac{\delta w_b}{L} + \frac{1}{2} \frac{\delta w_s}{L} \right) \end{aligned} \quad (3-35)$$

3.2.4 Deformation Mode Shapes: Inelastic Material

The determination of deformation mode shapes for inelastic action in the frame element is not feasible in a general analytical formulation. For approximate treatment of the inelastic case the elastic mode shapes of Eqs. (3-33) are used. For consistency of assumptions, however, it can be shown [19] that the linear axial deformation mode-shape of Eq. (3-25a) has to be replaced by a quadratic variation of

axial displacement u along the length of the element. This is achieved by the introduction of an additional node, r , at the center of the frame element. Only the axial displacement u_r of this node is monitored.

Thus

$$\frac{u}{L} = \frac{u_p}{L} + 3\eta \frac{\delta u_1}{L} - \eta \frac{\delta u_2}{L} - 2\eta^2 \frac{\delta u_1}{L} + 2\eta^2 \frac{\delta u_2}{L} \quad (3-36)$$

where

$$\delta u_1 = u_r - u_p$$

$$\text{and } \delta u_2 = u_q - u_r.$$

The transformation relation between the global displacement ΔU_1 and δu_1 can be shown to be

$$\frac{\delta u_1}{L} = \frac{1}{A_1} \left[\frac{\Delta U_1}{L} - A_2 \frac{\delta v^*}{L} - A_3 \frac{\delta w^*}{L} + \frac{1}{2L} (A_4 + A_5 + A_6) \right] \quad (3-37)$$

where

$$A_1 = T_{2p}^{11} T_1^{11} + T_{2p}^{21} T_1^{12} + T_{2p}^{31} T_1^{13}$$

$$A_2 = T_{2p}^{11} T_1^{21} + T_{2p}^{21} T_1^{22} + T_{2p}^{31} T_1^{23}$$

$$A_3 = T_{2p}^{11} T_1^{31} + T_{2p}^{21} T_1^{32} + T_{2p}^{31} T_1^{33}$$

$$A_4 = (T_{4p}^{11} \Delta x + T_{4p}^{12} \Delta y + T_{4p}^{13} \Delta z) T_{2p}^{11}$$

$$A_5 = (T_{4p}^{21} \Delta x + T_{4p}^{22} \Delta y + T_{4p}^{23} \Delta z) T_{2p}^{21}$$

$$A_6 = (T_{4p}^{31} \Delta x + T_{4p}^{32} \Delta y + T_{4p}^{33} \Delta z) T_{2p}^{31}$$

(3-38a-h)

$$\frac{\delta v^*}{L} = \frac{1}{2} \left(\frac{\delta v_b}{L} \right) - \frac{1}{8} \psi_z + \frac{1}{2} \frac{\delta v_s}{L} + \frac{1}{2} z_s \psi_x$$

$$\frac{\delta w^*}{L} = \frac{1}{2} \left(\frac{\delta w_b}{L} \right) + \frac{1}{8} \psi_y + \frac{1}{2} \frac{\delta w_s}{L} - \frac{1}{2} y_s \psi_x$$

and T_k^{ij} is the i - j th element of the matrix \underline{T}_k of Section 3.2.1. Equation

(3-37) assumes that A_1 is nonzero. If this is not the case, similar equations can be derived in terms of ΔV_1 or ΔW_1 .

It seems appropriate to remark in passing that this feature of the frame element using a quadratic variation for the axial displacement field is not necessary for the linear case wherein the deformations are referenced with respect to the centroidal axis. However, if used with deformations being referenced with respect to the centroidal axes, the quadratic variation degenerates to a linear variation. More importantly, the feature could be exploited to analyze linear response using reference axes which are not coincident with the centroidal axes and/or for the purposes of simulating rigid links. Of course, this then implies that the strain energy of deformations cannot be computed using the usual closed form expression of the linear elastic case but rather be computed using numerical integration as in the inelastic case to be described in Section 6.4.

For inelastic response, the relative contributions of bending and shear to the total lateral deformations are initially unknown. An iterative solution for the magnitude of shear deformation is required. The iterative solution is implemented by adjusting the relative contributions of bending and shear iteratively until the shear deformation as measured by the effective shear strain, converges. The following steps are involved:

1. Initial magnitudes of shear and bending deformation are assumed based on the elastic solutions of Eqs. (3-30c,d) and (3-34).

2. An analysis is performed for the stresses and strains in the element. The effective shear strains γ_{sxy} , γ_{sxz} are evaluated and Eqs. (3-27a,b) and (3-30a,b) are used to obtain new measures of the shear

deformation components,

$$(\delta v_s)_{\text{new}} = \gamma_{sxy} L, \quad (\delta w_s)_{\text{new}} = \gamma_{sxz} L \quad (3-39a,b)$$

3. The new shear deformations are compared to the old, normalized by a measure of the total deformations from Eqs. (3-30c,d).

$$\frac{|(\delta v_s)_{\text{new}} - (\delta v_s)_{\text{old}}|}{|\delta v_b| + |\delta v_s| + |1/2 \psi_z L|} \ll 1 \quad (3-40a,b)$$

$$\frac{|(\delta w_s)_{\text{new}} - (\delta w_s)_{\text{old}}|}{|\delta w_b| + |\delta w_s| + |1/2 \psi_y L|} \ll 1$$

If these ratios are sufficiently small (equal to 0.10) the iteration is stopped, if not, the iteration is repeated from step "2" with the new values of shear deformation.

Consideration of shear deformation requires a considerable calculation effort for the inelastic case. Therefore, shear deformation should be considered only for those elements where it is judged to be of significance.

3.2.5 Shear Flow Theory:

Figure 3-6 shows the forces acting on an element of a thin-walled frame member. With the usual assumptions of shear flow theory of thin-walled members [18] equilibrium of forces in the longitudinal direction yields

$$q = - \int_0^s \frac{d\sigma}{dx} t ds + q_0 \quad (3-41)$$

where q_0 is the shear flow at the origin of s . Equation (3-41) gives the variation of shear flow around the perimeter and along the length of the beam as a function of the longitudinal stress σ .

Subsequent treatment of shear stress by the shear flow theory varies depending upon whether the cross-section is open or closed. For thin-

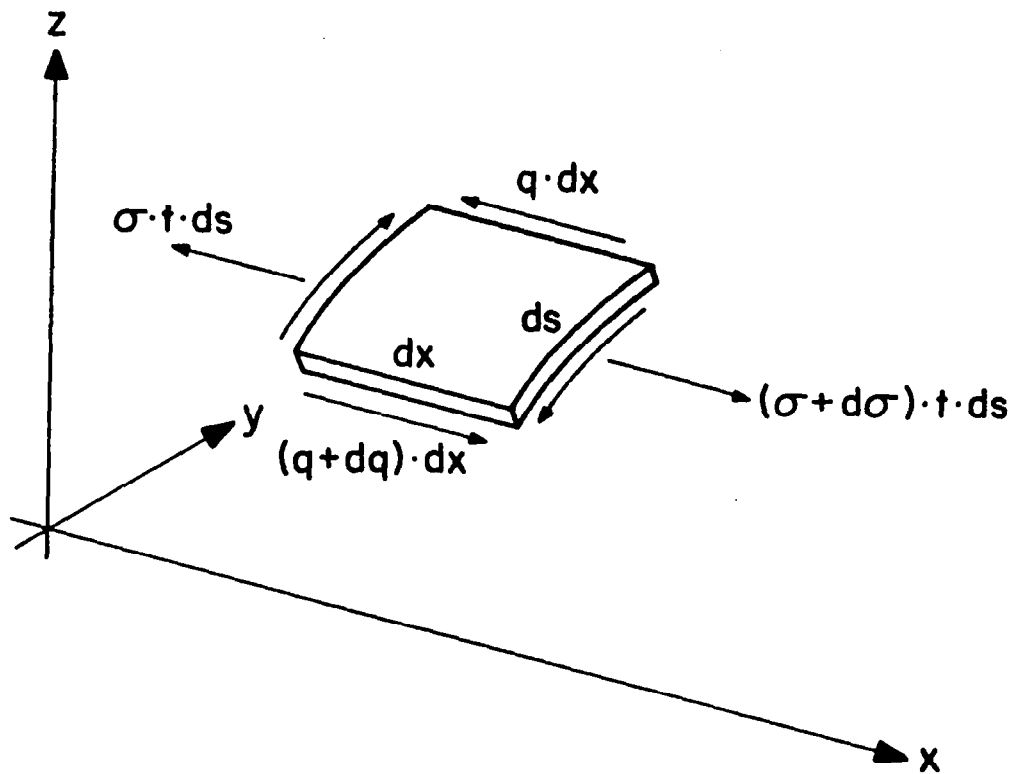


Fig. 3-6 Free Body Diagram of a Thin-walled Section.

walled open cross section, the torsional shear stresses vary while the shear stresses due to bending shear are constant across the thickness. For thin-walled closed sections the torsional and bending stresses are constant across the wall thickness hence both are described by the shear flow theory. Thus, in the case of the IE section element (a thin-walled open section) the shear stresses due to torsion are neglected both for the elastic and inelastic cases, although for the elastic case the strain energy due to torsion is accounted for. In this regard the treatment of the IE section element is inconsistent.

For closed cross-sections, Eq. (3-41) describes the change in q around the perimeter. The integration constant q_0 in Eq. (3-41) is selected so that the shear strain, when integrated around the perimeter gives the prescribed twist i.e.

$$\frac{d\beta}{dx} = \frac{1}{2A_0} \oint \gamma ds \quad (3-42)$$

where A_0 is the area enclosed by the section and γ is the shear strain.

Since, in the formulation of the material model of Section 4, it is assumed that the shear response is elastic. In this case Eq. (3-42) becomes

$$\frac{d\beta}{dx} = \frac{1}{2A_0 G} \oint \frac{q}{t} ds \quad (3-43)$$

Substitution for q from Eq. (3-41) in the above equation yields

$$\frac{d\beta}{dx} = \frac{1}{2A_0 G} \oint \frac{1}{t} \left[- \int_0^s \frac{d\sigma}{dx} t ds \right] ds + \oint \frac{q_0}{t} ds$$

or

$$q_0 = \frac{2A_0 G \frac{d\beta}{dx} - \oint \frac{q'}{t} ds}{\oint \frac{1}{t} ds} \quad (3-44a)$$

where

$$q' = \oint_0^s \frac{d\sigma}{dx} t \, ds \quad (3-44b)$$

It can be shown that the denominator of Eq. (3-44a) is given by

$$\oint \frac{1}{t} \, ds = \frac{4A_0^2}{J} \quad (3-45)$$

where J is the torsional constant for the section.

If $q(s)$ denotes the total shear flow due to bending and torsion, $q_b(s)$ the shear flow due to bending alone and $q_t(s)$ the shear flow due to torsion then the latter is given by

$$q_t(s) = \frac{1}{s_0} \oint q \, ds \quad (3-46)$$

where s_0 is the perimeter of the section. Hence

$$q_b(s) = q(s) - q_t(s) \quad (3-47)$$

3.3 MEMBRANE ELEMENT

A membrane element is a plane triangular thin element which undergoes only in-plane deformations resulting from displacements of its vertices. No out-of-plane deformations are admitted, but the element can undergo large rigid body motions. The usual assumptions of the engineering theory of membranes are implied in the development of the element stiffness properties.

3.3.1 Geometry of Deformation of a Membrane Element

Figure 3-7 shows the initial and deformed positions of a typical membrane element. The initial undeformed position of the triangular element is specified by the co-ordinates of its three vertices, p^0 , q^0 and r^0 (taken in a counterclockwise sense) with respect to the fixed system of global axes X , Y and Z . The vertices of this triangle after deformation are labeled as p , q and r . Local x' and y' axes are chosen to lie in the plane of the deformed triangle with the x' -axis coinciding

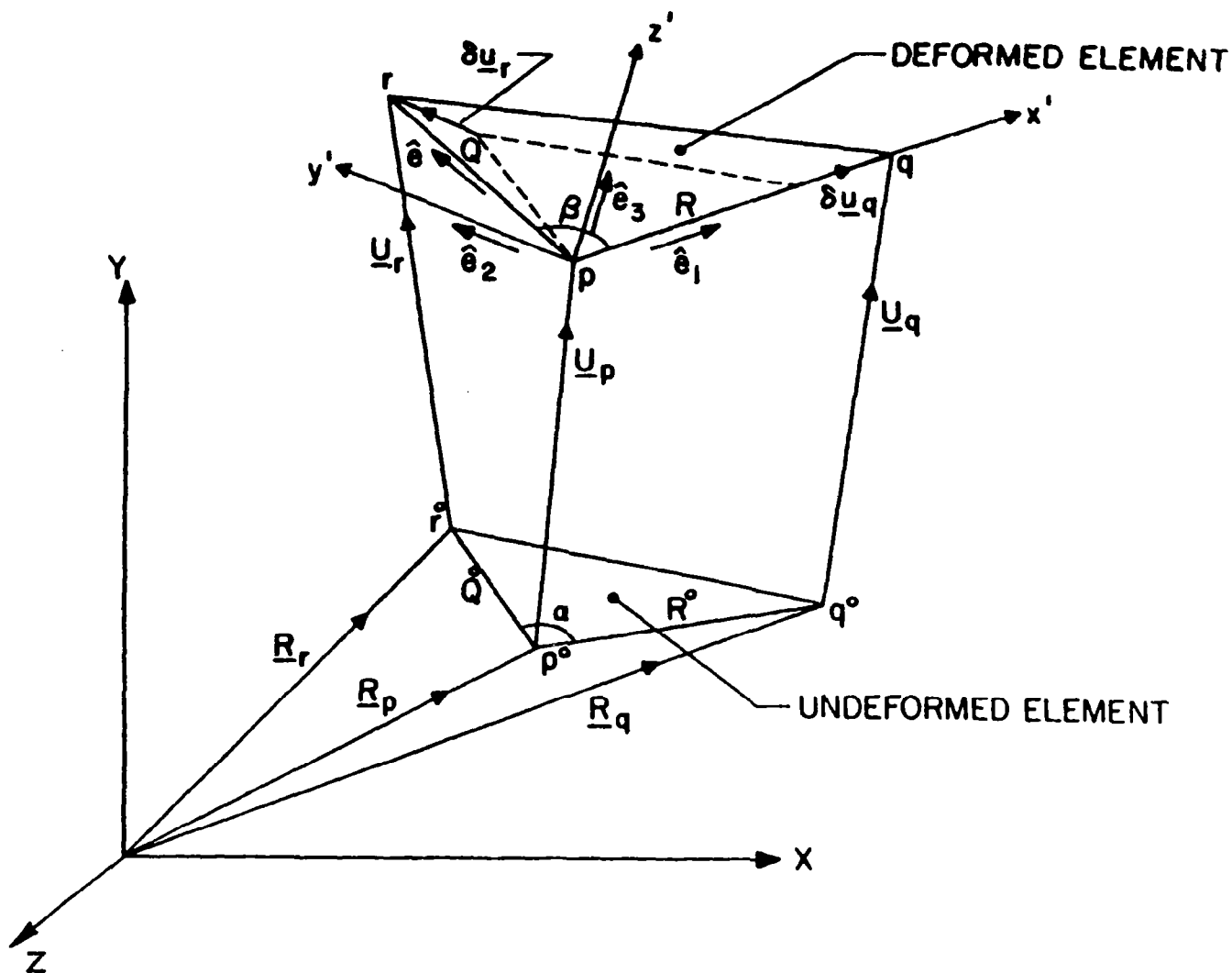


Fig. 3-7 Deformation of the Membrane Element.

with the side pq. The z' -axis is accordingly perpendicular to the plane of the deformed triangle. α and β denote the angles at the vertices p° and p before and after deformation respectively. If U_i , V_i and W_i ($i = p^\circ, q^\circ, r^\circ$) are the displacement components of the i th vertex referenced with respect to the X , Y and Z axes respectively, then the co-ordinates of the vertices, p , q and r with respect to these axes are

$$x_i = X_i + U_i; \quad y_i = Y_i + V_i, \quad z_i = Z_i + W_i \quad (i = p, q, r). \quad (3-48)$$

Unit vectors \hat{e}_1 and \hat{e} along the sides pq and pr are given by

$$\hat{e}_1 = \frac{x_{qp}\hat{i} + y_{qp}\hat{j} + z_{qp}\hat{k}}{\sqrt{x_{qp}^2 + y_{qp}^2 + z_{qp}^2}} = (x_{qp}\hat{i} + y_{qp}\hat{j} + z_{qp}\hat{k})/R \quad (3-49a, c)$$

$$\hat{e} = \frac{x_{rp}\hat{i} + y_{rp}\hat{j} + z_{rp}\hat{k}}{\sqrt{x_{rp}^2 + y_{rp}^2 + z_{rp}^2}} = (x_{rp}\hat{i} + y_{rp}\hat{j} + z_{rp}\hat{k})/Q$$

where

$$x_{ij} = x_i - x_j, \quad y_{ij} = y_i - y_j, \quad z_{ij} = z_i - z_j$$

Accordingly, unit vector \hat{e}_3 normal to the plane of the triangle is

$$\hat{e}_3 = \frac{\hat{e}_1 \times \hat{e}}{\sin\beta} = \frac{[(y_{qp}z_{rp} - y_{rp}z_{qp})\hat{i} + (z_{qp}x_{rp} - z_{rp}x_{qp})\hat{j} + (x_{qp}y_{rp} - x_{rp}y_{qp})\hat{k}]}{D} \quad (3-50a)$$

where

$$D = [(y_{qp}z_{rp} - y_{rp}z_{qp})^2 + (z_{qp}x_{rp} - z_{rp}x_{qp})^2 + (x_{qp}y_{rp} - x_{rp}y_{qp})^2]^{1/2} \quad (3-50b)$$

The unit vector \hat{e}_2 (along the y' -axis) is then given by

$$\begin{aligned} \hat{e}_2 &= \hat{e}_3 \times \hat{e}_1 \\ &= \frac{1}{DR} \begin{bmatrix} \{x_{rp}(y_{qp}^2 + z_{qp}^2) - x_{qp}(y_{qp}y_{rp} + z_{qp}z_{rp})\}\hat{i} \\ + \{y_{rp}(z_{qp}^2 + x_{qp}^2) - y_{qp}(z_{qp}z_{rp} + x_{qp}x_{rp})\}\hat{j} \\ + \{z_{rp}(x_{qp}^2 + y_{qp}^2) - z_{qp}(x_{qp}x_{rp} + y_{qp}y_{rp})\}\hat{k} \end{bmatrix} \end{aligned} \quad (3-51)$$

Equations (3-49) through (3-51) together yield the required transformation matrix between global and local co-ordinate systems, i.e.,

$$\begin{Bmatrix} \hat{e}_1 \\ \hat{e}_2 \\ \hat{e}_3 \end{Bmatrix} = \begin{bmatrix} \lambda_1 & \lambda_2 & \lambda_3 \\ \mu_1 & \mu_2 & \mu_3 \\ \nu_1 & \nu_2 & \nu_3 \end{bmatrix} \begin{Bmatrix} \hat{i} \\ \hat{j} \\ \hat{k} \end{Bmatrix} \quad (3-52a)$$

or

$$\begin{Bmatrix} \hat{i} \\ \hat{j} \\ \hat{k} \end{Bmatrix} = \begin{bmatrix} \lambda_1 & \mu_1 & \nu_1 \\ \lambda_2 & \mu_2 & \nu_2 \\ \lambda_3 & \mu_3 & \nu_3 \end{bmatrix} \begin{Bmatrix} \hat{e}_1 \\ \hat{e}_2 \\ \hat{e}_3 \end{Bmatrix} \quad (3-52b)$$

where

$$\begin{aligned} \lambda_1 &= \frac{x_{qp}}{R}, \quad \lambda_2 = \frac{y_{qp}}{R}, \quad \lambda_3 = \frac{z_{qp}}{R} \\ \mu_1 &= [x_{rp}(y_{qp}^2 + z_{qp}^2) - x_{qp}(y_{qp}y_{rp} + z_{qp}z_{rp})]/DR \\ \mu_2 &= [y_{rp}(z_{qp}^2 + x_{qp}^2) - y_{qp}(z_{qp}z_{rp} + x_{qp}x_{rp})]/DR \\ \mu_3 &= [z_{rp}(x_{qp}^2 + y_{qp}^2) - z_{qp}(x_{qp}x_{rp} + y_{qp}y_{rp})]/DR \\ \nu_1 &= (y_{qp}z_{rp} - y_{rp}z_{qp})/D, \quad \nu_2 = (z_{qp}x_{rp} - z_{rp}x_{qp})/D \\ \text{and } \nu_3 &= (x_{qp}y_{rp} - x_{rp}y_{qp})/D \end{aligned} \quad (3-52c, g)$$

3.3.2 Deformation Mode Shapes, Stresses and Strains

The simplest form of a plane stress triangular element is the constant strain element. The assumed displacement field as a function of the local co-ordinates is

$$\begin{aligned} u &= a_0 + a_1x + a_2y \\ v &= b_0 + b_1x + b_2y \end{aligned} \quad (3-53a, b)$$

The constants in Eq. (3-53) are evaluated from the conditions

$$\begin{aligned}
u(0,0) &= u_p, \quad v(0,0) = v_p \\
u(R^0,0) &= u_q, \quad v(R^0,0) = v_q \\
u(Q^0 \cos \alpha, Q^0 \sin \alpha) &= u_r, \quad v(Q^0 \cos \alpha, Q^0 \sin \alpha) = v_r
\end{aligned} \tag{3-54a,c}$$

Substitution of Eqs. (3-54) into (3-53) yields

$$\begin{aligned}
u &= u_p + \left(\frac{\delta u_q}{R^0}\right)x + \left[\frac{\delta u_r}{Q^0 \sin \alpha} - \frac{\delta u_q}{R^0} \cot \alpha\right]y \\
v &= v_p + \left(\frac{\delta v_q}{R^0}\right)x + \left[\frac{\delta v_r}{Q^0 \sin \alpha} - \frac{\delta v_q}{R^0} \cot \alpha\right]y
\end{aligned} \tag{3-55a,b}$$

where

$$\delta u_q = u_q - u_p, \quad \delta v_q = v_q - v_p \tag{3-55c}$$

$$\delta u_r = u_r - u_p, \quad \delta v_r = v_r - v_p \tag{3-55d}$$

The rigid body motion of the element in the local co-ordinate system is eliminated by setting $u_p = v_p = v_q = 0$. The strains ϵ_{xx} , ϵ_{yy} and γ_{xy} for finite deformations are the components of the Green's strain tensor which for the two dimensional case reduce to:

$$\begin{aligned}
\epsilon_{xx} &= \frac{\partial u}{\partial x} + \frac{1}{2} \left(\frac{\partial u}{\partial x}\right)^2 + \frac{1}{2} \left(\frac{\partial v}{\partial x}\right)^2 \\
&= \left(\frac{\delta u_q}{R^0}\right) + \frac{1}{2} \left(\frac{\delta u_q}{R^0}\right)^2
\end{aligned} \tag{3-56a}$$

$$\begin{aligned}
\epsilon_{yy} &= \frac{\partial v}{\partial y} + \frac{1}{2} \left(\frac{\partial u}{\partial y}\right)^2 + \frac{1}{2} \left(\frac{\partial v}{\partial y}\right)^2 \\
&= \frac{\delta v_r}{Q^0 \sin \alpha} + \frac{1}{2} \left[\frac{\delta u_r}{Q^0 \sin \alpha} - \frac{\delta u_q}{R^0} \cot \alpha\right]^2 + \frac{1}{2} \left(\frac{\delta v_r}{Q^0 \sin \alpha}\right)^2
\end{aligned} \tag{3-56b}$$

$$\begin{aligned}
\gamma_{xy} &= \frac{\partial u}{\partial y} + \frac{\partial v}{\partial x} + \frac{\partial u}{\partial x} \frac{\partial u}{\partial y} + \frac{\partial v}{\partial x} \frac{\partial v}{\partial y} \\
&= \left(\frac{\delta u_r}{Q^0 \sin \alpha} - \frac{\delta u_q}{R^0} \cot \alpha\right) + \left(\frac{\delta u_q}{R^0}\right) \left(\frac{\delta u_r}{Q^0 \sin \alpha} - \frac{\delta u_q}{R^0} \cot \alpha\right)
\end{aligned} \tag{3-56c}$$

From Fig. 3-15 it is evident that

$$\delta u_q = (R - R^0); \delta u_r = (Q \cos \beta - Q^0 \cos \alpha); \delta v_r = (Q \sin \beta - Q^0 \sin \alpha) \quad (3-57)$$

where

$$\cos \alpha = (X_{qp} X_{rp} + Y_{qp} Y_{rp} + Z_{qp} Z_{rp}) / Q^0 R^0 \quad (3-58a)$$

$$\cos \beta = (x_{qp} x_{rp} + y_{qp} y_{rp} + z_{qp} z_{rp}) / QR \quad (3-58b)$$

Equations (3-56) through (3-58) complete the description of the strain field as a function of the relative nodal displacements which in turn are functions of the global displacements. It should be noted that non-linear terms in the strain displacement relations, Eqs. (3-56) imply that the formulation admits arbitrarily large rotations but at best moderately large strains.

3.3.2.1 Stresses and Nodal Forces of the Elastic Membrane Element: The stresses in the constant strain membrane element, assumed to occur at its centroid, are given by

$$\begin{aligned} \sigma_{xx} &= \frac{E}{(1-\nu^2)} (\epsilon_{xx} + \nu \epsilon_{yy}); \quad \sigma_{yy} = \frac{E}{(1-\nu^2)} (\epsilon_{yy} + \nu \epsilon_{xx}); \\ \tau_{xy} &= \frac{E}{2(1+\nu)} \gamma_{xy} \end{aligned} \quad (3-59)$$

The corresponding nodal loads in local co-ordinates can then be obtained by the relations [20]

$$\begin{aligned} Q_{px} &= -\frac{h}{2} \left\{ [\sigma_{xx} (1 + \frac{\delta u_q}{R^0}) + \tau_{xy} (\frac{\delta u_r}{Q^0 \sin \alpha} - \frac{\delta u_q}{R^0} \cot \alpha)] Q^0 \sin \alpha + \tau_{xy} (1 + \frac{\delta u_q}{R^0}) (Q^0 \cos \alpha - R^0) \right\} \\ Q_{py} &= \frac{h}{2} \left\{ [\sigma_{yy} (1 + \frac{\delta v_r}{Q^0 \sin \alpha})] (Q^0 \cos \alpha - R^0) - \tau_{xy} (1 + \frac{\delta v_r}{Q^0 \sin \alpha}) Q^0 \sin \alpha \right\} \\ Q_{qx} &= \frac{h}{2} \left\{ [\sigma_{xx} (1 + \frac{\delta u_q}{R^0}) + \tau_{xy} (\frac{\delta u_r}{Q^0 \sin \alpha} - \frac{\delta u_q}{R^0} \cot \alpha)] Q^0 \sin \alpha - \tau_{xy} (1 + \frac{\delta u_q}{R^0}) Q^0 \cos \alpha \right\} \\ Q_{qy} &= \frac{h}{2} \left\{ [\sigma_{yy} (1 + \frac{\delta v_r}{Q^0 \sin \alpha})] Q^0 \cos \alpha + \tau_{xy} (1 + \frac{\delta v_r}{Q^0 \sin \alpha}) Q^0 \sin \alpha \right\} \\ Q_{rx} &= \frac{h}{2} \tau_{xy} (1 + \frac{\delta u_q}{R^0}) R^0; \quad Q_{ry} = \frac{h}{2} \sigma_{yy} (1 + \frac{\delta v_r}{Q^0 \sin \alpha}) R^0 \end{aligned} \quad (3-60)$$

Section 4

MATERIAL MODEL

4.1 Basic Assumptions

This section provides the theoretical basis along with its underlying assumptions for the material behavior in the inelastic range. By material behavior, we imply the prediction of the stress state and the strain energy density at a point in a material for a known strain state. Two theories are available for describing the material behavior in the inelastic range: (i) the deformation or total-strain theory and (ii) the flow or incremental strain theory. The difference between the two theories lies in the fact that the deformations predicted for the volume element by the former theory are independent of the loading path while those predicted by the latter theory are path dependent. Furthermore, the deformation or total strain theory postulates the existence of a strain energy density function in terms of total strains while the flow or incremental theory postulates the existence of an incremental strain energy density function in terms of the incremental strains. Incremental strain theory has the advantage that it describes more fully the behavior of a volume element but it has the disadvantage that the theory requires time consuming numerical analysis. The total strain theory on the other hand has the advantage of mathematical simplicity but does not conform to physical reality for some problems [21]. Because of its mathematical simplicity ACTION uses the deformation or total-strain theory. It is believed, however, that even at the expense of the complexity of the material model there may be a slight computational advantage, in terms of the performance of the solution algorithm, to be

gained by the use of the incremental strain theory [22].

Both the total strain and the incremental flow theories assume that the total strain or the strain increment, as the case may be, can be decomposed additively into an elastic and a plastic component. Lee [23] has shown that such a decomposition is in general not valid for large strains but may be justified if the plastic strains are predominant. Incidentally, Hencky's total strain theory assumes that in the strain hardening range the inelastic component of the total strain is predominant. Thus, in view of [23], of the two theories Hencky's total strain theory would appear to be more consistent for cases wherein the strains are large.

Hencky's theory [21] embodies three hypotheses: (i) the principal axes of stress and strain coincide; (ii) Mohr's circle diagram of stress and strain are similar at any stage in the inelastic deformation; and (iii) volume changes are elastic i.e., the inelastic deformations are incompressible or that $v_p = \frac{1}{2}$. These hypotheses lead to the following relation

$$\frac{\epsilon_{xx} - \epsilon_{yy}}{\sigma_{xx} - \sigma_{yy}} = \frac{\gamma_{xy}}{2\tau_{xy}} = \text{constant} \quad (4-1)$$

Furthermore, Hencky's total strain theory assumes that the strain energy density, W , is a function of the effective strain, $\bar{\epsilon}$, defined as

$$\bar{\epsilon} = \begin{cases} \frac{2}{\sqrt{3}} (\epsilon_{xx}^2 + \epsilon_{yy}^2 + \epsilon_{xx}\epsilon_{yy} + \frac{1}{2}\gamma_{xy}^2)^{1/2} & \text{for a two dimensional stress state} \\ \epsilon_{xx} & \text{for a uniaxial stress state} \end{cases} \quad (4-2)$$

such that

$$\frac{dW}{d\bar{\epsilon}} = \bar{\sigma} = \begin{cases} (\sigma_{xx}^2 + \sigma_{yy}^2 - \sigma_{xx}\sigma_{yy} + 3\tau_{xy}^2)^{1/2} & \text{for a two dimensional stress state} \\ \sigma_{xx} & \text{for a uniaxial stress state.} \end{cases} \quad (4-3)$$

The stress strain relations

$$\frac{\partial W}{\partial \epsilon_{xx}} = \sigma_{xx}, \quad \frac{\partial W}{\partial \epsilon_{yy}} = \sigma_{yy} \quad \text{and} \quad \frac{\partial W}{\partial \gamma_{xy}} = 2\tau_{xy} \quad (4-4)$$

obtained from Eq. (4-2) satisfy Eq. (4-1).

Equations (4-2) and (4-3) imply the use of Hencky's total strain theory along with its assumption that in the strain hardening range the inelastic component of the total strain is predominant [21]. This in a way is consistent with the assumption that the total strain can be decomposed into an elastic and a plastic part especially in cases where the strains are large [23]. According to reference [23] it is only when the plastic strains are predominant that such a decomposition is justified. Thus, the present formulation appears to be consistent in the strain-hardening range.

Next, Von Mises criterion is used to predict yielding. According to this criterion yielding is assumed to occur when the effective stress, $\bar{\sigma}$, which incidently is also the second invariant of the stress tensor or equivalently the octahedral shear stress, reaches the value $\bar{\sigma}_y$, the yield point of a uniaxial tension test.

4.2 Modeling of stress-strain curve and the treatment of stress-strain history [15]

The stress-strain curve of the material under uniaxial tension and compression is used as the effective stress-effective strain curve. This curve is modeled by eight straight line segments as shown in Fig. 4-1. Four of the eight segments describe the tensile side of the curve and the remaining four describe the compressive side. The left and right hand ends of the curve represent material failure. The sign of the quantity $(\epsilon_{xx} + \epsilon_{yy})$ i.e., the sign of the first invariant of the strain tensor is

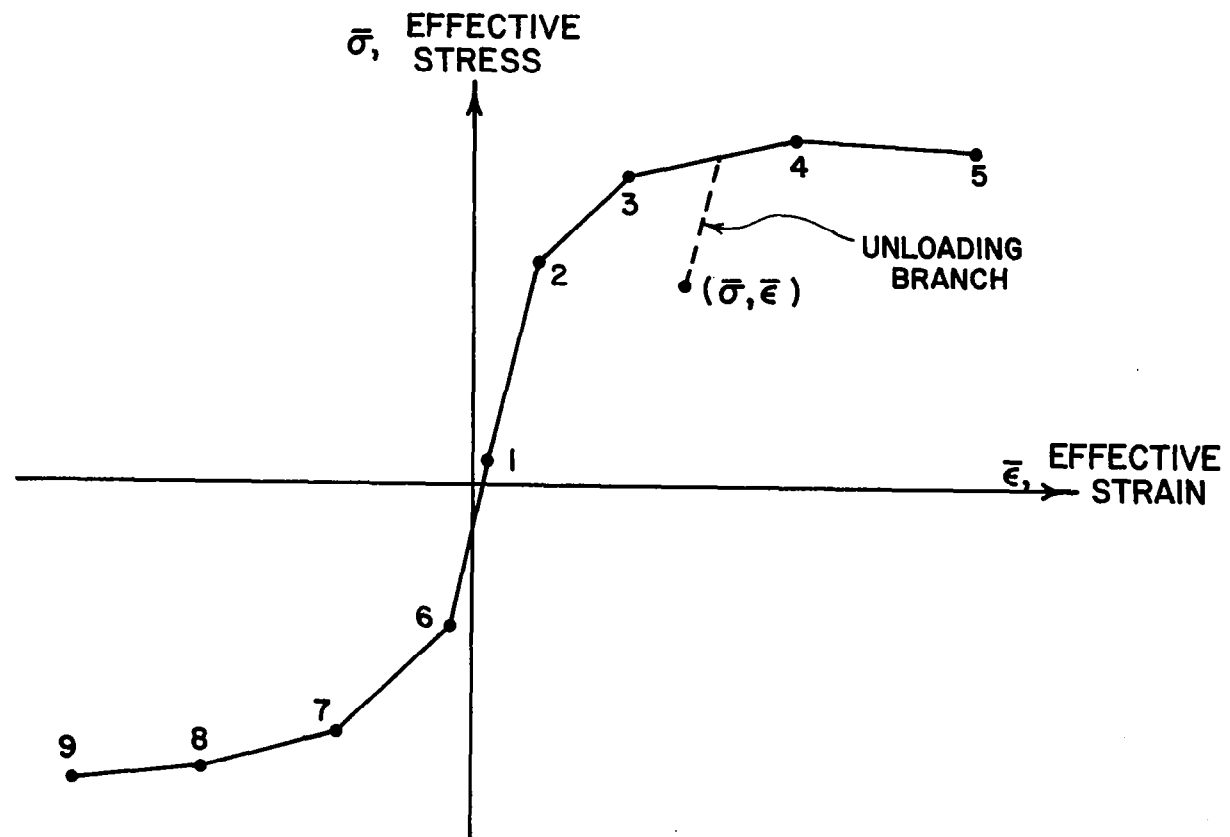


Fig. 4-1 Representation of the Stress-Strain Curve.

used for the selection of the tensile or the compressive branch of the curve. It is assumed, however, that the material has the same modulus in tension and compression. The model permits situations involving initial stress and strain. It is required that all points on the curve be uniquely determined by the strain parameter and certain indeterminate conditions requiring special treatment are not considered.

From an unloaded state the loading for cyclic increasing or decreasing strain follows the initial linear elastic portion of the curve as long as the effective stress does not exceed the stresses corresponding to tensile and compressive yield points. For increasing effective strain beyond the yield points, the loading follows the effective stress-strain curve with yielding occurring as described in the previous section. Once into the plastic region, when the effective strain starts to decrease, unloading occurs. Unloading in the plastic region is assumed to be elastic with the load path described by the shape of the initial elastic portion of the curve. Points 'b' and 'd' in Fig. 4-2 denote the new tensile and compressive yield points. Loading for additional decreasing and increasing strain follows the new elastic curve as long as the effective stress does not once again exceed the stresses corresponding to the new yield points. For straining beyond the new yield points, the subsequent loading and unloading is treated as described earlier except that the portion of the stress-strain curve between points 'b₀', 'd₀' in Fig. 4-2 is for all practical purposes forever lost from the "memory" of the material. This type of stress-strain behavior gives a larger tensile yield stress and a smaller compressive yield stress as a result of plastic deformation in tension. The converse is true for plas-

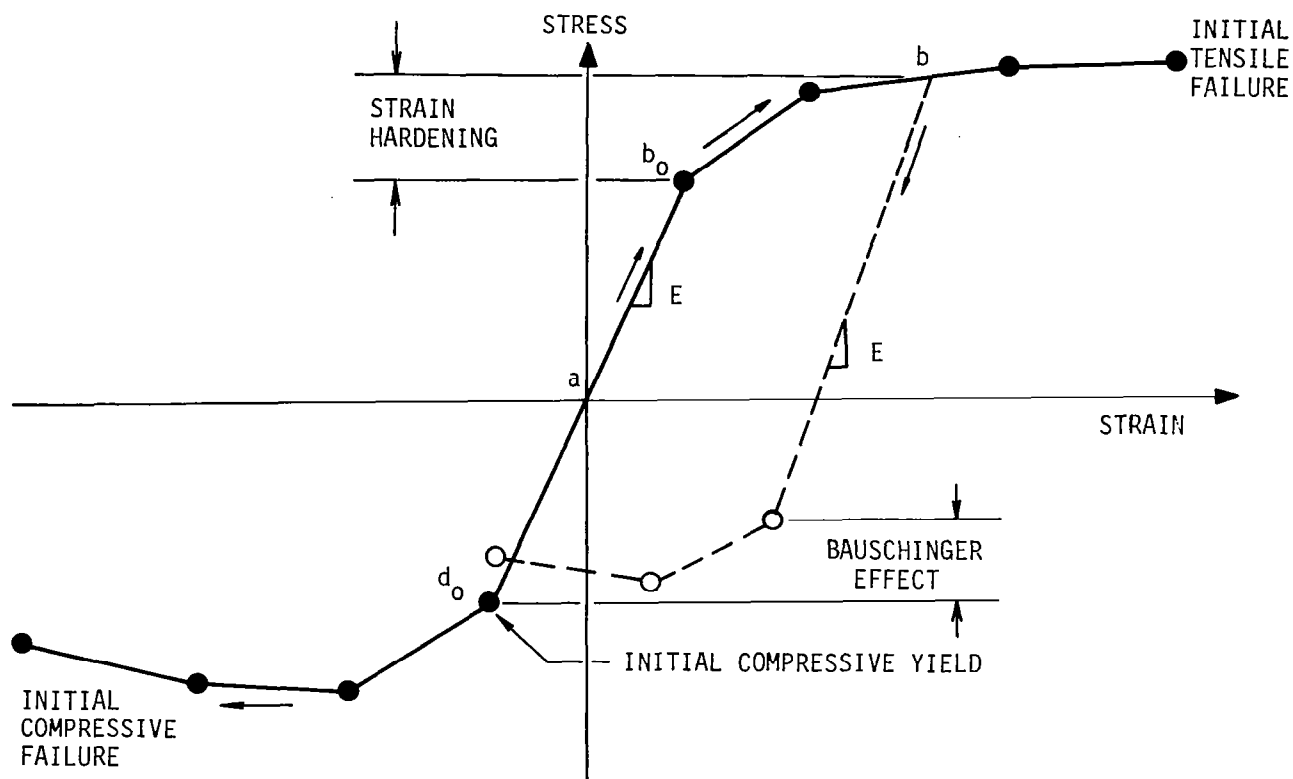


Fig. 4-2 Typical Stress-Strain Curve.

tic deformation in compression. These changes to the stress-strain curve are the strain-hardening and Bauschinger effects.

Recall that the transient response is based on a stepwise integration in time. Each time step corresponds to a loading or an unloading increment on the stress-strain curve. Let $\bar{\sigma}_0, \bar{\epsilon}_0$ correspond to a previous time point and $\bar{\sigma}_1, \bar{\epsilon}_1$ represent the state at the current time point. If $\bar{\epsilon}_1$ is greater than $\bar{\epsilon}_0$, it is assumed that the material "loads up" only. Likewise if $\bar{\epsilon}_1$ is less than $\bar{\epsilon}_0$, it is assumed that the material loads down only. This is illustrated in Fig. 4-3. It must be recognized that for any given loading two or more solutions all of which satisfy equilibrium are possible but all these solutions correspond to different strain histories. Hence, for $\bar{\epsilon}_1$ greater than $\bar{\epsilon}_0$ the only possible solution is the one corresponding to the point 'a'. The solution corresponding to the point 'c' satisfies the constitutive relation but violates equilibrium for a member loading up. The point 'c' is a possible solution for $\bar{\epsilon}_1$ greater than $\bar{\epsilon}_0$ if and only if the member is first loaded up to the point 'b' and loaded down from this point to the point 'c'. Such two step loading processes are not admitted in the formulation.

4.3 Evaluation of Dissipative Strain Energy Density

For the elastic-plastic response the strain energy density is decomposed into an elastic part and an incremental dissipative part. Thus, if 'a₀' in Fig. 4-4 denotes the state at some previous time t_0 and if 'a' denotes the state at time $(t_0 + \Delta t)$ then the incremental dissipative strain energy density ΔW_d and the elastic strain energy density W_e are, by assumptions, the appropriate areas under the idealized effective stress-effective strain curve as shown in Fig. 4-4.

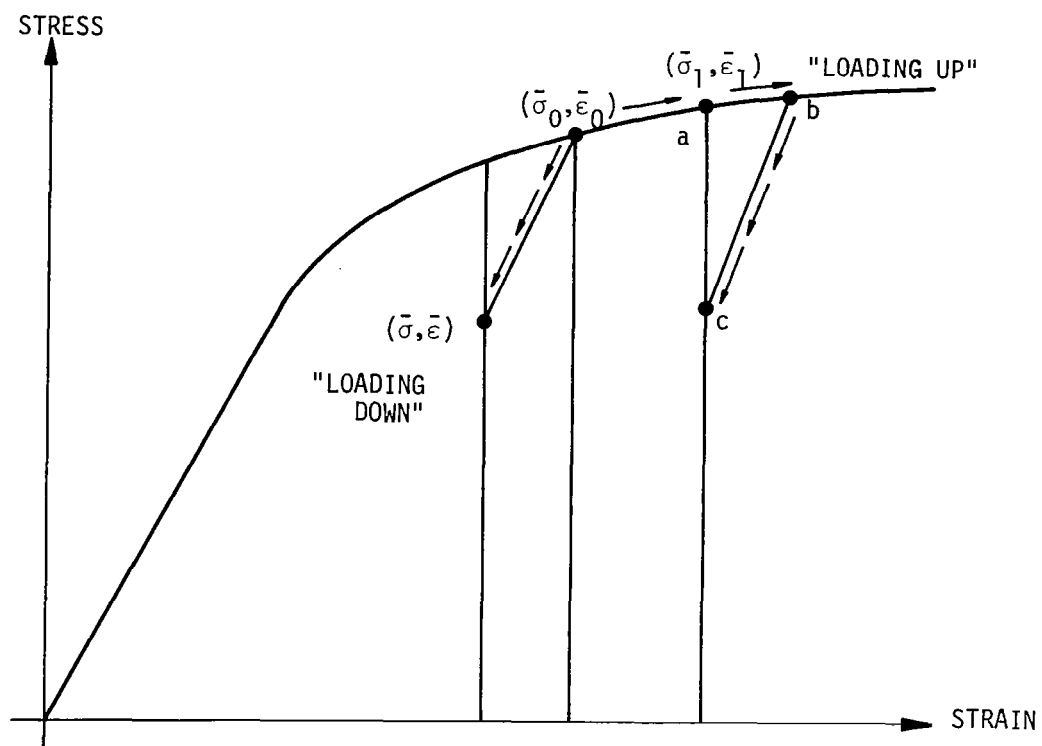


Fig. 4-3 Loading and Unloading Paths.



Fig. 4-4 Evaluation of Strain Energy Densities.

For the truss element ϵ_x is the only strain prescribed and the corresponding stress σ_x is assumed constant over the length of the element. For the frame element, however, stresses vary throughout the volume of the element. Certain number of Lobatto quadrature or reference points are used to describe the stress distribution throughout the element. At each of these points, the material model is used to determine the stress and the strain energy density ($W_e + \Delta W_d$). In the interest of simplicity, it is assumed that the shear stress-strain behavior is adequately described by linear elastic response. This implies that the plastic action is adequately described by the effects of normal stresses and strains alone. This approximation should be appropriate for elements wherein plastic axial or bending actions predominate. In the case of a membrane element all the three stress components are by assumption, constant throughout the element and hence as in the case of the truss element the stresses and the strain energy density need be evaluated at a single point.

The above ingredients comprise the treatment of loading and unloading in the plastic regions with strain-hardening and Bauschinger effects. Although, the model used here is typical of most material behavior it is relatively simple and not all material behavior will fit this model. Caution should particularly be exercised when this simplified material model is used in conjunction with membrane elements (two-dimensional stress states) undergoing cyclic loading.

Section 5

KINEMATIC CONSTRAINTS

Practical modeling considerations demand that equations of motion be augmented by constraint equations. This section describes constraint models in ACTION which facilitate representing a rigid tie between joints and an impenetrable contact plane.

5.1 Rigid Link Element

A "rigid link" is a finite element which does not deform appreciably. As the nodes in the structure undergo displacements, the rigid element merely translates and rotates without any appreciable deformations. Such a link can be used as a connector between two members meeting at a joint whose ends do not coincide thereby simulating eccentrically connected members. Rigid links may also be employed advantageously when entire sections of the structure undergo very little deformation. During these periods the sections can be treated as assemblages of rigid links to greatly reduce the number of unknown displacements and thereby reduce the computing time. The nodes of a rigid link are located with reference to a global co-ordinate system and they are identified as belonging to the same rigid link by input specification to ACTION. Points in each rigid link are referenced by a local co-ordinate system originating at the primary node of the link. The local co-ordinate system translates and rotates with the primary node as deformation takes place.

Since there is no relative displacement due to deformation in the rigid link, the right hand side of Equation (3-15) set equal to zero will provide the relationships necessary to describe the motion of the q-end or secondary node of the link in terms of the translation components and rotation components of the p-end or primary node of the link.

Solving this equation for the global displacement vector of the secondary node of the link yields

$$\{U\}_q = \{U\}_p + [T_3]_p^T \{L\} + \{R\}_p - \{R\}_q \quad (5-1)$$

This equation is invoked whenever the displacement components of the nodes are updated.

The equation is implemented by searching the list of elements for those designated as rigid links. When one is found, the displacement components of the secondary nodes are replaced by those calculated by Equation (5-1). Furthermore, given the translation and rotation components of the velocities and accelerations of the primary node, the motion of a secondary node is determined using simple rigid body kinematics. Finally, knowing the kinematics of the secondary nodes the contribution to the total potential energy, of inertia forces and loads applied directly to such secondary nodes, can be determined.

5.2 Impenetrable Contact Plane (Terrain Model)

The ACTION code includes a model of an impenetrable terrain to simulate a ground plane. The ground plane is assumed to be rigid and flat i.e., like a concrete runway. Penetration of the ground is not allowed. Resistance to forward motion along the ground plane is provided by coulomb friction. Impact with the plane is represented as a plastic collision.

The paragraphs that follow explain the ground plane model in ACTION.

5.2.1 Node Capture and Release

The model detects when the nodes of the aircraft model contact the ground plane. Once contact has been made these nodes are constrained to remain on the ground plane until they are pulled off by the release

of internal energy stored within the aircraft model. Thus a node of the aircraft model does not bounce off the ground plane due to the effect of the coefficient of restitution, but is pulled off when tension would otherwise be implied between the structure and the impenetrable plane.

Nodal displacements are obtained by solving the equations of motion for a particular time step. The current position of each node is then determined relative to the ground plane. If a node penetrates the ground plane, the time step is reduced and integration of the equations of motion is repeated. When a node penetrates the ground plane using the minimum time step, a check is made to see if its previous position above the ground plane was closer to the ground plane than its current position which is beneath the ground plane. (The likelihood of a node falling exactly on the ground plane at the end of a time step is remote.) If the node's previous position was closer to the ground plane, integration is backed up to the beginning of the current time step and a flag is set to signify contact between the node and the ground plane. If the node's position at the end of the current time step is closer to the ground plane, this position is used to mark the ground plane and a similar flag is set. Thus a node is considered to lie on the ground plane when it is as close to the ground plane as permitted by the minimum integration time step. (In terms of the logic of the code, the ground plane moves up or down to coincide with the position of the node.)

Once contact has been made between a node and the ground plane, it must be determined whether or not the node is to be constrained to remain on the ground plane during the next integration time step. This requires calculation of the total vertical resultant force acting on the structural model of the aircraft at the captured node. This force, which

is normal to the ground plane and positive upward, is the derivative of the strain energy function with respect to a displacement of the node in the direction of the outward normal to the ground plane. A positive normal force means the structural model is in compression in the vicinity of the captured node. In this case the vertical degree of freedom of the node is constrained for the next time step, but the node is still free to move horizontally along the ground plane. The vertical degree of freedom is constrained in the sense that the vertical displacement of the node corresponding to its current position on the ground plane is fixed for the next time step. A negative normal force means the structural model is in tension at the captured node. Then the vertical velocity, acceleration and all the higher order time derivatives of displacement of the node implied in the temporal algorithm are set equal to zero. The free equations of motion provide the basis for predicting subsequent behavior of the node until it is recaptured.

Due to the discretization of time it is assumed that the best approximation to the point in time when a negative normal force is found is based on the minimum integration time step. Thus if a negative normal force is discovered at the end of a non-minimum time step, the time step is reduced and the integration is repeated.

A coulomb friction force is applied to each node captured by the plane. The force is applied in the direction opposite to that of the horizontal velocity components of the captured node. The magnitude of the force is equal to the coefficient of friction input by the user times the positive resultant nodal force normal to the ground plane.

Section 6

ANALYSIS BY ENERGY MINIMIZATION

6.1 Background Information

It was indicated in Section 2 that two distinct solution approaches exist: (i) the vector approach and (ii) the scalar approach. In the former approach, the mathematical model is derived on the basis of the principle of virtual work and reduced to a system of non-linear second-order differential equations in time. In the latter approach, a scalar or a potential function associated with the energy of the model is introduced, minimization of which yields the desired equilibrium configuration. In both approaches a temporal finite difference scheme is utilized to effectively eliminate time as a variable. As a result, in the vector approach the equations of motion are reduced to a system of nonlinear algebraic equations in the unknown nodal parameters of the finite element model. In the scalar approach which is of relevance to this report the problem is reduced to a well known problem in mathematical programming namely the unconstrained minimization of a nonlinear function of several variables.

For all structural problems with geometric and material nonlinearities of the type considered herein the required potential function always exists. Although, this technique has been hitherto used for mainly positive or negative definite systems, other systems which fail to be positive or negative definite can be handled by using the least squares method or the modified conjugate gradient method with preconditioning [24]. In some cases, for such systems displacement incrementation rather than load incrementation in conjunction with conventional unconstrained minimization techniques can also be effective [25].

6.2 Solution Basis

The minimization scheme as applied to the solution of transient nonlinear structural analysis problems consists of minimizing a potential function associated with the system for an assumed relationship between displacements and time. The displacement-time relation for each generalized nodal displacement of a finite element model is assumed to be of the form [26]

$$q_{ei} = \beta(\Delta t)^2 \ddot{q}_{ei} + \left(\frac{1}{2} - \beta\right)(\Delta t)^2 \ddot{q}_{0i} + (\Delta t) \dot{q}_{0i} + q_{0i} \quad (6-1a)$$

$$\dot{q}_{ei} = \gamma(\Delta t) \ddot{q}_{ei} + (1-\gamma)(\Delta t) \ddot{q}_{0i} + \dot{q}_{0i} \quad (6-1b)$$

where q_{ei} is the i -th generalized nodal displacement at the end of the time step and β and γ are constants. The quantities \dot{q}_{ei} and \ddot{q}_{ei} can now be expressed in terms of the i -th generalized nodal displacement, q_{0i} , velocity, \dot{q}_{0i} and acceleration, \ddot{q}_{0i} at the beginning of the time step and the generalized nodal displacement, q_{ei} , at the end of the time step. Thus,

$$\dot{q}_{ei} = \dot{q}_{0i} + \ddot{q}_{0i}(\Delta t) + \frac{\gamma}{\beta} \frac{1}{(\Delta t)} \{ (q_{ei} - q_{0i}) - (\Delta t) \dot{q}_{0i} - \frac{(\Delta t)^2}{2} \ddot{q}_{0i} \} \quad (6-2a)$$

$$\ddot{q}_{ei} = \ddot{q}_{0i} + \frac{1}{\beta(\Delta t)^2} \{ (q_{ei} - q_{0i}) - (\Delta t) \dot{q}_{0i} - \frac{(\Delta t)^2}{2} \ddot{q}_{0i} \} \quad (6-2b)$$

The equations of equilibrium

$$M_i \ddot{q}_{ei} - F_i + \frac{\partial U}{\partial q_{ei}} = 0, \quad i = 1, 2, \dots, N \quad (6-3)$$

for an N degree-of-freedom system with lumped masses can then be written as

$$M_i \left[\ddot{q}_{0i} + \frac{1}{\beta(\Delta t)^2} \{ (q_{ei} - q_{0i}) - (\Delta t) \dot{q}_{0i} - \frac{(\Delta t)^2}{2} \ddot{q}_{0i} \} \right] - F_i + \frac{\partial U}{\partial q_{ei}} = 0, \quad i = 1, 2, \dots, N \quad (6-3a)$$

It can be easily verified that Eqs. (6-3a) correspond to the necessary

conditions for the functional

$$S = \sum_{i=1}^N \left\{ \left[\frac{1}{2\beta(\Delta t)^2} q_{ei}^2 - \left(\frac{1}{\beta(\Delta t)^2} q_{0i} + \frac{1}{\beta(\Delta t)} \dot{q}_{0i} + \left(\frac{1}{2\beta} - 1 \right) \ddot{q}_{0i} \right) q_{ei} \right] M_i - F_i \right\}_{(t+\Delta t)} q_{ei} \} + U + C \quad (6-4)$$

to be stationary. In Eq. (6-4), U is the strain energy and C is an arbitrary constant. Thus, knowing q_{0i} , \dot{q}_{0i} and \ddot{q}_{0i} at time t for any given load F_i at time $(t+\Delta t)$, the functional S may be minimized with respect to the generalized nodal displacements, q_{ei} ($i=1, \dots, N$), in order to determine the corresponding stable equilibrium configuration. Although, the coefficient of M_i in Eq. (6-4) is quadratic in q_{ei} , the strain energy, U , will in general be a nonlinear function (at the very least a quadratic for a linear problem) of the generalized nodal displacements q_{ei} (see Section 3). Thus, in general the functional S is highly nonlinear. Since, U is a positive semi-definite function for most structural materials, the functional S can be seen to be convex.

6.3 Minimization Algorithms

Of all the algorithms for unconstrained minimization only the quasi-Newton or the variable metric algorithms have been more frequently used for such nonlinear problems, because of their higher effectiveness [27]. Again, unless there exists an algorithm which exploits and maintains sparsity of the Hessian approximation during its passage to the minimum, one has to resort to some form of a first order conjugate gradient algorithm for problems wherein N is an extremely large number.

Beginning with an arbitrary initial guess, these algorithms seek a direction of travel and the amount of travel in that direction. The manner in which these are sought depends upon the sophistication of

the particular algorithm invoked. Most often the directions of travel are sought in a manner which guarantees not only a decrease in the value of the function but also convergence to the minimum in a finite number of iterations (usually $N+1$ for an N dimensional space) in the case of quadratic functionals. It is important to note that all functionals in question are very nearly quadratic in the neighborhood of the minimum.

6.3.1 BFGS Variable Metric Algorithm

The present formulation uses the well-known BFGS (Broyden-Fletcher-Goldfarb-Shanno) variable metric algorithm [28] which is supposedly the best current variable metric update formula for use in unconstrained minimization. This algorithm dispenses with the exact line searches while using an update formula which, in the case of a quadratic functional, guarantees a monotonic convergence of the eigenvalues of the approximating matrix to the inverse Hessian. The iterative scheme which is begun with the null vector as the initial guess is defined by

$$\{q\}^{(k+1)} = \{q\}^{(k)} - \alpha^{(k)} [H]^{(k)} \{g\}^{(k)} \quad (6-5a)$$

where

$$\{g\}^{(k)} = \nabla S(q^{(k)}) = \text{gradient of } S \text{ at } q^{(k)}$$

$[H]^{(k)}$ is a matrix which is designed to approximate in some sense the inverse Hessian matrix of S at $\{q\}^{(k)}$ and $\alpha^{(k)}$ is an appropriately chosen scalar. The BFGS update formula is given by

$$[H]^{(k+1)} = ([I] - \frac{1}{\beta} [P])[H]^{(k)} ([I] - \frac{1}{\beta} [P]) + \{\sigma\}\{\sigma\}^T / \beta \quad (6-5b)$$

where

$$[P] = \{\sigma\}\{y\}^T \quad (6-5c)$$

$$\beta = \{\sigma\}^T \{y\} \quad (6-5d)$$

$$\{\sigma\} = \{q\}^{(k+1)} - \{q\}^{(k)} \quad (6-5e)$$

$$\{y\} = \{g\}^{(k+1)} - \{g\}^{(k)} \quad (6-5f)$$

The $\alpha^{(k)}$ in Eq. (6-5a) is chosen either by a linear search or by a step length but so as to maintain the positive definiteness of the matrix [H]. The details of the step length calculation may be found in reference [29] or reference [30].

The iterative scheme is begun with an initial guess which for the first time step is usually the null vector for {q}, the unknown generalized nodal displacements and the identity matrix for [H], the approximation to the inverse hessian. From thereon these quantities at the end of the previous time or load step are used as initial guesses for the next step and it is this reasonably good approximation to the inverse Hessian that is instrumental in giving the second order methods a significant advantage over the first order methods like the conjugate gradient techniques. The required gradient of S is evaluated analytically although doing so by a finite differencing scheme is also possible. The use of an analytic gradient however, results in a substantial saving in the computational effort. This saving is the result of not only a cheaper gradient evaluation but most often a faster convergence of the solution because of higher accuracy of all the computed quantities [27]. The i-th component of the gradient of S can be written as

$$\frac{\partial S}{\partial q_{ei}} = M_i \ddot{q}_{ei} - F_i + \frac{\partial U}{\partial q_{ei}} \quad (6-6)$$

The term in Eq. (6-6) requiring significant computational effort is $\frac{\partial U}{\partial q_{ei}}$ as it embraces the geometric and material nonlinearities. Thus,

$$\frac{\partial U}{\partial q_{ei}} = \sum_{k=1}^m \int_{V_k} \frac{\partial W}{\partial q_{ei}} dv_k = \sum_{k=1}^m \int_{V_k} \left(\frac{dW}{d\bar{\epsilon}} \right)_k \left(\frac{\partial \bar{\epsilon}}{\partial q_{ei}} \right)_k dv_k \quad (6-7)$$

where

W = strain energy density; $\bar{\epsilon}$ and $\bar{\sigma}$ the effective strain and stress effectively as defined in Eqs. (4-2) and (4-3).

6.3.2 Powell's Conjugate Gradient Algorithm

The algorithm [33] is designed to improve the linear convergence rate of the Fletcher-Reeves' conjugate gradient algorithm [34] by using a restart whose frequency is not the usual n or $(n+1)$ iterations but rather one which is dependent on the objective function. Thus the basic algorithm may be stated as follows.

Given $\{q\}$, the initial direction of travel $\{d\}$, is defined to be the steepest descent direction $-\{g\}_1 = -\{\nabla S\}_1$. For $k \geq 2$

$$\{q\}_{k+1} = \{q\}_k + \lambda_k \{d\}_k \quad (6-8a)$$

$$\{d\}_k = -\{g\}_k + \beta_k \{d\}_{k-1} + \gamma_k \{d\}_t \quad (6-8b)$$

$$\beta_k = \{g\}_k^T [\{g\}_k - \{g\}_{k-1}] / \{d\}_{k-1}^T [\{g\}_k - \{g\}_{k-1}] \quad (6-8c)$$

$$\gamma_k = \{g\}_k^T [\{g\}_{t+1} - \{g\}_t] / \{d\}_t^T [\{g\}_{t+1} - \{g\}_t] \quad (6-8d)$$

where t is initially set equal to one and for $k \geq 2$ t is set equal to $k-1$ if

$$|\{g\}_{k-1}^T \{g\}_k| \geq 0.2 ||\{g\}_k||^2. \quad (6-8e)$$

λ_k in Eq. (6-8a) is determined by a line search which yields not only a decrease in the directional derivative but also requires the angle between $\{g\}_{k+1}$ and $\{d\}_k$ to be close to ninety degrees. Next, if the inequalities

$$-1.2 ||\{g\}_k||^2 \leq \{d\}_k^T \{g\}_k \leq -0.8 ||\{g\}_k||^2 \quad (6-8f)$$

are not satisfied then $\{d\}_k$ is assumed to be not sufficiently downhill and the procedure is restarted by letting $t = k-1$ and redefining $\{d\}_k$ by letting γ_k in Eq. (6-8a) to be zero. The procedure is also restarted if $(k-t) \geq n$ by setting $t = k-1$ and assuming γ_k in Eq. (6-8a)

to be zero when $k = t+1$. For additional details of this algorithm along with its fortran listing the interested reader should refer to reference [35] which also provides a listing of the subroutine for the BFGS variable metric algorithm of the previous section.

The storage requirements of this algorithm exceeds those of Fletcher-Reeves' only slightly but they are certainly very small by comparison with those of the variable metric algorithms. Thus, this algorithm is intended for extremely large scale problems of the order of thousand degrees of freedom or above. However, the performance of this algorithm for the solution of such large scale problems of relevance to this report remains to be investigated.

6.4 Evaluation of the Function S and its Gradient

The function S and its gradient must be expressed explicitly or implicitly as a function of the global generalized nodal displacements of the finite element model.

6.4.1 Function Evaluation

From a known vector of the generalized nodal variables in the global co-ordinate system, consistent with the prescribed boundary conditions, a vector of local generalized variables in the co-rotational co-ordinate system of each element is established through transformations which are functions of its geometry and its rigid body rotations (see Section 3). The assumption of deformation patterns of the element as functions of these local generalized nodal variables (interpolating polynomials) yields element strains. Recourse to the element material model then yields the corresponding stresses and strain energy densities at various predetermined quadrature points over the extent of the element. Barring

purely elastic response, a simple weighted summation of these quantities over the element volume yields stress resultants and strain energies respectively. For purely elastic response these are provided by well-known closed form expressions which can be generated as follows based on the results of Section 3.

6.4.1.1 Strain Energy Evaluation for Elastic Response

The total strain energy U may be expressed as

$$U = \sum_{k=1}^m U_k \quad (6-9)$$

where for purely elastic response a closed form expression for U_k , the strain energy of the k -th element, can be obtained from the usual definition of the strain energy and the use of the results of Section 3. Outlined below are such expressions for the truss, the frame and the membrane elements.

6.4.1.1.1 Truss Element

The strain energy of the k -th truss element is given by

$$U_k = \frac{1}{2} \int_V \sigma_x \epsilon_x dv = \frac{E}{2} \int_V \epsilon_x^2 dv$$

which from Eq. (3-5) can be written as

$$U_k = \frac{EAL}{2} \left(\frac{DL}{L} \right)^2 \quad (6-10)$$

wherein E , A and L pertain to the k -th stringer element.

6.4.1.1.2 Frame Element

The total strain energy of deformations of finite element due to bending, tension and shear is given by

$$U_k = U_{kb} + U_{kt} + U_{ks} \quad (6-11)$$

where

$$u_{kb} = \frac{E}{2} \int_V \epsilon_x^2 dv$$

which from Eqs. (3-24), (3-25) and (3-32) reduces to

$$\begin{aligned} = & \frac{EL}{2} [K^2 A + \frac{12}{L^2} \{I_z [(\frac{\delta v_b}{L})^2 - (\frac{\delta v_b}{L})\psi_z + \frac{1}{3}\psi_z^2 + 2I_{yz} [(\frac{\delta v_b}{L})(\frac{\delta w_b}{L}) \\ & + \frac{1}{2}(\frac{\delta v_b}{L}\psi_y - \frac{\delta w_b}{L}\psi_z) - \frac{1}{3}\psi_y\psi_z] + I_y [(\frac{\delta w_b}{L})^2 + (\frac{\delta w_b}{L})\psi_y \\ & + \frac{1}{3}\psi_y^2]\}] \end{aligned} \quad (6-12)$$

$$u_{kt} = \frac{1}{2} \int_0^L T \frac{d\beta}{dx} dx$$

which from Eq. (3-33) reduces to

$$u_{kt} = \frac{GJ}{2L} \psi_x^2 \quad (6-13a)$$

and

$$u_{ks} = \frac{1}{2} \int_0^L (v_y \gamma_{sxy} + v_z \gamma_{sxz}) dx \quad (6-13b)$$

which from Eqs. (3-27), (3-28), (3-29) reduces to

$$u_{ks} = \frac{GAL}{2} \left[\frac{1}{k_y} \left(\frac{\delta v_s}{L} \right)^2 + I_{yz} \left(\frac{1}{k_y I_z} + \frac{1}{k_z I_y} \right) \left(\frac{\delta v_s}{L} \right) \left(\frac{\delta w_s}{L} \right) + \frac{1}{k_z} \left(\frac{\delta w_s}{L} \right)^2 \right] \quad (6-13c)$$

Frame elements with only five typical cross-sections namely BOX, IE, TUBE, ELIP and SORE (Solid Rectangle) are permitted. Explicit expressions for the various section constants associated with each of these cross-sections can be found in Appendix A.

6.4.1.4.3 Membrane Element

The strain energy of the k-th membrane element can be obtained by integrating the strain energy density function W_e^* over the volume of the element. The assumption of constant strain within the element simplifies this integration to yield

$$u_k = \frac{EAh}{(1-\nu)^2} [\epsilon_{xx}^2 + \epsilon_{yy}^2 + 2\nu\epsilon_{xx}\epsilon_{yy} + \frac{(1-\nu)}{2} \gamma_{xy}^2] \quad (6-14a)$$

where from Figure (3-7)

$$A = \frac{1}{2} Q^{\circ} R^{\circ} \sin \alpha \quad (6-14b)$$

and the strain terms are given by Eqs. (3-56) through (3-58).

6.4.1.2 Strain Energy Evaluation for Inelastic Response

Although closed form analytical expressions for U can be developed when the material is elastic the same is not true when the material yields. Then the response depends upon the current values of stress components and past history. As shown in Section 4 Von Mises' yield criterion together with Henckey's total strain theory provides a simple means of calculating strain energy density distributions throughout an element that has yielded. Because total stresses and total strains are no longer linearly related recourse must be made to numerical integration of the strain energy density over the volume of the element.

The strain energy density may be decomposed into an elastic part and an incremental dissipative part thereby providing an estimate of the total energy of the system that has been dissipated through inelastic deformations. Thus for a system with m elements

$$\begin{aligned} U = \text{strain energy} &= \sum_{i=1}^m U^i = \sum_{i=1}^m U_e^i + \Delta U_d^i \\ &= \sum_{i=1}^m \left(\int_{V_i} W_e^i dv + \int_{V_i} \Delta W_d^i dv \right) \end{aligned} \quad (6-15)$$

where W_e^i and ΔW_d^i are obtained from the material model as described in Section 4 (see Figure 4.3).

For open or closed cross-sections of the type shown in Fig. (6-1). The integrals in Eq. (6-15) are expressed as sums of integrals over a finite number of strips, n_s . In keeping with the assumptions of the thin-walled theory the integrands are assumed constant over the thickness

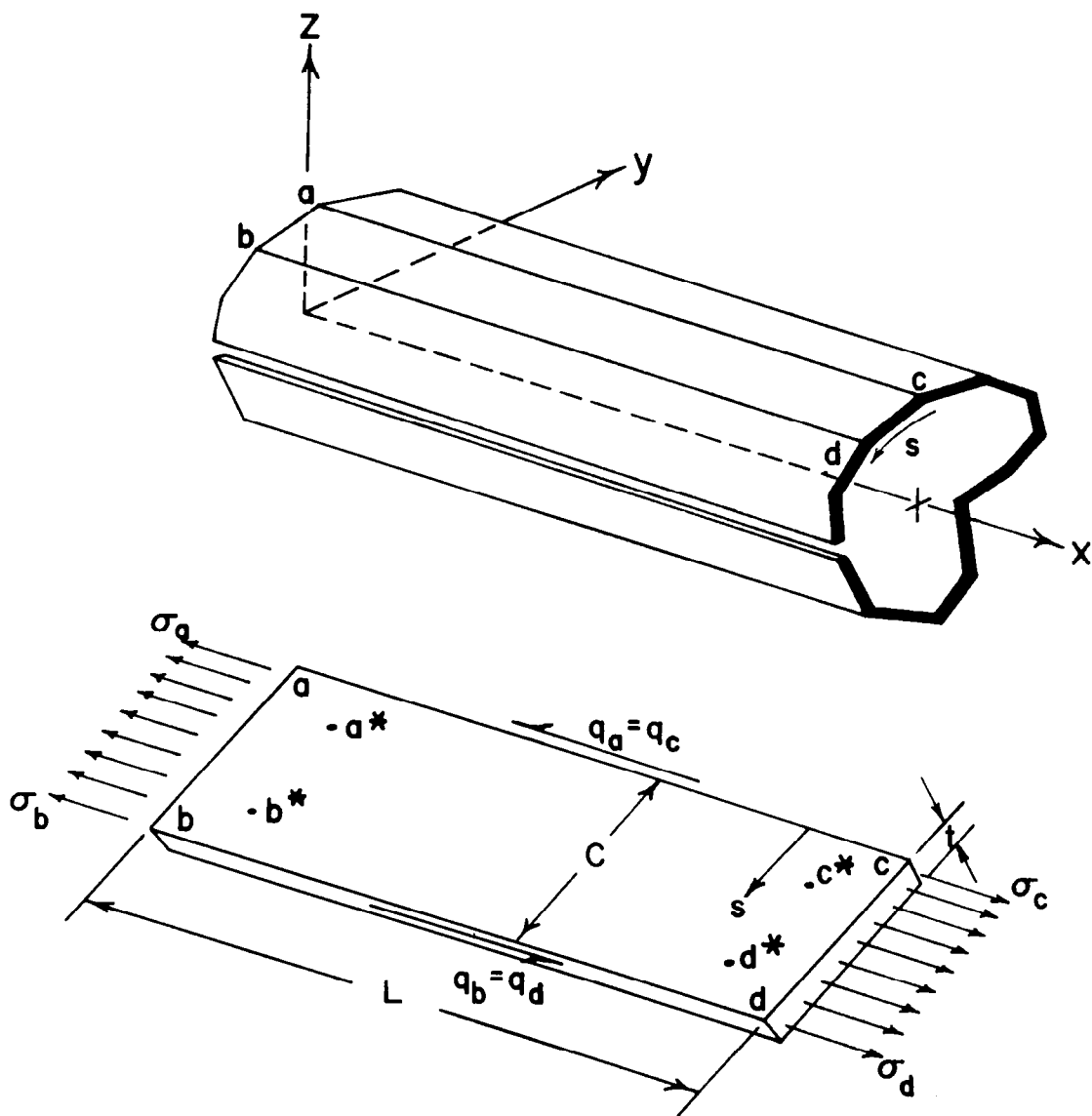


Fig. 6-1 A Model for Strain Energy Integration.

of these strips. Both integrals in Eq. (6-15) are of the form

$$\sum_{j=1}^{n_s} t_j \int_{A_j} f_j dA \quad (6-16)$$

which using a three point Lobatto quadrature rule in each of the two co-ordinate directions in the plane of the strip reduces to

$$\sum_{\ell=1}^3 \sum_{k=1}^3 \sum_{j=1}^{n_s} t_j A_j H_{\ell} H_k f_{j\ell k} \quad (6-17)$$

H_{ℓ} and H_k are the weights and $f_{j\ell k}$ is the value of f_j at the ℓ -kth quadrature point [31]. The exact locations of these quadrature points (or equivalently also the stress reference points) for the four different cross-sections can be found by referring to Appendix A.

6.4.2 Gradient Evaluation

The gradient of S as defined by Eq. (6-7) involves the acceleration vector \ddot{q}_{ei} which for a given vector q_{ei} , is provided by Eq. (6-12) as

$$\ddot{q}_{ei} = \frac{1}{\beta(\Delta t)^2} [(q_{ei} - q_{0i}) - \dot{q}_{0i}(\Delta t) - (\frac{1}{2} - \beta)\ddot{q}_{0i}(\Delta t)^2] \quad (6-18)$$

and the gradient of U with respect to q_{ei} is given by the general expressions in Eqs. (6-8). The expressions in Eqs. (6-8) can, however, be simplified and reduced to a closed form if the response is purely elastic.

6.4.2.1 Strain Energy Gradient Evaluation for Elastic Response

For purely elastic response the i -th component of the gradient of strain energy can be calculated as

$$\frac{\partial U}{\partial q_{ei}} = \sum_{k=1}^m \frac{\partial u_k}{\partial q_{ei}} = \sum_{k=1}^m \sum_{j=1}^{n_r} \left(\frac{\partial u_k}{\partial r_j} \right) \left(\frac{\partial r_j}{\partial q_{ei}} \right) \quad (6-19)$$

where r_j are the local relative degrees of freedom of the q -th node relative to the p -th node and n_r the total of such local relative degrees

of freedom. U_k is the strain energy of the k-th member, $k = 1, 2, \dots, m$ being the number of elements which have the q_{ei} degree of freedom in common.

6.4.2.1.1 Truss Element

The relative degree of freedom in this case, $\epsilon = DL/L$, is a function of the relative global displacements ΔU , ΔV and ΔW . Thus,

$$\frac{\partial U}{\partial U_q} = \sum_{i=1}^m (EAL)\epsilon \left[\frac{\partial \epsilon}{\partial U_q} \right] \quad (6-20)$$

From Eqs. (3-2) and (3-3) it follows that

$$\frac{\partial \epsilon}{\partial U_q} = \frac{(\Delta X + \Delta U)}{L^2(1+\epsilon)} ; \quad \frac{\partial \epsilon}{\partial U_p} = - \frac{\partial \epsilon}{\partial U_q} \quad (6-21a)$$

$$\frac{\partial \epsilon}{\partial V_q} = \left(\frac{(\Delta Y + \Delta V)}{L^2(1+\epsilon)} \right)_k ; \quad \frac{\partial \epsilon}{\partial V_p} = - \frac{\partial \epsilon}{\partial V_q} \quad (6-21b)$$

$$\frac{\partial \epsilon}{\partial W_q} = \left(\frac{(\Delta Z + \Delta W)}{L^2(1+\epsilon)} \right)_k ; \quad \frac{\partial \epsilon}{\partial W_p} = - \frac{\partial \epsilon}{\partial W_q} \quad (6-21c)$$

6.4.2.1.2 Frame Element [37]

The relative degrees of freedom in this case are δu , δv_b , δw_b , ψ_x , ψ_y and ψ_z and whereas Eqs. (6-12) through (6-14) provide U as a function of these relative generalized displacements, Eqs. (3-16) through (3-21) provide the necessary relationships between them and the relative global generalized displacements ΔU , ΔV , ΔW , $\Delta \theta_x$, $\Delta \theta_y$ and $\Delta \theta_z$.

Thus for the k-th element

$$\frac{\partial U_k}{\partial (\delta u)} = EA \left(\frac{\delta u}{L} \right) \quad (6-22a)$$

$$\begin{aligned} \frac{\partial U_k}{\partial (\delta v_b)} = & \frac{6E}{L^2} \{ I_z \left[2 \left(\frac{\delta v_b}{L} \right) - \psi_z \right] + 2I_{yz} \left[\left(\frac{\delta w_b}{L} \right) + \frac{1}{2} \psi_y \right] \} \\ & + \frac{12k_y EI_z}{L^2} \left\{ \frac{1}{k_y} \left(\frac{\delta v_s}{L} \right) + \frac{I_{yz}}{2} \left(\frac{1}{k_y I_z} + \frac{1}{k_z I_y} \right) \left(\frac{\delta w_s}{L} \right) \right\} \end{aligned} \quad (6-22b)$$

$$\begin{aligned}\frac{\partial u_k}{\partial(\delta w_b)} &= \frac{6E}{L^2} \{I_y [2(-\frac{\delta w_b}{L}) + \psi_y] + 2I_{yz} [(-\frac{\delta v_b}{L}) - \frac{1}{2} \psi_z]\} \\ &+ \frac{12k_z EI_y}{L^2} \{(\frac{I_{yz}}{2}) (\frac{1}{k_y I_z} + \frac{1}{k_z I_y}) (\frac{\delta v_s}{L}) + \frac{1}{k_z} (\frac{\delta w_s}{L})\} \quad (6-22c)\end{aligned}$$

$$\frac{\partial u_k}{\partial \psi_x} = \frac{GJ}{L} \psi_x \quad (6-22d)$$

$$\begin{aligned}\frac{\partial u_k}{\partial \psi_y} &= \frac{6E}{L^2} \{I_y [(-\frac{\delta w_b}{L}) + \frac{2}{3} \psi_y] + 2I_{yz} [\frac{1}{2} (-\frac{\delta v_b}{L}) - \frac{1}{3} \psi_z]\} \\ &+ \frac{6k_z EI_y}{L} \{(\frac{I_{yz}}{2}) (\frac{1}{k_y I_z} + \frac{1}{k_z I_y}) (\frac{\delta v_s}{L}) + \frac{1}{k_z} (\frac{\delta w_s}{L})\} \quad (6-22e)\end{aligned}$$

$$\begin{aligned}\frac{\partial u_k}{\partial \psi_z} &= \frac{6E}{L^2} \{I_z [(-\frac{\delta v_b}{L}) + \frac{2}{3} \psi_z] - 2I_{yz} [\frac{1}{2} (-\frac{\delta w_b}{L}) + \frac{1}{3} \psi_y]\} \\ &- \frac{6k_y EI_z}{L} \{(\frac{I_{yz}}{2}) (\frac{1}{k_y I_z} + \frac{1}{k_z I_y}) (\frac{\delta w_s}{L}) + \frac{1}{k_y} (\frac{\delta v_s}{L})\} \quad (6-22f)\end{aligned}$$

Furthermore, it can be easily verified from Eqs. (3-30c,d), (3-34 a, b)

that

$$\frac{\partial \delta v_b}{\partial q_{ei}} = \frac{1}{(1+\phi_z)} \left[\frac{\partial \delta v}{\partial q_{ei}} - z_s \frac{\partial \psi_x}{\partial q_{ei}} + \frac{\phi_z L}{2} \frac{\partial \psi_z}{\partial q_{ei}} \right] \quad (6-23a)$$

and

$$\frac{\partial \delta w_b}{\partial q_{ei}} = \frac{1}{(1+\phi_y)} \left[\frac{\partial \delta w}{\partial q_{ei}} + y_s \frac{\partial \psi_x}{\partial q_{ei}} + \frac{\phi_y L}{2} \frac{\partial \psi_y}{\partial q_{ei}} \right] \quad (6-23b)$$

It remains to derive expressions for the derivatives of the relative generalized displacements. For the case of large of deformations provided by Eqs. (3-16), (3-17) and (3-19)

$$\frac{\partial \{\delta u\}}{\partial \{U\}_p} = - [T_2]_p^T [T_1]^T \quad (6-24a,b)$$

$$\frac{\partial \{\delta u\}}{\partial \{U\}_q} = [T_2]_p^T [T_1]^T$$

$$\frac{\partial\{\delta u\}}{\partial\{\Theta\}_p} = [T_T]_p^T [T_1]^T$$

$$\frac{\partial\{\delta u\}}{\partial\{\Theta\}_q} = [0]$$

$$\frac{\partial\{\psi\}}{\partial\{U\}_p} = [0]$$

$$\frac{\partial\{\psi\}}{\partial\{U\}_q} = [0]$$

(6-24c,h)

$$\frac{\partial\{\psi\}}{\partial\{\Theta\}_p} = [T_R]_p^T [T_1]^T$$

$$\frac{\partial\{\psi\}}{\partial\{\Theta\}_q} = [T_2]^T [T_1]^T$$

where the components of $[T_T]_p$ are

$$T_T^{11} = 0$$

$$T_T^{21} = (s_x s_z + c_x s_y c_z)(\Delta X + \Delta U) + (-s_x c_z + c_x s_y s_z)(\Delta Y + \Delta V) + c_x c_y(\Delta Z + \Delta W)$$

$$T_T^{31} = (c_x s_z - s_x s_y c_z)(\Delta X + \Delta U) - (c_x c_z + s_x s_y s_z)(\Delta Y + \Delta V) - s_x s_y(\Delta Z + \Delta W)$$

$$T_T^{12} = -s_y c_z(\Delta X + \Delta U) - s_y s_z(\Delta Y + \Delta V) - c_y(\Delta Z + \Delta W)$$

(6-25a,h)

$$T_T^{22} = s_x c_y c_z(\Delta X + \Delta U) + s_x c_y s_z(\Delta Y + \Delta V) - s_x s_y(\Delta Z + \Delta W)$$

$$T_T^{32} = c_x c_y c_z(\Delta X + \Delta U) + c_x c_y s_z(\Delta Y + \Delta V) - c_x s_y(\Delta Z + \Delta W)$$

$$T_T^{13} = -c_y s_z (\Delta X + \Delta U) + c_y c_z (\Delta Y + \Delta V)$$

$$T_T^{23} = (-c_x c_z - s_x s_y s_z) (\Delta X + \Delta U) + (-c_x s_z + s_x s_y c_z) (\Delta Y + \Delta V) \quad (6-25g,1)$$

$$T_T^{33} = (s_x c_z - c_x s_y s_z) (\Delta X + \Delta U) + (s_x s_z + c_x s_y c_z) (\Delta Y + \Delta V)$$

and the components of $[T_R]_p$ are

$$T_R^{11} = -c_y c_z$$

$$T_R^{21} = (s_x x_z + c_x s_y c_z) \Delta\theta_x - (-c_x s_z + s_x s_y c_z) \Delta\theta_y + (-s_x c_z + c_x s_y s_z) \Delta\theta_z$$

$$T_R^{31} = (c_x s_z - s_x s_y c_z) \Delta\theta_x - (s_x s_z + c_x s_y c_z) \Delta\theta_y - (c_x c_z + s_x s_y s_z) \Delta\theta_z$$

$$T_R^{12} = -s_y c_z \Delta\theta_x - s_y s_z \Delta\theta_y - c_y s_z - c_y \Delta\theta_z$$

$$T_R^{22} = s_x c_y c_z \Delta\theta_x + s_x c_y s_z \Delta\theta_y - (c_x c_z + s_x s_y s_z) - s_x s_y \Delta\theta_z \quad (6-26a,h)$$

$$T_R^{32} = c_x c_y c_z \Delta\theta_x + c_x c_y s_z \Delta\theta_y - (-s_x c_z + c_x s_y s_z) - c_x s_y \Delta\theta_z$$

$$T_R^{13} = -c_y s_z \Delta\theta_x + c_y c_z \Delta\theta_y + s_y$$

$$T_R^{23} = (-c_x c_z - s_x s_y s_z) \Delta\theta_x + (-c_x s_z + s_x s_y c_z) \Delta\theta_y - s_x c_y$$

$$T_R^{33} = (s_x c_z - c_x s_y s_z) \Delta\theta_x + (s_x s_z + c_x s_y c_z) \Delta\theta_y - c_x c_y \quad (6-26i)$$

6.4.2.1.3 Membrane Element

The relative degrees of freedom in this case are δu_q , δu_r and δv_r (see Fig. 3-7). Thus for moderately large strains

$$\begin{aligned} \frac{\partial u_k}{\partial q_{ej}} = & \frac{Ehs \sin Q^\circ}{2(1-\nu^2)} \left\{ \left(\frac{\partial \delta u_q}{\partial q_{ej}} \right) \left\{ \left(\frac{1-\nu}{2} \right) \gamma_{xy} \left(\frac{\delta u_r}{Q^\circ \sin \alpha} - \cot \alpha \left(1 + 2 \frac{\delta u_q}{R^\circ} \right) \right) \right. \right. \\ & + (\epsilon_{xx} + \nu \epsilon_{yy}) \left(\frac{\delta u_q}{R^\circ} + 1 \right) + (\epsilon_{yy} + \nu \epsilon_{xx}) \cot \alpha \left(\frac{\delta u_q}{R^\circ} \cot \alpha - \frac{\delta u_r}{Q^\circ \sin \alpha} \right) \} \\ & + \left(\frac{\partial \delta u_r}{\partial q_{ej}} \right) \left\{ \left(\frac{1-\nu}{2} \right) \gamma_{xy} \left(\frac{R^\circ}{Q^\circ \sin \alpha} \right) \left(1 + \frac{\delta u_q}{R^\circ} \right) \right. \\ & + (\epsilon_{yy} + \nu \epsilon_{xx}) \left(\frac{R^\circ}{Q^\circ \sin \alpha} \right) \left(\frac{\delta u_r}{Q^\circ \sin \alpha} - \frac{\delta u_q}{R^\circ} \cot \alpha \right) \} \\ & \left. + \left(\frac{\partial \delta v_r}{\partial q_{ej}} \right) \left\{ (\epsilon_{yy} + \nu \epsilon_{xx}) \left(\frac{R^\circ}{Q^\circ \sin \alpha} \right) \left(1 + \frac{\delta v_r}{Q^\circ \sin \alpha} \right) \right\} \right\} \quad (6-27a) \end{aligned}$$

where

$$\frac{\partial \delta u_q}{\partial q_{ej}} = \frac{\partial R}{\partial q_{ej}} \quad (6-27b)$$

$$\frac{\partial \delta u_r}{\partial q_{ej}} = \frac{\partial Q}{\partial q_{ej}} \cos \beta + Q \frac{\partial \cos \beta}{\partial q_{ej}} \quad (6-27c)$$

$$\frac{\partial \delta v_r}{\partial q_{ej}} = \frac{\partial Q}{\partial q_{ej}} \sin \beta + Q \frac{\partial \sin \beta}{\partial q_{ej}} \quad (6-27d)$$

and

$$\frac{\partial R}{\partial q_{ej}} = \frac{1}{R} \left[x_{qp} \frac{\partial x_{qp}}{\partial q_{ej}} + y_{qp} \frac{\partial y_{qp}}{\partial q_{ej}} + z_{qp} \frac{\partial z_{qp}}{\partial q_{ej}} \right] \quad (6-27e)$$

$$\frac{\partial Q}{\partial q_{ej}} = \frac{1}{Q} \left[x_{rp} \frac{\partial x_{rp}}{\partial q_{ej}} + y_{rp} \frac{\partial y_{rp}}{\partial q_{ej}} + z_{rp} \frac{\partial z_{rp}}{\partial q_{ej}} \right] \quad (6-27f)$$

$$\begin{aligned} \frac{\partial \cos \beta}{\partial q_{ej}} = \frac{1}{QR} [& (\frac{\partial x_{qp}}{\partial q_{ej}}) x_{rp} + x_{qp} (\frac{\partial x_{rp}}{\partial q_{ej}}) + (\frac{\partial y_{qp}}{\partial q_{ej}}) y_{rp} \\ & + y_{qp} (\frac{\partial y_{rp}}{\partial q_{ej}}) + (\frac{\partial z_{qp}}{\partial q_{ej}}) z_{rp} + z_{qp} (\frac{\partial z_{rp}}{\partial q_{ej}})] \end{aligned} \quad (6-27g)$$

$$\frac{\partial \sin \beta}{\partial q_{ej}} = - \cot \beta (\frac{\partial \cos \beta}{\partial q_{ej}})$$

$$\frac{\partial x_{qp}}{\partial q_{ej}} = \begin{cases} 1 \\ -1 \text{ if } q_{ej} \\ 1 \end{cases} = \begin{cases} U_q \\ U_p \\ U_q \text{ or } U_p \end{cases} \quad (6-27h)$$

$$\frac{\partial y_{qp}}{\partial q_{ej}} = \begin{cases} 1 \\ -1 \text{ if } q_{ej} \\ 0 \end{cases} = \begin{cases} V_q \\ V_p \\ \neq V_q \text{ or } V_p \end{cases} \quad (6-27i)$$

$$\frac{\partial z_{qp}}{\partial q_{ej}} = \begin{cases} 1 \\ -1 \text{ if } q_{ej} \\ 0 \end{cases} = \begin{cases} W_q \\ W_p \\ \neq W_q \text{ or } W_p \end{cases} \quad (6-27j)$$

with similar relations for derivatives of x_{rp} , y_{rp} and z_{rp} with respect to q_{ej} .

6.4.2.2 Strain Energy Gradient Evaluation for Inelastic Response

For inelastic response the i -th component of the gradient of strain energy is evaluated as

$$\frac{\partial u}{\partial q_{ei}} = \sum_{k=1}^m \frac{\partial u_k}{\partial q_{ei}} = \sum_{k=1}^m \sum_{j=1}^{n_r} \int_{V_k} (\frac{\partial W}{\partial \bar{\epsilon}})_k (\frac{\partial \bar{\epsilon}}{\partial r_j}) dv_k (\frac{\partial r_j}{\partial q_{ei}}) \quad (6-30)$$

where W and $\bar{\epsilon}$ are defined as in Eqs. (4-4) and (4-5) and the remaining equations are defined in Section 6.4.1.2. As in the case of the strain energy, the gradient evaluation for inelastic response necessitates a similar integration using quadratures. Except for the change in the integrand this evaluation is identical to that described previously.

6.4.2.2.1 Truss Element

In this case $\bar{\epsilon}_k = \epsilon_k$ which is also the relative degree of freedom (j=1). Thus

$$\left(\frac{\partial \bar{\epsilon}}{\partial r_j}\right)_k = 1$$

Expressions for $(\partial r_j / \partial q_{ei})$ are provided by Eqs. (6-21).

6.4.2.2.2 Frame Element

In this case again $\bar{\epsilon}_k = (\epsilon_x)_k$. With the aid of Eqs. (3-24) and (3-32) this is seen to be

$$\begin{aligned} \bar{\epsilon}_k = K - \frac{y}{L} [6(1-2\eta) \frac{\delta v_b}{L} + 2(3\eta-1)\psi_z] \\ - \frac{z}{L} [6(1-2\eta) \frac{\delta w_b}{L} - 2(3\eta-1)\psi_y] \end{aligned} \quad (6-31)$$

where K is given by Eq. (3-35). Thus, for the case of large elastic deformations

$$\begin{aligned} \frac{\partial \bar{\epsilon}_k}{\partial (\delta u)} &= 1 \\ L \left(\frac{\partial \bar{\epsilon}_k}{\partial (\delta v_b)} \right) &= - \frac{6y}{L} (1-2\eta) + \frac{6}{5} \left(\frac{\delta v_b}{L} \right) - \frac{1}{10} \psi_z + \frac{\delta v_s}{L} \\ L \left(\frac{\partial \bar{\epsilon}_k}{\partial (\delta w_b)} \right) &= - \frac{6z}{L} (1-2\eta) + \frac{6}{5} \left(\frac{\delta w_b}{L} \right) + \frac{1}{10} \psi_y + \frac{\delta w_s}{L} \\ \frac{\partial \bar{\epsilon}_k}{\partial (\psi_y)} &= \frac{2z}{L} (3\eta-1) + \frac{1}{10} \left(\frac{\delta w_b}{L} \right) + \frac{2}{15} \psi_y \\ \frac{\partial \bar{\epsilon}_k}{\partial (\psi_z)} &= - \frac{2y}{L} (3\eta-1) - \frac{1}{10} \left(\frac{\delta v_b}{L} \right) + \frac{2}{15} \psi_z \\ L \left(\frac{\partial \bar{\epsilon}_k}{\partial (\delta v_s)} \right) &= \left(\frac{\delta v_b}{L} \right) + \left(\frac{\delta v_s}{L} \right) \end{aligned} \quad (6-32a, g)$$

$$L \left(\frac{\partial \bar{\epsilon}_k}{\partial (\delta w_s)} \right) = \left(-\frac{\delta w_b}{L} \right) + \left(\frac{\delta w_s}{L} \right)$$

Expressions for $(\partial r_j / \partial q_{ei})$ are provided by Eqs. (6-26), (6-27) and (6-28).

When a frame element responds inelastically, an additional node is added at the center of the element. The axial displacement field is then defined with the aid of two relative axial degrees of freedom δu_1 and δu_2 as evident from Eq. (3-36). Equation (3-37) provides the definition of δu_1 in terms of other usual quantities. The derivatives of δu_1 and δu_2 can thus be obtained by differentiation of relations in Eq. (3-38a-h). Explicit expressions for such derivatives are however too lengthy and cumbersome and have been omitted accordingly.

6.4.2.2.3 Membrane Element

The effective strain, $\bar{\epsilon}_k$ in this case is defined by Eq. (4-4).

Hence,

$$\frac{\partial \bar{\epsilon}_k}{\partial \epsilon_{xx}} = \frac{4}{3\bar{\epsilon}_k} (\epsilon_{xx} + \frac{1}{2} \epsilon_{yy})$$

$$\frac{\partial \bar{\epsilon}_k}{\partial \epsilon_{yy}} = \frac{4}{3\bar{\epsilon}_k} (\epsilon_{yy} + \frac{1}{2} \epsilon_{xx}) \quad (6-33a,c)$$

$$\frac{\partial \bar{\epsilon}_k}{\partial \gamma_{xy}} = \frac{2}{3} \frac{\gamma_{xy}}{\bar{\epsilon}}$$

Expressions for $(\partial r_j / \partial q_{ei})$ are provided by Eqs. (6-29).

Section 7

SOLUTION ERROR CONTROL

Errors in the present solution process arise from two sources:

(i) truncation errors which occur due to truncating the series representation of the response Eqs. (6-1) and (ii) round-off errors which occur due to the use of a computer with finite digit arithmetic precision. In addition to the accuracy considerations of the solution process due regard must be taken of its stability. For linear systems it has been shown by Goudreau and Taylor [32] that in order to maintain unconditional stability of the numerical integration scheme given by Eqs. (6-1) the parameter β should be chosen such that

$$\beta \geq 0.25 (0.5 + \gamma)^2$$

with $\gamma \geq 0.50$. No such criteria can be postulated for nonlinear problems however, with the optimum values of β and γ being very much problem dependent [25].

Proper choice of a step size (time or load) is thus crucial. If too large a time step is used truncation errors occur due to truncating the series representation of the response. Furthermore, there is a danger of instability of the numerical integration process. If too small a step size is used, computer accuracy limitations arise due to limited number of digits used by the computer to represent the response. In practice, irrespective of whether a problem is linear or not the determination of the optimum size is difficult because of the difficulties of accurately measuring the errors due to polynomial truncation and computer arithmetic truncation.

Automatic error control in ACTION consists of varying time steps

to assure that the truncation error is tolerable. The errors are controlled by adopting time steps so that the equations of motion are satisfied to user specified accuracies at midstep times. In other words, some norm of the gradient of S in Eq. (6-4) is required to be less than a user specified limit. Using Eqs. (6-1) responses are interpolated for midtime. An equilibrium check is made using these displacements and midtime forces and interpolated accelerations. Similar equilibrium checks are also made at the end of the time step. If the errors are excessive the time step is halved and equations resolved. If the error is excessively small, the current results are accepted, stress and strain histories are updated but the time step for the next solution is increased by an arbitrary factor of 1.50.

The following definition of error is adopted for checking equilibrium imbalance at the midstep or the end of the time step. For the i -th degree of freedom the equilibrium imbalance is given by $\partial S / \partial q_{ei}$. The imbalance is weighted depending upon the relative magnitudes of displacements. Thus, each gradient component is multiplied by the corresponding displacement component and the resulting work-like quantity is normalized with respect to the current value of the potential function S . Thus the i -th component of the error vector is defined to be

$$E_i = \frac{\left(\frac{\partial S}{\partial q_{ei}} \right) q_{ei}}{S} \quad (7-1)$$

The norm of the error vector is defined to be

$$||E|| = \max_i (E_i). \quad (7-2)$$

The errors at the beginning and at the end of the time step are

assumed to be due solely to convergence limits of the minimization process. Hence the allowable error at midstep due to truncation is assumed to be

$$||E||_{t_0 + \frac{\Delta t}{2}} = \frac{||E||_{t_0} + ||E||_{t_0 + \Delta t}}{2} \quad (7-3)$$

Δt being the size of the time step. It is this measure of error at midstep which is required to fall within user specified limits.

Section 8

APPENDIX A - FRAME ELEMENT CROSS-SECTION DETAILS

A.1 The Box Cross-Section [15]

In this section formulas for the box cross-section are given. The box cross-section is a thin-walled symmetric closed section composed of four pieces as shown in Fig. A-1. Each piece has a uniform thickness with the twoside pieces having the same thickness and the top and bottom pieces having the same thickness.

Because of the significant difference in the torsional rigidities of open and closed cross-sections, use of the box cross-section to represent an open section by omitting pieces will lead to gross errors in torsional response. Thin-walled open sections can be adequately modeled by making a recourse to the IE section to be described later.

The x, y, z axes of Fig. A-1 are the x_2, y_2, z_2 axes of Fig. 3-3.

The geometric parameters of the box cross section are given by

$$A = 2(d_1 t_1 + d_2 t_2)$$

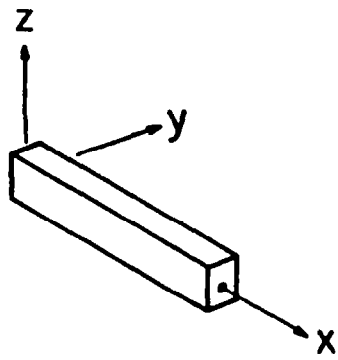
$$y_c = 0, \quad z_c = 0$$

$$I_y = \left(\frac{d_1 t_1}{2} + \frac{d_2 t_2}{6} \right) d_2^2, \quad I_z = \left(\frac{d_1 t_1}{6} + \frac{d_2 t_2}{2} \right) d_1^2 \quad (A-1a,g)$$

$$I_{yz} = 0, \quad J = \frac{2d_1^2 d_2^2}{\frac{d_1}{t_1} + \frac{d_2}{t_2}}$$

where A is the cross-sectional area, y_c and z_c are co-ordinates of the centroid, I_y , I_{yz} and I_z are area moments of inertia, and J is the torsional constant. From symmetry the position of the shear center is at the centroid of the section, hence

$$y_s = 0, \quad z_s = 0 \quad (A-1h,f)$$



c , CENTROID

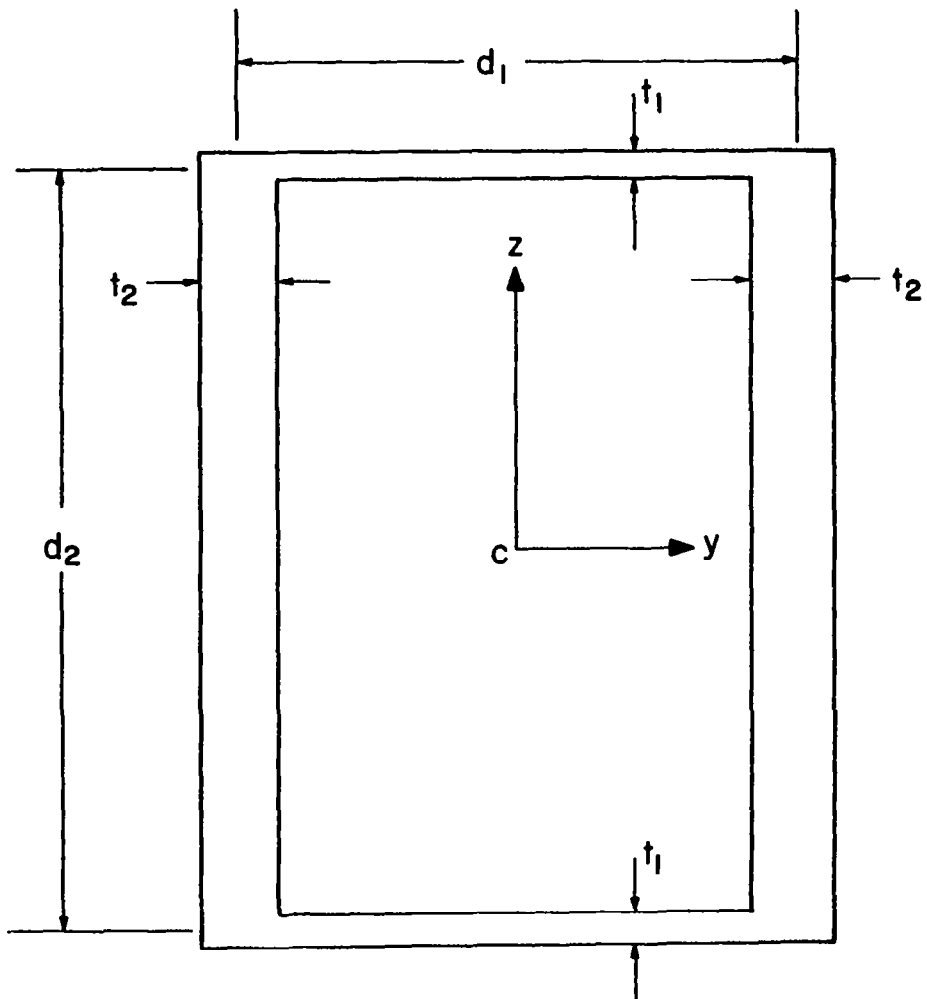


Fig. A-1 Box Cross-Section Definition.

Shear constants k_y and k_z for the cross-section are determined based on the maximum strain method [33]. Thus

$$k_y = \frac{A}{V_y} (\tau_y)_{\text{centroid}}, \quad k_z = \frac{A}{V_z} (\tau_z)_{\text{centroid}}$$

Calculating the centroidal shear stresses for elastic bending the above formulas reduce to

$$k_y = \frac{A}{4I_z} \frac{d_1}{t_1} \left(\frac{d_1 t_1}{2} + d_2 t_2 \right), \quad (A-2a,b)$$

$$k_z = \frac{A}{4I_y} \frac{d_2}{t_2} \left(d_1 t_1 + \frac{d_2 t_2}{2} \right)$$

With these k_y and k_z , the elastic shear deflection parameters α_y and α_z of Eq. (3-34a,b) are

$$\alpha_y = \frac{12k_y EI_z}{GAL^2}, \quad \alpha_z = \frac{12k_z EI_y}{GAL^2} \quad (A-2c,d)$$

For monitoring inelastic material response, five points are spaced equally along each of the four walls of the section dividing the box element into 16 volume elements for the calculation of strain energy using Lobatto quadratures. For reporting stress results the normal stress, σ , and the shear stress, τ , are determined at the 16 points in Fig. A-2 and the stresses are subscripted by the point numbers shown in the figure to identify their location.

For the box section, Eq. (3-44a) for the shear flow constant becomes

$$q_0 = \frac{\frac{2A_0 G}{L} \psi_x - \sum_i \frac{C_i}{2} [(\tau_a + \tau_b) + \frac{C_i}{6L} (\sigma_a - \sigma_b - \sigma_c + \sigma_d)]}{\frac{4A_0^2}{J}} \quad (A-3)$$

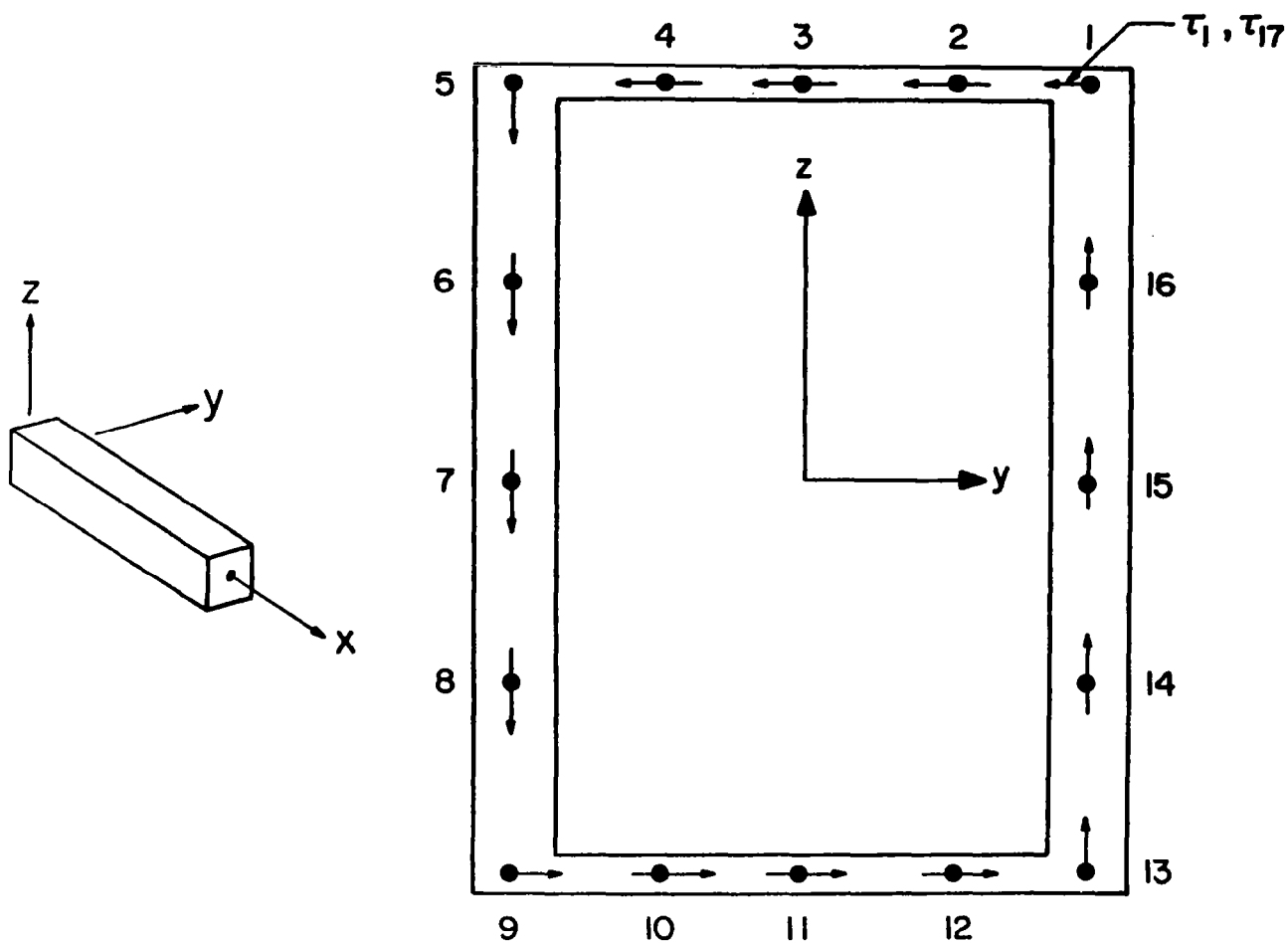


Fig. A-2 Quadrature Points for the Box Cross-section.

where the sum is over the 16 volume elements. Based on the centroidal strains, the measurements of the effective bending shear strains are

$$\gamma_{sy} = \frac{\Delta v_s}{L} = \frac{1}{2G} (\tau_{11} - \tau_3)$$

$$\gamma_{sz} = \frac{\Delta w_s}{L} = \frac{1}{2G} (\tau_{15} - \tau_7)$$
(A-4a,b)

All of the equations used to treat the frame member with box section are now available.

A.2 The IE Cross-Section [15]

In this section formulas for the IE cross-section are given. The IE cross-section is shown in Fig. A-3. It is made up of seven pieces--five flange pieces indicated by the subscripts 1, 2, 4, 6, 7 and two web pieces indicated by the subscripts 3, 5. Each piece has a uniform thickness which may be different from the thickness of any other piece. Any combination of the five flange pieces may be omitted by specifying the width or thickness, or both, to be zero. The web sections, indicated by subscripts 3 and 5, cannot be omitted. The x, y, z axes of Fig. A-3 are the x_2 , y_2 , z_2 axes of Fig. 3-3.

The geometric parameters of the IE cross-section are given by

$$A = \sum_{i=1}^7 A_i = \sum_{i=1}^7 d_i t_i$$

$$y_c = \frac{1}{2A} (A_1 d_1 - A_2 d_2 - A_4 d_4 + A_6 d_6 - A_7 d_7)$$

$$z_c = \frac{1}{A} \left[\left(\frac{A_5}{2} + A_6 + A_7 \right) d_5 - \left(A_1 + A_2 + \frac{A_3}{2} \right) d_3 \right]$$

$$I_y = (A_1 + A_2 + \frac{A_3}{3}) d_3^2 + (\frac{A_5}{3} + A_6 + A_7) d_5^2 - A z_c^2$$

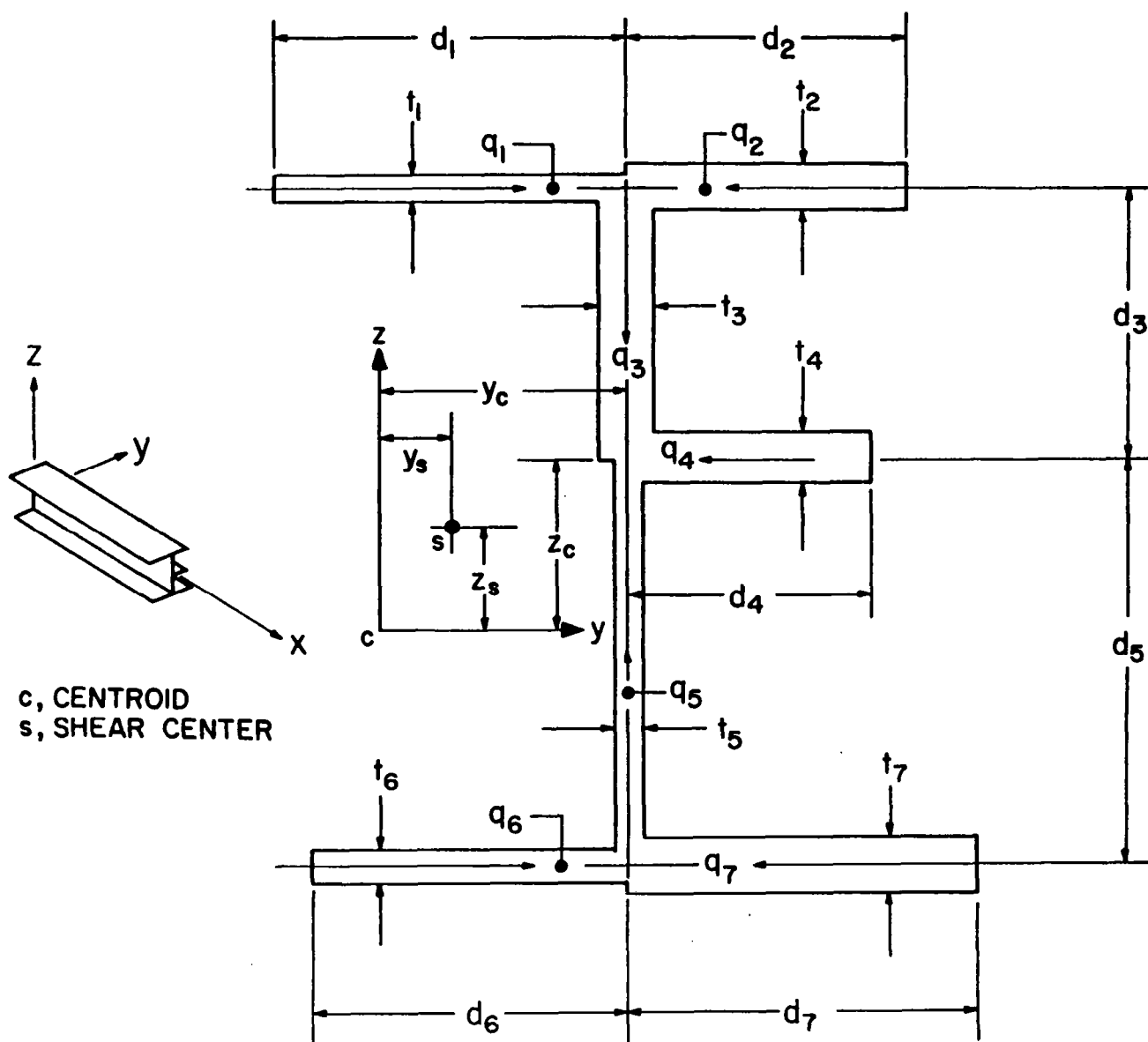


Fig. A-3 IE Cross-section Definition.

$$\begin{aligned}
I_z &= \frac{1}{3} (A_1 d_1^2 + A_2 d_2^2 + A_4 d_4^2 + A_6 d_6^2 + A_7 d_7^2) - A y_c^2 \\
I_{yz} &= \frac{1}{2} [(-A_1 d_1 + A_2 d_2) d_3 - (-A_6 d_6 + A_7 d_7) d_5] - A y_c z_c \\
J &= \frac{1}{3} \sum_{i=1}^7 A_i t_i^2 \quad (A-5a,g)
\end{aligned}$$

The elastic shear center is located as follows. For loading in the x-z plane the normal stress is given by

$$\sigma = \frac{I_z z - I_{yz} y}{I_y I_z - I_{yz}^2} M_y$$

where M_y is the bending moment about the y-axis. From Eq. (3-24) the shear flow is

$$q - q_0 = - \frac{V_z}{I_y I_z - I_{yz}^2} \int_0^s (I_z z - I_{yz} y) t ds$$

where $V_z = \frac{dM_y}{dx}$ is the resultant shear force. This result can be used to find the shear flow in each piece.

From the definition of the shear center, we have

$$V_z (y_c - y_s) = \int_0^{d_1} d_3 q_1 ds_1 - \int_0^{d_2} d_3 q_2 ds_2 - \int_0^{d_6} d_5 q_6 ds_6 + \int_0^{d_7} d_5 q_7 ds_7$$

where y_s is the y co-ordinate of the shear center as shown in Fig. A-4.

Substituting for the shear flow and integrating the following expression by y_s results

$$\begin{aligned}
y_s &= y_c - \frac{1}{2(I_y I_z - I_{yz}^2)} \{ -I_z [(z_c + d_3) d_3 (d_1^2 t_1 - d_2^2 t_2) \\
&\quad - (z_c - d_5) d_5 (d_6^2 t_6 - d_7^2 t_7)] \\
&\quad + I_{yz} [(y_c - \frac{2}{3} d_1) d_3 d_1^2 t_1 - (y_c + \frac{2}{3} d_2) d_3 d_2^2 t_2
\end{aligned} \quad (A-5h)$$

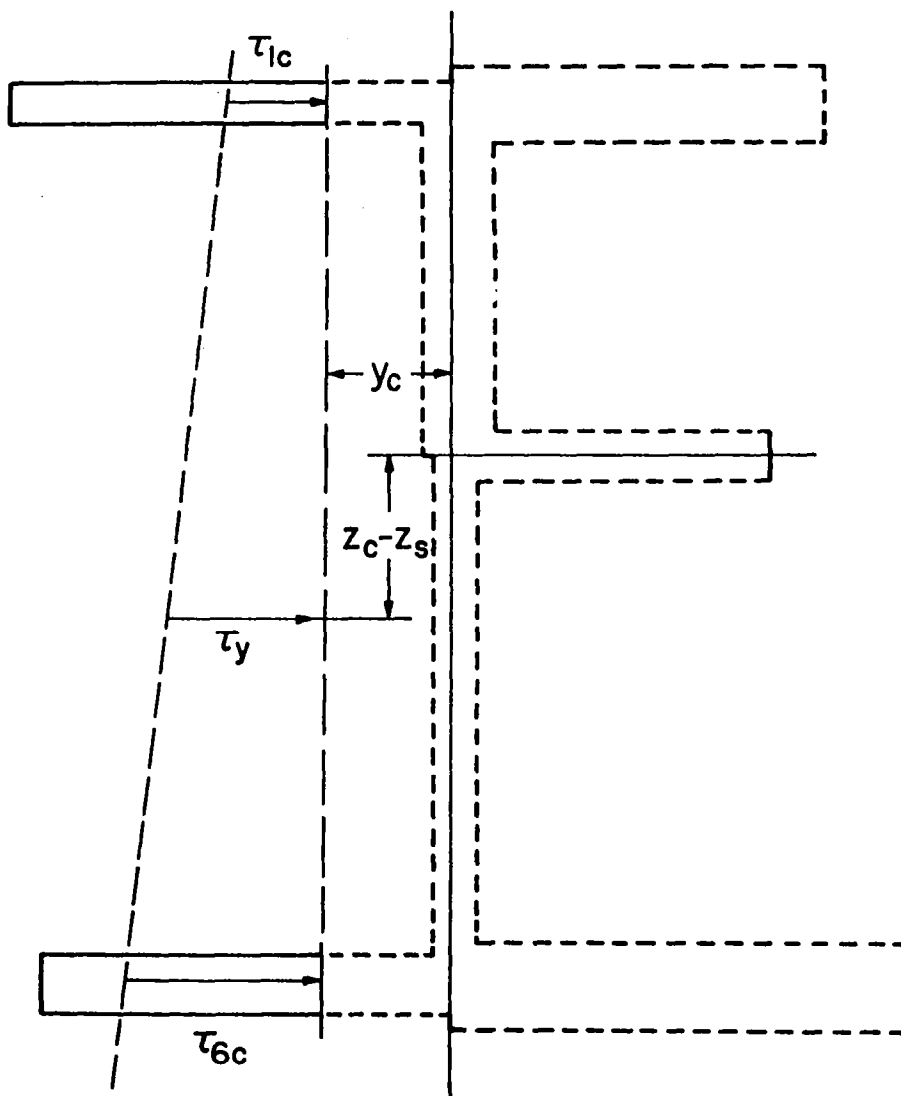


Fig. A-4 Method for Determining Shear Stresses τ_y .

$$- (y_c - \frac{2}{3} d_6) d_5 d_6^2 t_6 + (y_c + \frac{2}{3} d_7) d_5 d_7^2 t_7 \}}]$$

A similar treatment for loading in the x-y plane gives an expression for the z co-ordinate of the shear center

$$\begin{aligned} z_s = z_c - \frac{1}{2(I_y I_z - I_{yz}^2)} \{ & I_y [(y_c - \frac{2}{3} d_1) d_3 d_1^2 t_1 - (y_c + \frac{2}{3} d_2) d_3 d_2^2 t_2 \\ & - (y_c - \frac{2}{3} d_6) d_5 d_6^2 t_6 + (y_c + \frac{2}{3} d_7) d_5 d_7^2 t_7] \\ & - I_{yz} [(z_c + d_3) d_3 (d_1^2 t_1 - d_2^2 t_2) - (z_c - d_5) d_5 (d_6^2 t_6 - d_7^2 t_7)] \} \end{aligned} \quad (A-51)$$

The expressions for the shear flow in each piece can be used to determine the shear constants k_y and k_z required for the shear deflection calculations. Based on the maximum strain method formulas for these constants are

$$k_y = \frac{A}{V_y} (\tau_y)_{\text{centroid}}, \quad k_z = \frac{A}{V_z} (\tau_z)_{\text{centroid}}.$$

Calculation of the shear stress at the centroid based on elastic bending in the y-z plane and substitution into the above expression yields for y_c positive:

$$\begin{aligned} k_y = \frac{A}{(I_y I_z - I_{yz}^2) (d_3 + d_5)} \{ & [I_y (\frac{d_1 - y_c}{2}) + I_{yz} (d_3 + z_c)] (d_5 - z_s) (d_1 - y_c) \\ & + [I_y (\frac{d_6 - y_c}{2}) - I_{yz} (d_5 - z_c)] (d_6 - y_c) (d_3 + z_s) \} \end{aligned} \quad (A-6a)$$

and for y_c negative

$$\begin{aligned} k_y = \frac{A}{(I_y I_z - I_{yz}^2) (d_3 + d_5)} \{ & [I_y (\frac{d_2 + y_c}{2}) - I_{yz} (d_3 + z_c)] (d_2 + y_c) (d_5 - z_s) \\ & + [I_y (\frac{d_7 + y_c}{2}) + I_{yz} (d_5 - z_c)] (d_3 + z_s) (d_7 + y_c) \} \end{aligned} \quad (A-6b)$$

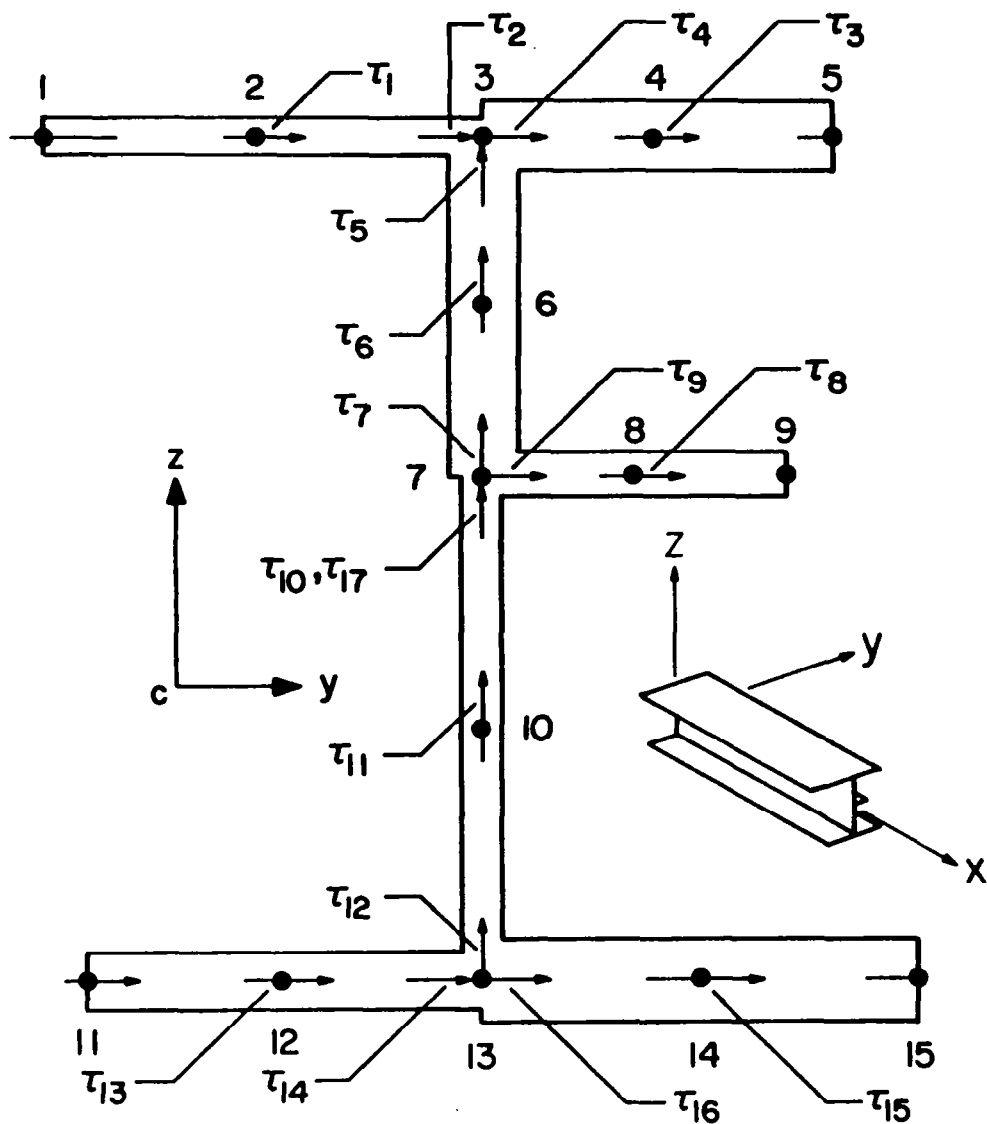


Fig. A-5 Quadrature Points for IE Cross-Section.

The shear stress at the shear center is used to measure the effective centroidal stress, as shown in Fig. A-4 for the case of positive y_c .

A similar treatment for loading in the x-z plane gives the following expressions for the shear constant k_z :

z_c positive:

$$k_z = \frac{A}{(I_y I_z - I_{yz}^2) t_5} \{ I_z [A_6 + A_7 + \frac{1}{2} t_5 (d_5 - z_c)] (d_5 - z_c) + I_{yz} [-A_6 (\frac{d_6}{2} - y_c) + A_7 (\frac{d_7}{2} + y_c) + t_5 (d_5 - z_c) y_c] \}$$

z_c negative:

$$k_z = \frac{A}{(I_y I_z - I_{yz}^2) t_3} \{ I_z [A_1 + A_2 + \frac{1}{2} t_3 (d_3 + z_c)] (d_3 + z_c) + I_{yz} [A_1 (\frac{d_1}{2} - y_c) - A_2 (\frac{d_3}{2} + y_c) - t_3 (d_3 + z_c) y_c] \} \quad (A-6c)$$

With k_y and k_z determined, the elastic shear deflection parameters α_y and α_z of Eqs. (3-34a,b) can be calculated. These are

$$\alpha_y = \frac{12k_y EI}{GAL^2} \frac{y}{z}, \quad \alpha_z = \frac{12k_z EI}{GAL^2} \frac{z}{y} \quad (A-6d)$$

Equations (A-5) through (A-6) represent the principal cross-section and member parameters used in the analysis of the IE section. They are based upon geometry and the elastic deflection responses.

For monitoring inelastic material response, stress reference points are selected so that the end and mid-points of each of the seven cross-section pieces are represented. This selection divides the IE element into 14 volume elements for the calculation of strain energy through the use of Lobatto quadratures. The normal stress, σ is calculated at each reference point as defined in Fig. A-5. The shear stress, τ , is determined only at selected reference points as shown in Fig. A-5. The shear

stress at the free ends of the flanges is zero.

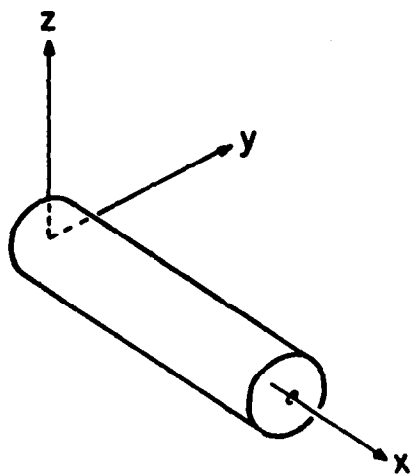
It is evident that the shear flow theory does not contain torsional components and hence cannot describe torsion of an open cross-section like the IE cross-section. Thus, the torsional response is assumed to be elastic and Eq. (6-13) is used to account for the torsional strain energy.

For treating inelastic bending shear deformations, measurements of the effective shear strains are required. Based on the maximum strain method the centroidal shear stresses may be used to estimate effective shear strains. However, in general the centroidal stresses are a result of bending about both the y and z axes; hence it is necessary to separate the centroidal stresses into components associated with bending about the y-axis and with bending about the z-axis. For the box, tube and elliptical sections this is done easily based on geometric symmetry of the sections and the results are obtained in terms of centroidal stresses. For the non-symmetric IE section the analysis is more complex. Therefore a slightly different approach is taken. From Eqs. (3-29a,b), the effective strains are

$$\gamma_{sy} = k_y \frac{V_y}{AG}, \quad \gamma_{sz} = k_z \frac{V_z}{AG}$$

In these expressions, the parameters, V_y and V_z are the force resultants of the shear stresses in the y and z directions. The forces V_y and V_z are determined by integrating the shear stresses over the cross-section. Assumption of a linear variation of shear stress between the stress reference points, yields the following results:

$$\begin{aligned} \gamma_{sy} = \frac{\Delta v_s}{L} = \frac{k_y}{2GA} [& (\tau_1 + \frac{\tau_2}{2})d_1t_1 + (\tau_3 + \frac{\tau_4}{2})d_2t_2 + (\tau_8 + \frac{\tau_9}{2})d_4t_4 \\ & + (\tau_{13} + \frac{\tau_{14}}{2})d_6t_6 + (\tau_{15} + \frac{\tau_{16}}{2})d_7t_7], \end{aligned} \quad (A-7a)$$



16 EQUALLY SPACED STRESS
REFERENCE POINTS

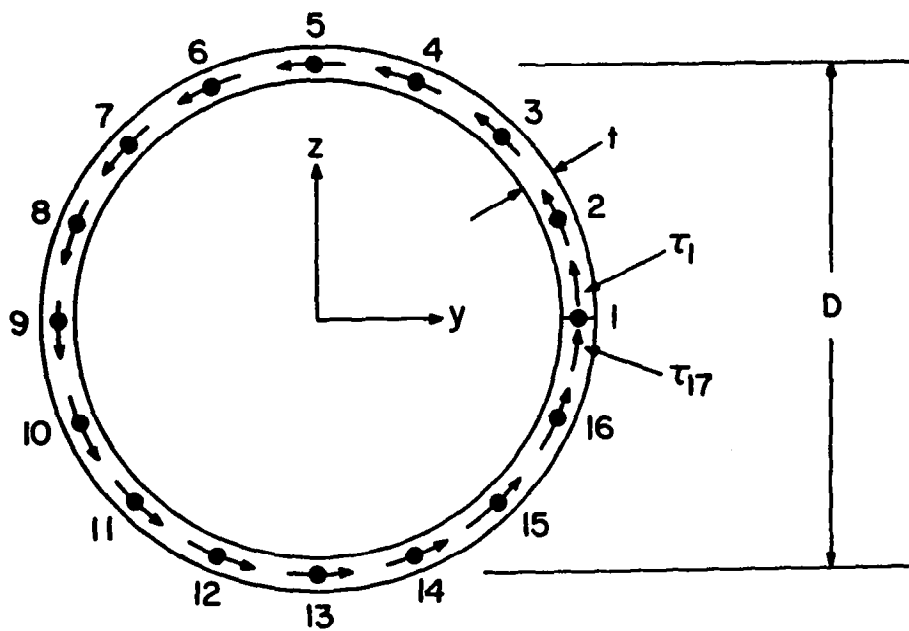


Fig. A-6 Circular Tube Cross-Section Details.

$$\gamma_{sz} = \frac{\Delta w_s}{L} = \frac{k_z}{2GA} \left[\left(\frac{\tau_5}{2} + \tau_6 + \frac{\tau_7}{2} \right) d_3 t_3 + \left(\frac{\tau_{10}}{2} + \tau_{11} + \frac{\tau_{12}}{2} \right) d_5 t_5 \right] \quad (A-7b)$$

The shear constants k_y and k_z in the above equations are those determined on the basis of elastic bending, i.e., as given by Eqs. (A-6).

All of the equations required for the analysis of a frame member with IE cross-section are now available. The procedure for evaluating the strain energy is the same as that described for the box section.

A.3 The Circular Tube Cross-Section [15]

In this section formulas for the circular tube cross-section are given. The circular tube cross-section is described by the mean diameter, D , and the constant wall thickness, t , as shown in Fig. A-6. The x, y, z axes of Fig. A-6 are the x_2, y_2, z_2 axes of Fig. 3-2.

The geometric parameters of the circular tube cross-section are given by

$$A = \pi D t, \quad y_c = z_c = 0$$

$$I_y = I_z = \frac{AD^3}{8}, \quad I_{yz} = 0 \quad (A-8a,b)$$

$$J = 2I_y = \frac{AD^3}{4}$$

where A is the cross-sectional area, y_c and z_c are the co-ordinates of the centroid, I_y , I_z and I_{yz} are area moments of inertia and J is the torsional constant. As a result of symmetry the shear center coincides with the centroid of the section, hence

$$y_s = z_s = 0 \quad (A-8c,d)$$

The shear constants k_y and k_z determined on the basis of the maximum strain method are

$$k_y = \frac{A}{V_y} (\tau_y)_{\text{centroid}}, \quad k_z = \frac{A}{V_z} (\tau_z)_{\text{centroid}}$$

Calculating the centroidal shear stresses for elastic bending and substituting into the above formulas gives

$$k_y = 2 \text{ and } k_z = 2 \quad (\text{A-9a,b})$$

With these k_y and k_z known, the elastic shear deflection parameters α_y and α_z of Eqs. (3-25) are

$$\alpha_y = \frac{12k_y EI_z}{GAL^2}, \quad \alpha_z = \frac{12k_z EI_y}{GAL^2} \quad (\text{A-9c,d})$$

Equations (A-8) and (A-9) constitute the principal cross-section and member parameters used in the analysis of the circular tube cross-section based on elastic deflection response.

For monitoring inelastic material response, 16 stress reference points spaced equally around the circumference as shown in Fig. A-6 are used. These points divide the circular tube section into 16 equal volume elements which are used for the calculation of the strain energy by Lobatto quadratures. These 16 reference points are used for reporting the normal stress, σ , and the shear stress, τ , which are subscripted using these reference numbers as shown in Fig. A-6.

Some of the general expressions developed for the inelastic material response simplify considerably for the circular tube section. Equation (3-40) for the shear flow may be simplified to

$$q_o = t \left(\frac{DG}{2L} \psi_x - \frac{1}{16} \sum_{i=1}^{16} \tau_i \right) \quad (\text{A-10})$$

where the sum is over the 16 reference points at the p-end of the element. Based on centroidal shear strain, measurements of the effective shear strains caused by bending are

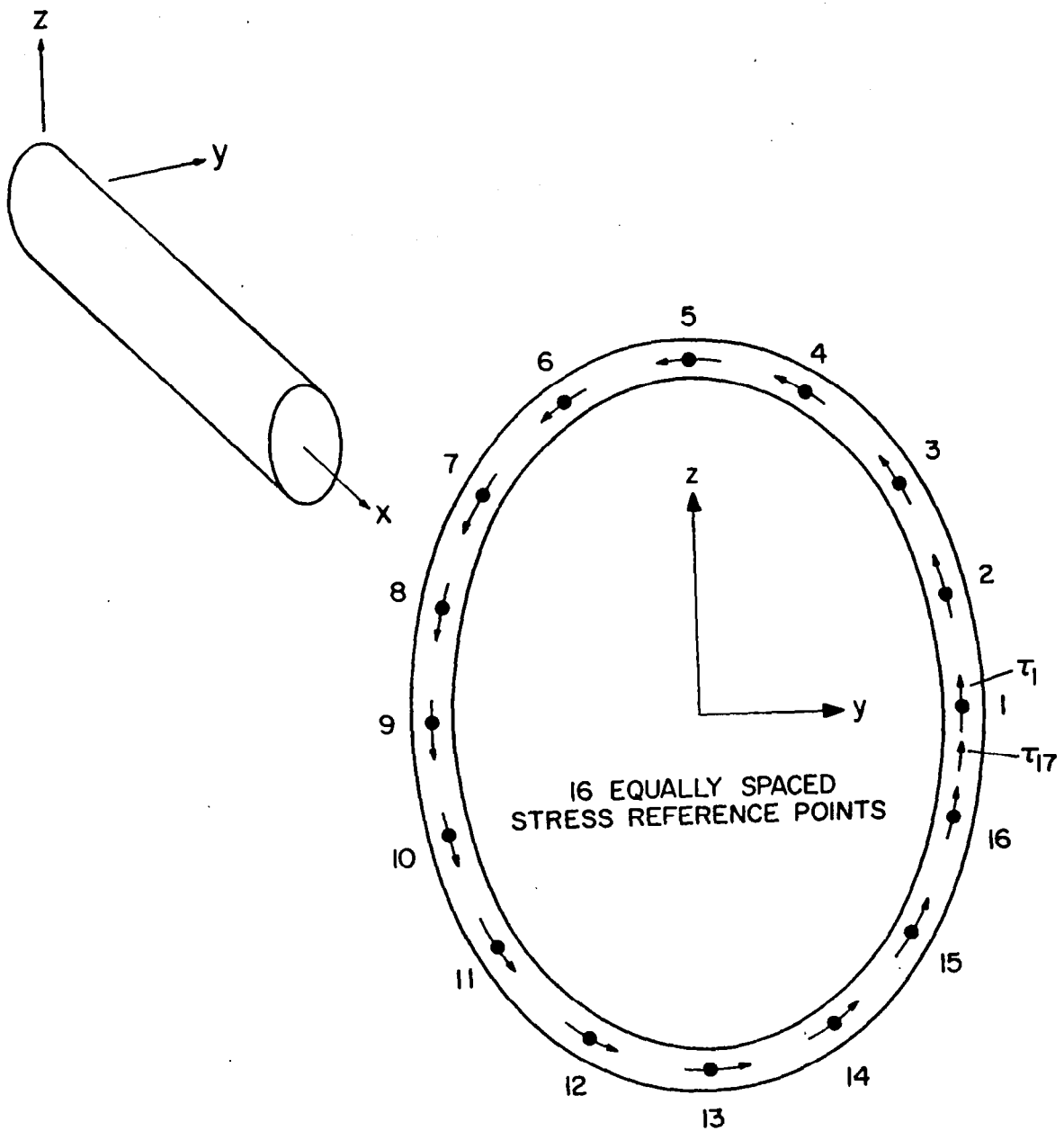


Fig. A-7 Elliptical Tube Cross-Section Details.

$$\gamma_{sy} = \frac{\Delta v_s}{L} = \frac{1}{2G} (\tau_{13} - \tau_{5}), \quad \gamma_{sz} = \frac{\Delta w_s}{L} = \frac{1}{2G} (\tau_{1} - \tau_{9}) \quad (A-11)$$

All of the equations used to treat the frame member with circular tube cross-section are now available.

A.4 The Elliptical Tube Cross-Section

In this section formulas for the elliptical tube cross-section are given. The elliptical tube cross-section is described by the two diameters $2a$ and $2b$ along the major and minor axis respectively and the constant wall thickness, t , as shown in Fig. A-7. The x , y , z axes of Fig. A-7 are the x_2 , y_2 , z_2 axes of Fig. 3-2.

The geometric parameters of the elliptical tube cross-section are

$$A = \pi(a+b)t, \quad y_c = z_c = 0$$

$$I_y = \frac{\pi t}{4} [(3b+a)a^2 + (3a+b)\frac{t^2}{4}] \quad (A-12a,f)$$

$$I_z = \frac{\pi t}{4} [(3a+b)b^2 + (3b+a)\frac{t^2}{4}]$$

$$I_{yz} = 0$$

$$J = \frac{4(\pi ab)^2 t}{E(e, \pi/2)}$$

where

$$e = \frac{\sqrt{a^2 - b^2}}{a} \quad \text{and } E(e, \pi/2) \text{ is the elliptic integral}$$

of the second kind.

The shear center coincides with the center as a consequence of the symmetry of the cross-section and hence

$$y_s = z_s = 0 \quad (A-12g)$$

The shear constants k_y and k_z determined on the basis of the maximum strain method are

$$k_y = \frac{A}{V_y} (\tau_y)_{\text{centroid}}, \quad k_z = \frac{A}{V_z} (\tau_z)_{\text{centroid}}$$

Calculating the centroidal shear stresses for elastic bending and substituting into the above formulas gives

$$k_y = \frac{aA^2}{3\pi I_z t}, \quad k_z = \frac{bA^2}{3\pi I_y t} \quad (\text{A-13,a,b})$$

With these k_y and k_z known, the elastic shear deflection parameters α_y and α_z of Eqs. (3-25) are

$$\alpha_y = \frac{12k_y EI_z}{GAL^2}, \quad \alpha_z = \frac{12k_z EI_y}{GAL^2} \quad (\text{A-14,a,b})$$

Equations (A-13) through (A-14) constitute the principal cross-section and member parameters used in the analysis of the elliptical tube cross-section based on elastic deflection response.

For monitoring inelastic material response, 16 stress reference points spaced equally around the circumference as shown in Fig. A-7 are used. These points divide the elliptical tube cross-section into 16 equal volume elements which are used for the calculation of the strain energy by Lobatto quadratures. These 16 reference points are used for reporting the normal stress, σ , and the shear stress, τ , which are subscripted using these reference numbers as shown in Fig. A-7.

Some of the general expressions developed for the inelastic material response simplify for the elliptical tube cross-section also. Equation (3-40) for the shear flow may be simplified to

$$q_o = \frac{t[2\pi ab \frac{\psi}{L} - \frac{1}{16} \sum_{i=1}^{16} \tau_i]}{4aE(e)} \quad (\text{A-15})$$

Where $E(e)$ is the elliptical integral of the second kind and where the sum in Eq. (A-15) is over the 16 reference points at the p-end of the

element. Based on the centroidal shear strain, measurements of the effective shear strains caused by bending are

$$\gamma_{sy} = \frac{\Delta V_s}{L} = \frac{1}{2G} (\tau_{13} - \tau_{15}), \quad \gamma_{sz} = \frac{\Delta W_s}{L} = \frac{1}{2G} (\tau_{11} - \tau_{19}) \quad (A-16)$$

All of the equations used to treat the frame member with elliptical tube cross-section are now available.

A.5 The Solid Rectangular Cross-Section [37]

This section provides formulas for the solid rectangular cross-section which is described by its two dimensions D_1 and D_2 as shown in Fig. A-8. The x, y, z axes of Fig. A-8 are the x_2, y_2, z_2 axes of Fig. 3-2.

The geometric parameters of the rectangular cross-section are

$$A = D_1 D_2, \quad y_c = z_c = 0$$

$$I_y = \frac{D_1^3 D_2}{12}, \quad I_z = \frac{D_1 D_2^3}{12}, \quad I_{yz} = 0 \quad (A-17a,c)$$

$$J = \frac{1}{3} (2a^3)(2b) \left(1 - \frac{192}{\pi^5} \frac{a}{b} \sum_{n=1,3,\dots}^{\infty} \frac{1}{n^5} \tanh \frac{n\pi b}{2a}\right)$$

Where A is the cross-sectional area, y_c and z_c the co-ordinates of the centroid, I_y , I_z and I_{yz} are the are moments of inertia, J is the torsional rigidity constant and b is the larger and a is the shorter of the two dimensions D_1 and D_2 [36]. As a result of symmetry the shear center coincides with the centroid of the section, hence

$$y_s = z_s = 0 \quad (A-17d)$$

The shear constants k_y and k_z determined on the basis of the maximum strain are

$$k_y = \frac{A}{V_y} (\tau_y)_{\text{centroid}}, \quad k_z = \frac{A}{V_z} (\tau_z)_{\text{centroid}}$$

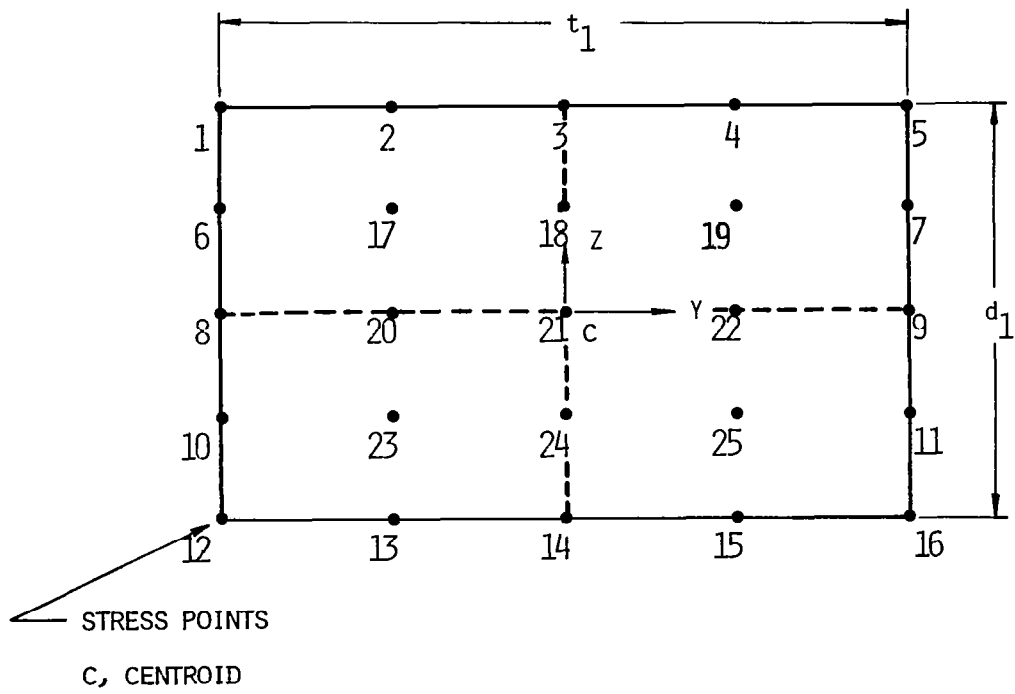
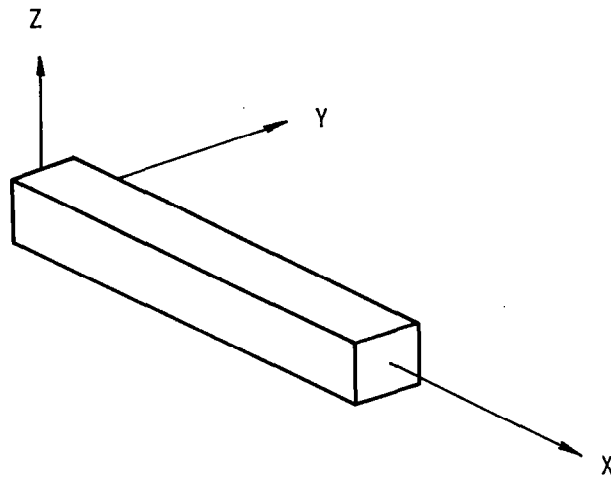


FIGURE A-8. SOLID RECTANGULAR CROSS-SECTION DETAILS.

Calculating the centroidal shear stresses for elastic bending and substituting into the above formulas gives

$$k_y = k_z = \frac{3}{2} \quad (\text{A-17e})$$

With these k_y and k_z known, the elastic shear deflection parameters α_y and α_z of Eqs. (3-25) are

$$\alpha_y = \frac{12k_y EI_z}{GAL^2}, \quad \alpha_z = \frac{12k_z EI_y}{GAL^2} \quad (\text{A-18a,b})$$

Equations (A-17) and (A-18) constitute the principal cross-section and member parameters used in the analysis of the solid rectangular cross-section based elastic response.

For monitoring inelastic material response, 2x2 Gauss quadrature points for each of the four subrectangles and 25 stress reference points spaced equally around the periphery as shown in Fig. A-8 are used. The stresses at the stress reference points are calculated by simple linear extrapolation of the stresses at the Gauss points.

Section 9

BIBLIOGRAPHY

1. I. K. McIvor, "Modeling and Simulation as Applied to Vehicle Structures and Exteriors." Vehicle Safety Research Integration Symposium, Rep. No. DOT HS-820 306, U.S. Dept. Transp., May 1973, pp. 5-18.
2. M. P. Kamat, "Survey of Computer Programs for Prediction of Crash Response and of its Experimental Validation," in "Measurement and Prediction of Structural Biodynamic Crash-Impact Response," Winter Annual Meeting, ASME, 1976.
3. M. P. Kamat, "Users' Manual to the ACTION Computer Code," NASA CR-144973, 1980.
4. M. J. Turner, E. H. Dill, H. C. Martin and R. J. Melosh, "Large Deflection Analysis of Complex Structures Subjected to Heating and External Loads," J. Aerospace Sci., 27, 1960.
5. H. C. Martin, "Derivation of Stiffness Matrices for the Analysis of Large Deflection and Stability Problems," Proc. 1st Conf. on Matrix Methods in Structural Mechanics, 1966.
6. J. T. Oden, "Numerical Formulation of Non-linear Elasticity Problems," J. Struct. Div., ASCE, 93, 1967.
7. H. D. Hibbit, P. V. Marcal and J. R. Rice, "A Finite Element Formulation for Problems of Large Strain and Large Displacement," Int. J. Solids and Struct., 6, 1970.
8. W. Haisler, J. Stricklin, and F. Stebbins, "Development and Evaluation of Solution Procedures for Geometrically Nonlinear Structural Analysis," AIAA J., 10, 1972.
9. H. Armen, H. Levine, A. Pifko, and A. Levy, "Nonlinear Analysis of Structures," NASA CR-2351, 1974.
10. A. Pifko, H. Levine and H. Armen, Jr., "PLANS - A Finite Element Program for Nonlinear Analysis of Structures. Volume I - Theoretical Manual," NASA CR-2568, 1975.
11. T. Belytschko, N. Holmes and R. Mullen, "Explicit Integration - Stability, Solution Properties, Cost," Winter Annual Meeting, ASME, AMD-14, 1975.
12. T. Belytschko, and Hsieh, B. J., "Nonlinear Transient Finite Element Analysis with Convected Co-ordinates," Int. J. Num. Meths. Engr. 9, 1975.
13. F. K. Bogner, R. H. Mallet, M. D. Minich and L. A. Schmit, "Development and Evaluation of Energy Search Methods of Nonlinear Structural Analysis," AFFDL-TR-65-113, WPAFB, Dayton, OH, 1965.

14. R. H. Mallet and L. Berke, "Automated Method for Large Deflection and Instability Analysis of Three-Dimensional Truss and Frame Assemblies," AFFDL-TR-66-102, WPAFB, Dayton, OH, 1966.
15. J. W. Young, "CRASH: A Computer Simulator of Nonlinear Transient Response of Structures," DOT-HS-091-1-125-B, 1972.
16. H. Goldstein, Classical Mechanics, Addison-Wesley Publishing Co., Inc., 1950.
17. I. S. Sokolnikoff, Mathematical Theory of Elasticity, McGraw-Hill Book Co., 1956.
18. J. T. Oden, "Mechanics of Elastic Structures," McGraw-Hill Book Co., 1967.
19. M. P. Kamat and D. E. Killian, "Some Inconsistencies of the Finite Element Method as Applied to Inelastic Response," NASA CR-2732, 1976.
20. J. T. Oden, Finite Elements of Nonlinear Continua, McGraw-Hill, N.Y., 1972.
21. O. J. Smith and O. M. Sidebottom, Inelastic Behavior of Load Carrying Members, John Wiley and Sons, Inc. 1965.
22. K. Washizu, Variational Methods in Elasticity and Plasticity, Pergamon Press, 1968.
23. E. H. Lee, "Elastic-Plastic Deformation at Finite Strains," J. Appl. Mech., Trans. ASME, 1969.
24. O. Widlund, "Conjugate Gradient Methods for Systems of Linear Equations which fail to be Positive Definite Symmetric Type," Lecture delivered at ICASE, NASA Langley Research Center, Hampton, VA, 1978.
25. M. P. Kamat, "Nonlinear Transient Analysis of Aircraft-Like Structures - Theory and Validation," Virginia Polytechnic Institute and State University Report, VPI-E-79-10, 1979.
26. N. M. Newmark, "A Method of Computation for Structural Dynamics," J. EM. Div., ASCE, 85, 1959.
27. M. P. Kamat, and N. F. Knight, Jr., "Efficiency of Unconstrained Minimization Techniques in Nonlinear Analysis," NASA CR-2991, 1978.
28. J. E. Dennis, Jr., and J. J. Moré, "Quasi-Newton Methods, Motivation and Theory," SIAM Review, 19, 1977.
29. D. F. Shanno, and K. H. Phua, "Algorithm 500 Minimization of Unconstrained Multivariate Functions," ACM Trans. Math. Software, 2, 1976.

30. R. Fletcher, "A New Approach to Variable Metric Algorithms", Computer J., 13, 1970.
31. M. Abramowitz and I. A. Stegun, Handbook of Mathematical Functions, Dover Publications Inc., 1965.
32. G. L. Goudreau and R. L. Taylor, "Evaluation of Numerical Integration Methods in Elastodynamics," Computer Meth. in Appl. Mech. and Engr., 2, 1972.
33. M. J. Powell, "Restart Procedures for the Conjugate Gradient Method," C.S.S.24, Computer Science and Systems Division, A.E.R.E., Harwell, Oxfordshire, England, 1975.
34. R. Fletcher and C. M. Reeves, "A Rapidly Convergent Descent Method for Minimization," Computer Journal, 6, 1963.
35. Harwell Subroutine Library, compiled by M. J. Hopper, Theoretical Physics Division, U.K.A.E.A. Research Group, Atomic Energy Research Establishment, Harwell, Vol. 2, 1973.
36. S. P. Timoshenko and J. N. Goodier, Theory of Elasticity, McGraw-Hill Book Co., 1951.
37. N. F. Knight, Jr., "An Efficiency Assessment of Selected Unconstrained Minimization Techniques as Applied to Nonlinear Structural Analysis", M.S. Thesis, Virginia Polytechnic Institute and State University, Blacksburg, Va., August 1977.

1. Report No. NASA CR-3287		2. Government Accession No.		3. Recipient's Catalog No.	
4. Title and Subtitle NONLINEAR TRANSIENT ANALYSIS BY ENERGY MINIMIZATION - A THEORETICAL BASIS FOR THE "ACTION" COMPUTER CODE				5. Report Date July 1980	
				6. Performing Organization Code	
7. Author(s) Manohar P. Kamat				8. Performing Organization Report No.	
9. Performing Organization Name and Address Virginia Polytechnic Institute and State University Blacksburg, VA 24061				10. Work Unit No.	
				11. Contract or Grant No. NAS1-15080-T10	
12. Sponsoring Agency Name and Address National Aeronautics and Space Administration Washington, DC 20546				13. Type of Report and Period Covered Contractor Report	
				14. Sponsoring Agency Code	
15. Supplementary Notes Technical Monitor: Robert J. Hayduk, NASA Langley Research Center Topical Report					
16. Abstract <p>This report provides the formulation basis for establishing the static or dynamic equilibrium configurations of finite element models of structures which may behave in the nonlinear range. With both geometric and time independent material nonlinearities included, the development is restricted to simple one and two dimensional finite elements which are regarded as being the basic elements for modeling full aircraft-like structures under crash conditions. Representations of a rigid link and an impenetrable contact plane are added to the deformation model so that any number of nodes of the finite element model may be connected by a rigid link or may contact the plane.</p> <p>Equilibrium configurations are derived as the stationary conditions of a potential function of the generalized nodal variables of the model. Minimization of the nonlinear potential function is achieved by using the best current variable metric update formula (BFGS) for use in unconstrained minimization. Powell's conjugate gradient algorithm which offers very low storage requirements at some slight increase in the total number of calculations, is the other alternative algorithm to be used for extremely large scale problems.</p> <p>Automatic time step control for transient analysis is available. The process is controlled by monitoring equilibrium errors due to truncation of the series representation of the response at midstep time.</p>					
17. Key Words (Suggested by Author(s)) Transient analysis Nonlinear structures Unconstrained minimization			18. Distribution Statement Unclassified - Unlimited Subject Category 39		
19. Security Classif. (of this report) Unclassified	20. Security Classif. (of this page) Unclassified	21. No. of Pages 107	22. Price A06		